



Parametric sensitivity for analysis of dc networks

Noé Barrera Gallegos

► To cite this version:

Noé Barrera Gallegos. Parametric sensitivity for analysis of dc networks. Other [cs.OH]. Ecole Centrale de Lille, 2016. English. NNT : 2016ECLI0021 . tel-01449925v2

HAL Id: tel-01449925

<https://hal.science/tel-01449925v2>

Submitted on 14 Mar 2017

HAL is a multi-disciplinary open access archive for the deposit and dissemination of scientific research documents, whether they are published or not. The documents may come from teaching and research institutions in France or abroad, or from public or private research centers.

L'archive ouverte pluridisciplinaire **HAL**, est destinée au dépôt et à la diffusion de documents scientifiques de niveau recherche, publiés ou non, émanant des établissements d'enseignement et de recherche français ou étrangers, des laboratoires publics ou privés.

N° d'ordre : 304

CENTRALE LILLE

THESE

Présentée en vue
d'obtenir le grade de

DOCTEUR

En

Automatique, Génie Informatique, Traitement du Signal et des Images
Par

Noe BARRERA GALLEGOS

DOCTORAT DELIVRE PAR CENTRALE LILLE

Titre de la thèse :

Sensibilité Paramétrique pour l'Analyse Dynamique des Réseaux à Courant Continu

Soutenue le 16 Décembre 2016 devant le jury d'examen :

Président	M. Christophe Sueur, Professeur Centrale Lille
Rapporteur	M. Sandip Roy, Professeur Washington State University U. S. A.
Rapporteur	M. Pierre-Yves Richard, Professeur CentraleSupélec
Examineur	M. Salvatore D'Arco, Docteur, Research Scientist SINTEF
Directeur de thèse	Mme. Geneviève Dauphin-Tanguy, Professeur Centrale Lille
Co-Directeur de thèse	M. Xavier Guillaud, Professeur Centrale Lille

Thèse préparée au **Centre de Recherche en Informatique, Signal et Automatique de Lille**
CRISTAL CNRS UMR 9189
Ecole Doctorale SPI 072

“The essence of mathematics lies on its freedom”

-Georg Ferdinand Ludwig Philipp Cantor

Acknowledgments

This work of thesis is the start of an adventure of knowledge, it started with the encouraging work of **Prof. Gilberto** and the research of **Mme. Prof. Genevieve Dauphin-Tanguy** and **Prof. Xavier Guillaud**. Their patience was key for the success of this research. For all the time invested in me, I would like to thank them.

I am grateful to be part of two different teams MOCIS and L2EP and I would like to thank them for its input in the presentations and collaboration. Thanks **Julian** for all the help with the models, simulations, and the great discussions about our work and the different ideas we have.

I would like to thank my family my mother **Margarita** she encouraged me all the time to keep working in which I enjoy the most, My father **Javier** who taught me the value of hard work, My brothers **Alejandro** and **Eduardo** they have help me to be humble. Their words of wisdom during the difficult moments helped to motivate me and focus on the objectives.

I am grateful to be part of a joyful office; I will always cherish the discussions with **Mayank** and **Mohamed** about the meaningless stuff or the very deep insightful thoughts.

I am grateful of having the best friends from Mexico here in France, **Gerardo** and **Joel** for being generous and trust worthy.

Thanks my beloved **Andreina** for your patience through the last months.

I would like to thank the council of science and technology of México (**CONACyT**) in collaboration of the with the regional council of science and technology (**CECTI**) who financed this work of thesis.

Noe Barrera Gallegos

RESUME

Cette thèse a été préparée au sein de l'équipe de recherche « Méthodes et Outils pour la Conception Intégrée de Systèmes (MOCIS) » au Centre de Recherche en Informatique, Signal et Automatique de Lille (CRISTAL) en collaboration avec l'équipe « Réseaux » du Laboratoire d'Electronique et d'Électrotechnique de Puissance de Lille (L2EP).

La thèse se concentre sur le développement d'un outil d'analyse modale pour les réseaux à courant continu.

Les systèmes traditionnels ont des dynamiques qui sont connues pour avoir des oscillations au niveau des rotors des générateurs d'une zone par rapport à une autre. Dans les réseaux électriques de puissance il y a des composants avec des dynamiques non linéaires, une linéarisation est nécessaire pour son analyse.

La théorie fondamentale de l'analyse de sensibilité s'applique pour l'analyse des systèmes électriques de puissance dans les différentes étapes de la production et la transmission de l'énergie.

Pour ce type de systèmes l'analyse modale sélective (SMA) a été développée au MIT en 1982. Le SMA fournit des algorithmes pour le calcul, la sélection et la réduction des variables d'état dans les grands systèmes électriques. Des outils de base concernant cette théorie sont devenus populaires et très utilisés.

Les facteurs de participation représentent un exemple de ces outils, utilisés depuis longtemps. Ils ont été proposés par (I.J. Perez-Arriaga, Verghese, and Schweppe 1982). Les facteurs de participation groupés dans une matrice de participation donnent l'importance des

variables d'état sur les valeurs propres du système. Il est important de dire que cette l'analyse se fait sur le modèle linéaire ou linéarisé du système. L'hypothèse associée à cet outil est d'avoir un modèle du système de type « diagonal dominant » ; en d'autres termes, les éléments diagonaux de la matrice du système sont les plus importants pour les valeurs propres.

Le but des facteurs de participation est la réduction des modèles des systèmes ayant une dynamique particulière comme celle des systèmes électromécaniques.

Dans les nouveaux réseaux à courant continu, les dynamiques sont différentes de celles des systèmes traditionnels. Les dynamiques rapides des composants d'électronique de puissance n'étaient pas considérées dans les objectifs des analyses menées avec les facteurs de participation. Dans ce contexte, des besoins de nouveaux outils sont apparus pour l'analyse modale dans les réseaux à courant continu.

Les objectifs de ce travail de thèse sont :

- Appliquer la théorie actuelle pour l'analyse modale dans les systèmes à courant continu multi-terminal (MTDC).
- Développer une nouvelle méthodologie pour l'analyse dynamique des réseaux à courant continu.

Le Chapitre 2 rappelle la théorie fondamentale de la sensibilité analytique sur laquelle les facteurs de participation sont basés. Pour une bonne compréhension des éléments de base de cette théorie, quelques exemples sont présentés mettant en oeuvre la formulation des facteurs de participation et les hypothèses pour l'utilisation de cette méthodologie.

Avec quelques exemples mettant en évidence les effets des hypothèses, il apparaît que les facteurs de participation sont limités à un type des modèles particuliers. Dans la pratique, les facteurs de participation sont utilisés sur plusieurs modèles de réseaux de puissance sans vérifier

les hypothèses fondamentales. Pour cette raison, il est important de trouver une méthode ou un outil applicable à tous les modèles linéaires des réseaux de puissance.

Dans le Chapitre 3, une formulation différente est proposée pour l'analyse par sensibilité paramétrique (Barrera-Gallegos, Dauphin-Tanguy, and Guillaud 2016). Cette méthodologie est basée sur la théorie de la sensibilité analytique. Quelques exemples sont présentés pour montrer l'utilité de cette approche et sont comparés avec les facteurs de participation.

Le chapitre 4 concerne la modélisation des convertisseurs à courant continu. La première partie s'intéresse au convertisseur source de tension (VSC) qui est un des convertisseurs les plus populaires dans la conversion alternatif continu. La deuxième partie étudie le convertisseur modulaire multiniveaux (MMC) qui s'utilise de plus en plus en raison des avantages offerts par rapport aux modèles classiques des convertisseurs. Pour les deux cas, ces modèles linéaires sont présentés en vue de leur analyse paramétrique.

Dans le chapitre 5, l'étude d'un modèle réduit didactique valide l'utilisation de l'analyse paramétrique. Un modèle plus complexe montre progressivement le couplage des paramètres dans un convertisseur VSC. La comparaison entre l'analyse paramétrique et les facteurs de participation permet d'exposer les limites de l'utilisation des facteurs de participation sur des réseaux HVDC.

Ensuite, l'analyse du convertisseur MMC est présentée. Elle montre quelles sont les différentes façons de contrôler l'énergie stockée dans le convertisseur et leur influence sur les différents couplages entre des paramètres de la partie AC et DC du convertisseur.

En conclusion, il apparaît que la nouvelle méthodologie, par l'étude de la sensibilité est plus générale que l'approche par facteurs de participation et donne plus d'informations sur les caractéristiques dynamiques des réseaux HVDC.

Avec quelques exemples les effets des hypothèses et on montre que les facteurs de participation sont limités sur un type des modèles particulières. Dans la actualité, les facteurs de participation sont utilisés sur plusieurs de modèles des réseaux de puissance sans regarder les hypothèses fondamentales. Pour cette raison est important de trouver une méthode ou utile avec pour appliquer dans tous les modèles linéaires des réseaux de puissance.

Table of Contents

General introduction	1
Chapter 1 State of the art.....	1
1.1 Context and motivation.....	1
1.2 Small signal stability.....	2
1.2.1 Modal Analysis in power electrical systems	3
1.2.2 Modal Analysis of Multi-terminal DC grids	5
1.3 Conclusions.....	6
Chapter 2 Modal sensitivity and participation factors	7
2.1 Introduction.....	7
2.2 Sensitivity matrices	7
2.3 Participation factors	12
2.3.1 Change of basis.....	16
2.3.2 Per-unit representation.....	16
2.4 Usage and interpretation of sensitivity matrices and participation factors	20
2.5 Conclusions.....	26
Chapter 3 Sensitivity analysis	27
3.1 Introduction.....	27
3.2 New definition of parametric sensitivity matrix	27
3.2.1 Example 3.1: Simple Circuit sensitivity of the eigenvalues to the elements..	29
3.2.2 Normalization	31
3.2.3 Example 3.2: Simple Circuit with real eigenvalues	32
3.2.4 Example 3.3: Simple Circuit zero in a diagonal element	35
3.2.5 Example 3.4: Simple Circuit with diagonal dominant elements	37
3.3 Remarks and uses.....	38
3.4 Conclusions.....	40
Chapter 4 State-space modeling of HVDC systems.....	41
4.1 Introduction.....	41
4.2 Context of the HVDC development.....	41

4.3	Voltage source converter	44
4.3.1	General control scheme	44
4.3.2	Per-unit in HVDC grids	51
4.3.3	Reduced linear equivalent	53
4.3.4	Three terminal DC grid model.....	56
4.4	Modular Multi-level Converter reduced model	61
4.4.1	Simplification of the AAM.....	65
4.4.2	Control strategy	67
4.4.3	Linearization.....	69
4.4.4	One station MMC in a MTDC network.....	70
4.4.5	Two stations MMC in a HVDC.....	72
4.5	Conclusions.....	73
Chapter 5	Modal analysis on HVDC systems	75
5.1	Objectives of the analysis	75
5.2	Simplified equivalent DC link	75
5.3	Dynamic analysis of a three terminal MTDC	81
5.4	Dynamic analysis of HVDC system with MMC	88
5.4.1	One MMC connected to a fixed voltage source: energy controlled by DC power 88	
5.4.2	One MMC connected to a fixed voltage source: DC power mode and energy controlled by AC power	92
5.4.3	One MMC connected to a variable DC bus – energy reference constant.....	94
5.4.4	Two terminal MMC DC link (MMC1 Power mode W controlled by dc Power, MMC2 voltage mode W controlled by Ac Power)	97
5.5	Conclusions.....	106
Chapter 6	General Conclusions and Perspectives	107
	Scientific contribution	108
	Bibliography	109
Appendix A.	Automatic routine for parametric sensitivity analysis	114

List of Figures

Figure 1.1 Classification of power system stability	1
Figure 1.2 Modal analysis	3
Figure 2.1 Circuit diagram.	14
Figure 2.2 Current in L (a) and voltage in C (b).	23
Figure 2.3 Response with complex eigenvalues.....	24
Figure 2.4 Diagonal dominant response in pu.	25
Figure 2.5 Gershgorin circles for equation (2.104).	26
Figure 3.1 Eigenvalue trajectories for a small change in H_L	34
Figure 3.2 Eigenvalue trajectories for small change in H_C	34
Figure 3.3 Comparison for an equal change.	35
Figure 3.4 Eigenvalue trajectories for L.....	37
Figure 4.1 Phasorial representation of the three-phase voltage.....	42
Figure 4.2 Two generation systems connected.....	43
Figure 4.3 Voltage source station control diagram.....	44
Figure 4.4 VSC converter.....	45
Figure 4.5 Reduced model of a VSC.....	46
Figure 4.6 dq0 model of a VSC.....	46
Figure 4.7 Current loop	48
Figure 4.8 Decoupled current loops	49
Figure 4.9 Voltage and power control.	49
Figure 4.10 Voltage droop characteristic.	50
Figure 4.11 Linear model.	50
Figure 4.12 HVDC link with two stations.....	53
Figure 4.13 HVDC link equivalent circuit.	53
Figure 4.14 HVDC link equivalent circuit.	55
Figure 4.15 Block diagram of the equivalent HVDC link.....	55
Figure 4.16 Three terminal MTDC grid with droop controlled VSC.....	57
Figure 4.17 Block diagram of the MTDC system	58
Figure 4.18 diagram of the modular multilevel converter.....	62
Figure 4.19 MMC models in decreasing complexity.	63
Figure 4.20 Model type 3.	63
Figure 4.21 Reduced phase-arm circuit.	65
Figure 4.22 Equivalent dq0 MMC average model.	66
Figure 4.23 Inner controllers.	67
Figure 4.24 v_{dc} voltage controller.	68
Figure 4.25 Block diagram of the complete non-linear system.....	69
Figure 4.26 Linearized physical system.	70
Figure 4.27 MMC station connected to a MTDC network.....	70

Figure 4.28 Block diagram of a power controlled MMC.....	70
Figure 4.29 Block diagram of a voltage controlled MMC	71
Figure 4.30 HVDC link with MMC stations.	72
Figure 5.1 Topology of the simplified HVDC	75
Figure 5.2 Dynamic response of the voltage in the link for a change of 0.1pu in the voltage reference.	77
Figure 5.3 Eigenvalue trajectories changing L_{ab}	79
Figure 5.4 Eigenvalue trajectories changing the equivalent capacitance C_{eq1}	79
Figure 5.5 Eigenvalue Trajectories with a change on k_{droop1} and k_{droop2}	80
Figure 5.6 Voltage response.	82
Figure 5.7 Eigenvalue evolution for changing $C_{eq1} \pm 0.5$ pu	84
Figure 5.8 Eigenvalue evolution for changing $L_{ab1} \pm 0.5$ pu	84
Figure 5.9 Voltage response of the VSC stations.....	85
Figure 5.10 Voltage response.	86
Figure 5.11 MMC connected to a fixed voltage source.	88
Figure 5.12 MMC connected to a variable voltage source.....	94
Figure 5.13 Voltage response for a change of voltage reference	98
Figure 5.14 Eigenvalues changing the cable length from 300Km to 100Km.	106
Figure A.1 General flow chart for the parametric sensitivity analysis.....	114

List of tables

Table 1.1 Different advantages and drawbacks of HVDC systems	5
Table 2.1 Parameters of the circuit	21
Table 2.2 Per unit base parameters	21
Table 2.3 Changes in the parameters.....	23
Table 2.4 Parameters	24
Table 3.1 Parameters of the circuit.....	32
Table 3.2 Parameters for a zero in the diagonal	36
Table 3.3 Parameters in diagonal dominant case	37
Table 3.4 Comparison of different approaches	39
Table 4.1 Base values for a VSC station	51
Table 4.2 Parameters of the HVDC system.....	60
Table 4.3 Eigenvalues for $k_{droop} = 0.5$	60
Table 4.4 State variables of the MMC power controlled in a MTDC	71
Table 4.5 State variables of the MMC voltage controlled in a MTDC	72
Table 4.6 State variables of the MMC1.....	72
Table 4.7 State variables of the MMC2.....	73
Table 4.8 State variables of the cable	73
Table 5.1 Parameters of the HVDC network.....	76
Table 5.2 Eigenvalues.....	76
Table 5.3 Association between state variables and parameters.....	77
Table 5.4 Association between state variables and parameters.....	81
Table 5.5 Eigenvalues for $k_{droop} = 0.5$	81
Table 5.6 Eigenvalues for $k_{droop} = 0.2$	84
Table 5.7 Eigenvalues for $k_{droop} = 0.1$	86
Table 5.8 Parameter values of one MMC station connected to a MTDC grid.....	88
Table 5.9 Control settings.....	89
Table 5.10 Eigenvalues with energy controlled by DC power.....	89
Table 5.11 Eigenvalues for the DC link	92
Table 5.12 Control settings.....	94
Table 5.13 Eigenvalues for the DC link	95
Table 5.14 Parameters of the MMC stations	97
Table 5.15 Control settings MMC1	98
Table 5.16 Control settings MMC1	98
Table 5.17 Eigenvalues for the DC link	99
Table 5.18 Most important parameters for the eigenvalues	103
Table 5.19 State variables with most contribution to the eigenvalues.....	103

List of Abbreviations

HVDC	High voltage direct current
MTDC	Multi-terminal direct current
AC	Alternating current
DC	Direct current
VSC	Voltage source converter
MMC	Modular multi-level converter
LTI	Linear time-invariant
SMA	Selective modal analysis
VAR	Volt-ampere reactive

General introduction

This thesis work has been performed under the co-guidance of Prof. Geneviève DAUPHIN-TANGUY and Prof. Xavier GUILLAUD, in the context of the collaboration between the research group Méthodes et Outils pour la Conception Intégrée de Systèmes (MOCIS) at the Centre de Recherche en Informatique, Signal et Automatique de Lille (CRISAL) and the research group Réseaux in the Laboratoire d'Electrotechnique et d'Electronique de Puissance de Lille (L2EP).

This work was developed using the expertise in modelling and characterization of power electronic components of the L2EP and the diagnosis and analysis of complex models in the research group MOCIS.

The objectives of the work are

- to review the current methodologies used for the dynamic analysis of multi-terminal DC (MTDC) grids.
- to develop a new methodology for the dynamic analysis of MTDC grids, allowing a clear understanding of how the component parameters associated to the state variables are related to the eigenvalues.

It has been chosen to study the parametric sensitivity of variables which provides a deeper understanding on the importance of the parameters in the dynamics of the model.

Classically used for this kind of problems, such approach supposes some assumptions on the form of the used model, the validity of which will be discussed in the next chapter

The first chapter presents the state of the art for modal analysis of power electrical systems. It discusses the current problematics of the use of participation factors and its limitations.

The second chapter presents the mathematical background of the sensitivity analysis and participation factors. With didactic examples, the characteristics of participation factors are shown.

The third chapter proposes a new matrix for the analysis of parametric sensitivity. It is implemented on some didactic examples.

The fourth chapter presents first the models of the voltage source converter with very well-known for the AC/DC conversion. Recently, the Modular Multilevel topology is more and more used for high voltage DC systems. It is also described in the 4th chapter which proposes also a linearized approach of this converter.

In the fifth chapter, the methodology proposed in chapter 3 is applied on MMC. A comparison with participation factor is proposed and the analyze of the results shows the effectiveness of the proposed tool

A general conclusion summarizes the main contribution of the thesis.

Chapter 1 State of the art

1.1 Context and motivation

Power electrical systems analysis is particularly difficult due the quantity and the complexity of the dynamics. It has different objectives depending on the dynamics and properties analyzed in the system. The power system stability is a condition of equilibrium between the different phenomena in the electrical system. The stability of the system depends on different characteristics, Figure 1.1 presents an overall representation of the problems linked to power system stability (Kundur et al. 2004).

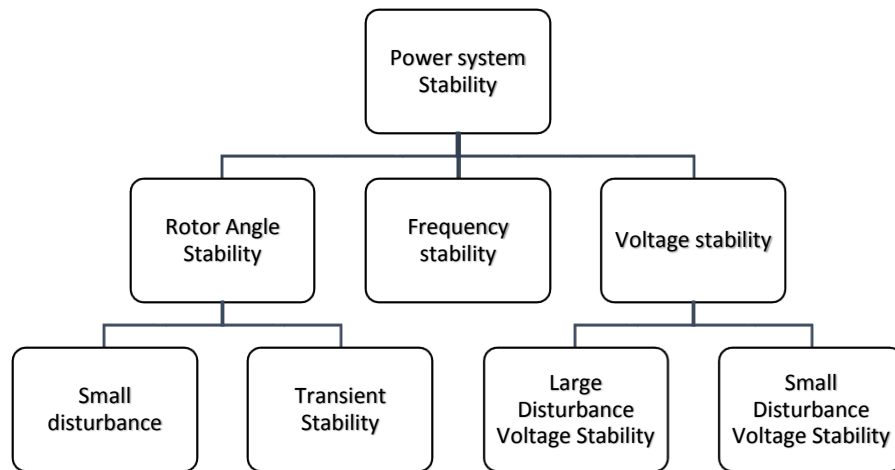


Figure 1.1 Classification of power system stability

This classification is based on the different kinds of disturbances applied to the system (Kundur et al. 2004)(Mondal, Chakrabarti, and Sengupta 2014).

- The rotor angle stability is the ability of the synchronous machines interconnected in a power system to remain synchronized after a small disturbance.
- The voltage stability refers to the ability of the system to maintain steady voltages at all busses during a disturbance.
- The frequency stability is the ability of the system to maintain a steady frequency during a severe disturbance in the generation or load on the system.

The rotor angle stability is one of the most studied characteristics of the power electrical systems, because it involves the stability of the complete system; however the analytical description of these dynamics is complex because of the nonlinearity of the involved phenomena.

The description of the dynamics under controlled circumstances is required to reduce the complexity of the analysis. There are some mathematical tools and methodologies for power stability analysis. For practical considerations and for reducing the complexity the system is considered to be under small disturbances.

1.2 Small signal stability

Small signal stability is the ability of the power system to maintain synchronism under small disturbances such as small variations in loads and generators. The non-linear differential equations are thus linearizable (Kundur et al. 2004).

If power oscillations caused by small disturbances in the system decrease with time and the deviations of the state variables remain small for long time, the system is considered as stable.

For the stability analysis, Lyapunov stability theory is widely used. It is related closely to the local stability in the non-linear system. Intuitively speaking, movement of a nonlinear system over a small range should have similar properties to its linearized approximation (X.-F. Wang, Song, and Irving 2008).

To study the stability of the non-linear system at the operating point, the following results of Lyapunov's stability theory apply:

- a) If the linearized system is asymptotically stable (all eigenvalues of A have negative real parts) the current non-linear system is asymptotically stable at the equilibrium point.
- b) If the linearized system is unstable (at least one of the eigenvalues of A has a positive real part), the current non-linear system is unstable at the equilibrium point.
- c) If the linearized system is critically stable (the real part of all eigenvalues of A are non-positive but at least one of them is zero) no conclusion is available about the non-linear system from its linearized approximation.

Modal analysis can bring more insight into the dynamics at the operating point.

In general, modal analysis is used in different applications as mechanical structures and electrical power networks. Figure 1.2 presents an example of the available tools for modal analysis in electrical and mechanical systems.

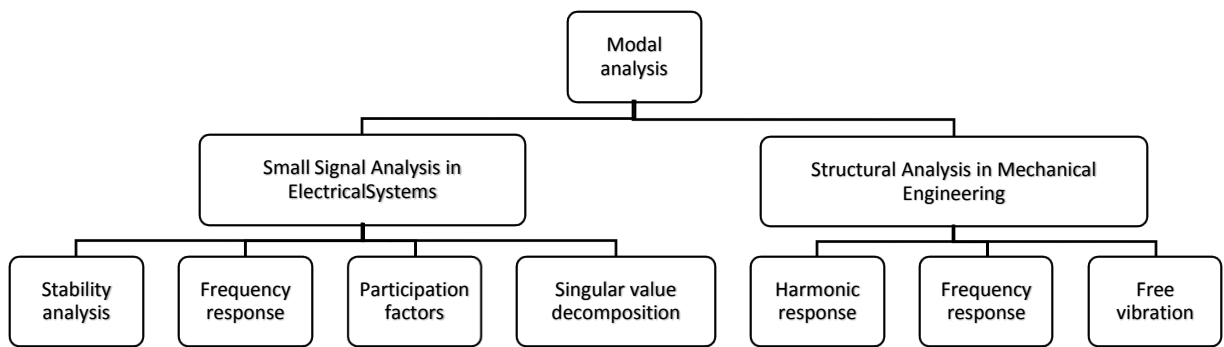


Figure 1.2 Modal analysis

1.2.1 Modal Analysis in power electrical systems

Power electrical systems have thousands of elements interacting. In order to simplify their study, the analysis of power electrical systems is divided in different subsets of dynamics (Pal and Chaudhuri 2005):

- Intra plant mode oscillations: Oscillations caused by the machines (interacting with each other) in the generation site.
- Local plant mode oscillations: Oscillations caused by the generator and the rest of the electrical system.
- Interarea mode oscillations: Caused by two or more groups of generators swinging against each other. This includes the dynamics of the transmission lines between the generators and some loads.
- Control mode oscillations: Oscillations associated with generators and poorly tuned exciters, governors, high voltage direct current (HVDC) converters, static volt-ampere reactive (VAR) compensators controls, among other power electronics components.
- Torsional mode oscillations: modes associated with the turbine generator shaft system.

Several powerful methods for the computation of eigenvalues associated with a small number of selected oscillation modes are published in the literature on power system stability (Morgan 1966; Determination, n.d.).

Particularly, the selective modal analysis (SMA) approach described in (Verghese, Perez-arriaga, and Schweppe 1982) and (Ignacio J. Perez-Arriaga et al. 1990) computes eigenvalues associated with selected modes of interest by using the so called “participation factors”. The objective is to identify variables that are relevant to the selected modes and then construct a reduced-order model involving only the relevant variables (Kundur 2007). The SMA was developed in the context of the local plant and inter-area mode oscillations, especially for low

frequency oscillatory modes, where these modes (eigenvalues) are often associated with the electromechanical elements in the system (Ignacio J. Perez-Arriaga et al. 1990).

These oscillatory modes are fundamental for the dynamical behavior of the system; however, all the dynamical elements have to be taken into account due to their couplings.

Indeed, all theories used until now have been based on the assumption that the grid was mainly fed by electromechanical systems as synchronous machines. Because frequency decoupling is possible between the electromagnetic frequencies and the so-called electromechanical frequencies under 10 Hz, the SMA is a widely used methodology for the analysis of this kind of systems.

The selective modal analysis provides (Ignacio J. Perez-Arriaga et al. 1990):

- Sensitivity-based tools for identifying physical state variables or components that are significant in producing the selected modes.
- Methods for constructing reduced-order models that involve only the significant variables.
- Representation of the influence of parts of the system on the selected modes with any desired accuracy.
- Algorithms for efficiently and accurately computing the few selected modes of interest.

For the reduction of the model, the methodology called “participation factors” has been proposed by (I.J. Perez-Arriaga, Verghese, and Schweppe 1982), based on the sensitivity analysis. This methodology gives a metric for relating states and eigenvalues. The participation factor approach is based on the assumption that some coupling between the state variables can be neglected. Chapter 2 presents a detailed discussion on the assumptions and basis of participation factors.

Recent versions of specialized books on power electrical systems, for example (Kundur 2007) and (Chaudhuri et al. 2014), dedicate some sections to the use of participation factors but without covering important assumptions.

For systems with strongly coupled dynamics, the dynamics can have covered different frequencies and the use of participation factors could be not suitable. This problematics has been addressed in different works to overcome the limitations of the participation factors.

In (Vasca and Verghese 1999) it is proposed an extension of the definition which leads to extended participation factors. Then in (Abed, Hassouneh, and Hashlamoun 2009) the original formulation is replaced for two cases with real and complex eigenvalues; a new definition including the output in the formulation is presented in (Sheng et al. 2010).

Still nowadays, the first definitions of participation factors are in use for modal analysis. For example in (Tschirhart, Sussman, and Abed 2014) the participation factors are used to improve the analysis for voltage stability and monitoring.

The use of power electronics for all stages of energy generation and transmission has increased, in a way that its dynamics are important for the global system behavior. Moreover, the increasing use of renewable energies using direct current networks brings the necessity of new analysis tools.

1.2.2 Modal Analysis of Multi-terminal DC grids

Due to the increase of renewable energy and direct current (dc) links, power electronic converter is taking more and more importance in the grid.

The energy management in a wind turbine is fundamentally different from a traditional power plant. There will be technical and operational implications for the power system at times of high shares of wind power. The power system should sustain disturbances, such as the loss of largest power plant or line, so that the frequency and voltage remain stable. Wind power is asynchronous generation that does not have the same inherent, physical support to the power system inertia as synchronous machines. The fundamental issues regarding frequency stability when losing a large unit or power line as well as large amounts of wind power tripping during network faults need further analyses (Holtinen 2012).

The advantages (see Table 1.1) of connecting different systems using DC links have changed the properties of the power electrical systems (Okba et al. 2012).

Table 1.1 Different advantages and drawbacks of HVDC systems

Advantages	Drawbacks
<ul style="list-style-type: none"> • Greater power per conductor. • Simpler line construction and smaller transmission towers. • A bipolar HVDC grid line uses only two insulated sets of conductors. • Ground return can be used. • Each conductor can be operated as an independent circuit. • No charging current at steady state. • No skin effect. • Lower line losses. • Line power factor is always unity. • Synchronous operation is not required. • No physical restriction limiting the distance or power level for HVDC underground or submarine cables. 	<ul style="list-style-type: none"> • Converters are expensive. • Converters require much reactive power. • Multi-terminal networks are not easy to operate. • Converters generate harmonics, hence require filters. • Break-even distance is influenced by the cost of right-of-way and line construction.

The analysis of HVDC and multi terminal direct current (MTDC) grids is being performed with tools designed for electrical systems based in alternant current (ac) models. This is the case of participation factors.

The participation factors are very effective and rather simple to calculate when the linearized state model is established. For MTDC dynamic analysis (Kalcon et al. 2012), the participation factors are used to analyze the influence of control parameters on some eigenvalues of the system. More recently (Beerten, D Arco, and Suul 2015) use the participation factors to analyze the level of association between subsystems in a three station MTDC. However, no work reconsiders the theory from the basis to assess whether the fundamental assumptions are still valid.

Clearly, the new electrical systems are a big challenge because of their multiple dynamics. The use of current analysis methodologies for traditional electrical systems could lead to unclear conclusions. To know more about these new ways of energy transmission new tools are needed.

1.3 Conclusions

For the analysis of power electrical systems, some tools and mathematical fundamentals are required. The analysis tools have to be adjusted and justified for their specific application.

The use of the participation factors in systems out of their scope of analysis can lead to non-adequate results.

The description on how the analysis is performed and what are the intended purposes is important to understand and also how it can be improved.

The following chapter presents a review of the fundamentals of modal analysis used in power electrical systems.

Chapter 2 Modal sensitivity and participation factors

2.1 Introduction

The modal analysis for linear models is an important tool to model characteristics as the stability of damping oscillations among others. These characteristic depend on the coupling between components whose parameters are supposed to be known without uncertainty, which is not always the case.

It is a common knowledge that there always exists a certain discrepancy between actual (real-operating) and nominal trajectories of any system. This discrepancy is partly due to various inherently approximation schemes in system identification, and partly due to possible further parameter variations stimulated by environmental changes as slow aging of components, variations in raw products or system components in process control applications, inaccuracy of measurement devices or methods, etc .(Eslami 1994).

The study of the changes in the eigenvalues due to parameter changes is important, not only for stability purposes but also for the control of the state variables. Fundaments on sensitivity analysis are hereafter presented.

2.2 Sensitivity matrices

Modal analysis is based on sensitivity analysis of the eigenvalues of the state matrix A to changes in the system parameters.

Consider a LTI model in free-response form,

$$\dot{x}(t) = Ax(t) \quad (2.1)$$

where the matrix A is,

$$A = \begin{bmatrix} a_{11} & a_{12} & \cdots & a_{1n} \\ a_{21} & a_{22} & \cdots & a_{2n} \\ \vdots & \vdots & \ddots & \vdots \\ a_{n1} & a_{n2} & \cdots & a_{nn} \end{bmatrix} \quad (2.2)$$

Assuming the eigenvalues λ_i ($i=1,2,\dots,n$) are distinct, the right eigenvectors v_i ($i=1,2,\dots,n$) are linearly independent and satisfy,

$$Av_i = \lambda_i v_i \quad (2.3)$$

u_j ($j=1,2,\dots,n$) are the correspondent eigenvectors of A^T , such that,

$$A^T u_j = \lambda_j u_j. \quad (2.4)$$

Or by transposition

$$u_j^T A = \lambda_j u_j^T \quad (2.5)$$

From (2.3) by pre-multiplication by u_j^T

$$u_j^T A v_i = \lambda_i u_j^T v_i \quad (2.6)$$

and post-multiplied by v_i

$$u_j^T A v_i = \lambda_j u_j^T v_i \quad (2.7)$$

it leads to

$$(\lambda_i - \lambda_j) u_j^T v_i = 0 \quad (2.8)$$

For $i \neq j$ the product $u_j^T v_i$ is zero and for $i = j$ can have any value. For normalization purposes it is considered that the product is

$$u_j^T v_i = 1 \quad (2.9)$$

The modal matrices are,

$$V = \begin{bmatrix} v_1 & v_2 & \cdots & v_n \end{bmatrix} = \begin{bmatrix} v_{11} & v_{21} & \cdots & v_{n1} \\ v_{12} & v_{22} & \cdots & v_{n2} \\ \vdots & \vdots & \ddots & \vdots \\ v_{1n} & v_{2n} & \cdots & v_{nn} \end{bmatrix} \quad (2.10)$$

$$U = \begin{bmatrix} u_1 & u_2 & \cdots & u_n \end{bmatrix} = \begin{bmatrix} u_{11} & u_{21} & \cdots & u_{n1} \\ u_{12} & u_{22} & \cdots & u_{n2} \\ \vdots & \vdots & \ddots & \vdots \\ u_{1n} & u_{2n} & \cdots & u_{nn} \end{bmatrix} \quad (2.11)$$

By defining a basis change as

$$x(t) = V \xi(t) \quad (2.12)$$

equation (2.1) becomes

$$\dot{\xi}(t) = V^{-1} A V \xi(t) \quad (2.13)$$

Or

$$\dot{\xi}(t) = \Lambda \xi(t) \quad (2.14)$$

where Λ is the diagonal matrix composed of the n eigenvalues of A .

The solution of this equation is,

$$\xi_i(t) = e^{\lambda_i t} \xi_i(0) \quad (2.15)$$

with

$$\xi(0) = U^T x(0) \quad (2.16)$$

Replacing (2.15) in (2.12) it becomes,

$$x(t) = V \begin{bmatrix} e^{\lambda_1 t} & 0 & \dots & 0 \\ 0 & e^{\lambda_2 t} & \dots & 0 \\ \vdots & \vdots & \ddots & \vdots \\ 0 & 0 & \dots & e^{\lambda_n t} \end{bmatrix} \xi(0) \quad (2.17)$$

Then, replacing the initial condition from (2.16),

$$x(t) = V \begin{bmatrix} e^{\lambda_1 t} & 0 & \dots & 0 \\ 0 & e^{\lambda_2 t} & \dots & 0 \\ \vdots & \vdots & \ddots & \vdots \\ 0 & 0 & \dots & e^{\lambda_n t} \end{bmatrix} U^T x(0) \quad (2.18)$$

In compact form thus,

$$x(t) = \left[\sum_{i=1}^n e^{\lambda_i t} v_i u_i^T \right] x(0) \quad (2.19)$$

The correspondent fundamental problem in sensitivity theory is to determine the sensitivities of λ_i , u_i and v_i to small changes in the elements of the matrix A .

If an element $[a_{kl}]$ in A matrix is perturbed due to changes in system parameters, then the eigenvalues and eigenvectors of A will change. Using (2.7) and (2.9),

$$u_i^T A v_i = \lambda_i u_i^T v_i$$

and considering that $u_i^T v_i = 1$, the partial differentiation of λ_i with respect to a_{kl} is,

$$\frac{\partial \lambda_i}{\partial a_{kl}} = \frac{\partial (u_i^T A v_i)}{\partial a_{kl}} \quad (2.20)$$

$$\frac{\partial \lambda_i}{\partial a_{kl}} = \frac{\partial u_i^T}{\partial a_{kl}} A v_i + u_i^T \frac{\partial (A v_i)}{\partial a_{kl}} \quad (2.21)$$

Developing the partial derivative of $A v_i$

$$\frac{\partial \lambda_i}{\partial a_{kl}} = \lambda_i \frac{\partial u_i^T}{\partial a_{kl}} v_i + u_i^T \left(\frac{\partial A}{\partial a_{kl}} v_i + A \frac{\partial v_i}{\partial a_{kl}} \right) \quad (2.22)$$

and organizing ,

$$\frac{\partial \lambda_i}{\partial a_{kl}} = \lambda_i \frac{\partial u_i^T}{\partial a_{kl}} v_i + u_i^T \frac{\partial A}{\partial a_{kl}} v_i + u_i^T A \frac{\partial v_i}{\partial a_{kl}} \quad (2.23)$$

it leads to,

$$\frac{\partial \lambda_i}{\partial a_{kl}} = u_i^T \frac{\partial A}{\partial a_{kl}} v_i + \lambda_i \frac{\partial u_i^T}{\partial a_{kl}} v_i + \lambda_i u_i^T \frac{\partial v_i}{\partial a_{kl}} \quad (2.24)$$

By reducing in terms of the partial derivative of $u_i^T v_i$ with respect to a_{kl} ,

$$\frac{\partial \lambda_i}{\partial a_{kl}} = u_i^T \frac{\partial A}{\partial a_{kl}} v_i + \lambda_i \frac{\partial (u_i^T v_i)}{\partial a_{kl}} \quad (2.25)$$

and, by definition, $u_i^T v_i = 1$ and its derivative is always 0, thus

$$\frac{\partial \lambda_i}{\partial a_{kl}} = u_i^T \frac{\partial A}{\partial a_{kl}} v_i \quad (2.26)$$

Partial derivative of A with respect to a_{kl} is zero for most of the elements except for a_{kl} , and equal to 1 for a_{kl} , which reduces (2.26) to the scalar (2.27)

$$\frac{\partial \lambda_i}{\partial a_{kl}} = u_{ik}^T v_{il} \quad (2.27)$$

Definition 2.1: Sensitivity matrices

The sensitivity matrices S_i are defined as the set of the partial derivatives of each eigenvalue λ_i with respect to the elements of the matrix A

$$S_i = \begin{bmatrix} \frac{\partial \lambda_i}{\partial a_{11}} & \frac{\partial \lambda_i}{\partial a_{12}} & \dots & \frac{\partial \lambda_i}{\partial a_{1n}} \\ \frac{\partial \lambda_i}{\partial a_{21}} & \frac{\partial \lambda_i}{\partial a_{22}} & \dots & \frac{\partial \lambda_i}{\partial a_{2n}} \\ \vdots & \vdots & \ddots & \vdots \\ \frac{\partial \lambda_i}{\partial a_{n1}} & \frac{\partial \lambda_i}{\partial a_{n2}} & \dots & \frac{\partial \lambda_i}{\partial a_{nn}} \end{bmatrix} = \begin{bmatrix} u_{i1} v_{i1} & u_{i1} v_{i2} & \dots & u_{i1} v_{in} \\ u_{i2} v_{i1} & u_{i2} v_{i2} & \dots & u_{i2} v_{in} \\ \vdots & \vdots & \ddots & \vdots \\ u_{in} v_{i1} & u_{in} v_{i2} & \dots & u_{in} v_{in} \end{bmatrix} = u_i v_i^T \quad (2.28)$$

Then the solution $x(t)$ can be expressed in terms of S_i

$$x(t) = \left[\sum_{i=1}^n e^{\lambda_i t} v_i u_i^T \right] x(0) = \left[\sum_{i=1}^n e^{\lambda_i t} S_i^T \right] x(0) \quad (2.29)$$

For every change in an element a_{kl} there will be a change in the eigenvalues of the model. This change can be linearly approximated by (Porter and Crossley 1972),

$$\lambda_i = \lambda_i + \frac{\partial \lambda_i}{\partial a_{kl}} \delta a_{kl} \quad (2.30)$$

where λ_i is the new value of a given eigenvalue and δ is the change of a_{kl} ,

For the stability problem, all the eigenvalues have to be in the open left side of the complex plane, which imposes,

$$\lambda_i + \frac{\partial \lambda_i}{\partial a_{kl}} \delta a_{kl} < 0 \quad (i = 1, 2, \dots, n) \quad (2.31)$$

For the case of conjugated complex eigenvalues it is known that the damping factor can be a restriction to an established ξ^* for some systems.

$$\frac{-\operatorname{real}\left(\lambda_i + \frac{\partial \lambda_i}{\partial a_{kl}} \delta a_{kl}\right)}{\sqrt{\operatorname{real}\left(\lambda_i + \frac{\partial \lambda_i}{\partial a_{kl}} \delta a_{kl}\right)^2 + \operatorname{Im}\left(\lambda_i + \frac{\partial \lambda_i}{\partial a_{kl}} \delta a_{kl}\right)^2}} < \xi^* \quad (2.32)$$

The solution of the free motion system equation (2.1)

$$x(t) = e^{At} x(0) \quad (2.33)$$

can be obtained by different methods depending on the way e^{At} is calculated (Moler and Van Loan 2003).

A function $f(A)$ of a matrix A can be defined as

$$f(A) = f(\lambda_1)Z_1 + \dots + f(\lambda_n)Z_n \quad (2.34)$$

where Z_i are the component matrices of A , assuming that A has n distinct eigenvalues. They are all related as,

$$\begin{cases} I = Z_1 + Z_2 + \dots + Z_n \\ A = \lambda_1 Z_1 + \lambda_2 Z_2 + \dots + \lambda_n Z_n \\ A^2 = \lambda_1^2 Z_1 + \lambda_2^2 Z_2 + \dots + \lambda_n^2 Z_n \\ \vdots \\ A^{n-1} = \lambda_1^{n-1} Z_1 + \lambda_2^{n-1} Z_2 + \dots + \lambda_n^{n-1} Z_n \end{cases} \quad (2.35)$$

Written in the form of a linear system,

$$\begin{bmatrix} I \\ A \\ \vdots \\ A^{n-1} \end{bmatrix} = \begin{bmatrix} 1 & 1 & \dots & 1 \\ \lambda_1 & \lambda_2 & \dots & \lambda_n \\ & \vdots & & \\ \lambda_1^{n-1} & \lambda_2^{n-1} & \dots & \lambda_n^{n-1} \end{bmatrix} \begin{bmatrix} Z_1 \\ Z_2 \\ \vdots \\ Z_n \end{bmatrix} \quad (2.36)$$

it shows up a Vandermonde type matrix which leads to

$$\begin{bmatrix} Z_1 \\ Z_2 \\ \vdots \\ Z_n \end{bmatrix} = \begin{bmatrix} 1 & 1 & \dots & 1 \\ \lambda_1 & \lambda_2 & \dots & \lambda_n \\ & \vdots & & \\ \lambda_1^{n-1} & \lambda_2^{n-1} & \dots & \lambda_n^{n-1} \end{bmatrix}^{-1} \begin{bmatrix} I \\ A \\ \vdots \\ A^{n-1} \end{bmatrix} \quad (2.37)$$

where the Vandermonde inverse matrix has been widely studied for different cases.

Then the exponential function of A is expressed by,

$$e^{At} = e^{\lambda_1 t} Z_1 + e^{\lambda_2 t} Z_2 + \dots + e^{\lambda_n t} Z_n \quad (2.38)$$

Hence the solution of the free-motion system can be expressed

$$x(t) = \sum_{i=1}^n e^{\lambda_i t} Z_i x(0) \quad (2.39)$$

This result is linked to the assumption that A has n distinct eigenvalues.

The matrices Z_i have similar properties to the sensitivity matrices S_i such as the sum of all matrices Z_i gives the identity matrix,

Property 2.1 The relation between both matrices is,

$$S_i^T = Z_i \quad (2.40)$$

In the particular case of repeated eigenvalues, it is not possible to obtain the solution, because the right and left eigen-matrices are not orthogonal.

For the solution of the system, a so-called “confluent” Vandermonde matrix can be used but is not related with the sensitivity of the eigenvalues.

2.3 Participation factors

The PF are used in the modal control theory better known as sensitivity analysis. Participation factors focus their application in electrical power systems in which having a prior knowledge of the system is recommendable. As it is mentioned in (I.J. Perez-Arriaga 1981) “*A crucial feature of the Dynamic stability problem (in the power systems context) and one that makes it particularly suitable for selective modal analysis (SMA), is that only a few, lightly damped, oscillatory modes are of interest, out of the hundreds of modes that the model may have*”. It is also said that the SMA is not restricted to any particular kind of physical systems but it is focused on electrical power systems.

Considered a linear system with distinct eigenvalues, as mentioned in (I.J. Perez-Arriaga et al. 1988) “*The term (PF) reflects the activity of the k^{th} state variable when the i^{th} mode (eigenvalue) is excited*”.

Definition 2.2 Participation factors (I.J. Perez-Arriaga, Verghese, and Schweppe 1982)

The participation factor (PF) matrix is defined as

$$P = \begin{bmatrix} \frac{\partial \lambda_1}{\partial a_{11}} & \frac{\partial \lambda_2}{\partial a_{11}} & \dots & \frac{\partial \lambda_n}{\partial a_{11}} \\ \frac{\partial \lambda_1}{\partial a_{22}} & \frac{\partial \lambda_2}{\partial a_{22}} & \dots & \frac{\partial \lambda_n}{\partial a_{22}} \\ \vdots & \vdots & \ddots & \vdots \\ \frac{\partial \lambda_1}{\partial a_{nn}} & \frac{\partial \lambda_2}{\partial a_{nn}} & \dots & \frac{\partial \lambda_n}{\partial a_{nn}} \end{bmatrix} = \begin{bmatrix} u_{11}v_{11} & u_{21}v_{21} & \dots & u_{n1}v_{n1} \\ u_{12}v_{12} & u_{22}v_{22} & \dots & u_{n2}v_{n2} \\ \vdots & \vdots & \ddots & \vdots \\ u_{1n}v_{1n} & u_{2n}v_{2n} & \dots & u_{nn}v_{nn} \end{bmatrix} \quad (2.41)$$

Remark:

It is assumed that A is diagonal dominant, and that all $a_{ij} \neq 0$, $\forall i, j = 1, 2, \dots, n$ (I.J. Perez-Arriaga, Verghese, and Schweppe 1982).

Properties of participation factors (Pagola, Perez-Arriaga, and Verghese 1989)

- a) The participation factors given by P_{ki} are not dependent on the units of the state variables.

- b) The sum of all elements by rows or by columns of P is 1.
- c) The PF represent the sensitivity of the eigenvalues λ_i to the diagonal elements a_{ii} ($i = 1, 2, \dots, n$) of the matrix A .
- d) For diagonal transformations, the numeric value of the PF does not change (to be presented later).

Definition 2.3: Solution of the free-motion system using participation factors (I.J. Perez-Arriaga, Verghese, and Schweppe 1982)

The approximated solution for the free-motion system is

$$x^*(t) = \begin{pmatrix} x_1^*(t) \\ \vdots \\ x_i^*(t) \\ \vdots \\ x_n^*(t) \end{pmatrix} \quad (2.42)$$

with,

$$x_i^*(t) = \begin{bmatrix} P_{1i} & P_{2i} & \dots & P_{ni} \end{bmatrix} \begin{bmatrix} e^{\lambda_1 t} \\ e^{\lambda_2 t} \\ \vdots \\ e^{\lambda_n t} \end{bmatrix} x_i^*(0) \quad (2.43)$$

considering $x_i(0) = 1$.

Remark:

This affirmation is only valid if A is diagonal dominant, as it will be shown in following examples.

The approximated solution for the i^{th} state variable is,

$$x_i^*(t) = \begin{bmatrix} \frac{\partial \lambda_1}{\partial a_{ii}} & \frac{\partial \lambda_2}{\partial a_{ii}} & \dots & \frac{\partial \lambda_n}{\partial a_{ii}} \end{bmatrix} \begin{bmatrix} e^{\lambda_1 t} \\ e^{\lambda_2 t} \\ \vdots \\ e^{\lambda_n t} \end{bmatrix} x_i^*(0) \quad (2.44)$$

to be compared with the complete solution of (2.29)

$$x_i(t) = \left[\left[\frac{\partial \lambda_1}{\partial a_{1i}} e^{\lambda_1 t} + \dots + \frac{\partial \lambda_n}{\partial a_{1i}} e^{\lambda_n t} \right] \dots \left[\frac{\partial \lambda_1}{\partial a_{ii}} e^{\lambda_1 t} + \dots + \frac{\partial \lambda_n}{\partial a_{ii}} e^{\lambda_n t} \right] \dots \left[\frac{\partial \lambda_1}{\partial a_{ni}} e^{\lambda_1 t} + \dots + \frac{\partial \lambda_n}{\partial a_{ni}} e^{\lambda_n t} \right] \right] \begin{bmatrix} x_1(0) \\ \vdots \\ x_i(0) \\ \vdots \\ x_n(0) \end{bmatrix} \quad (2.45)$$

The following example presents analytically the complete solution and the participation factors approximation.

Example 2.1 Consider the diagram in Figure 2.1 of a simple circuit with two resistances, one capacitor and one inductor.

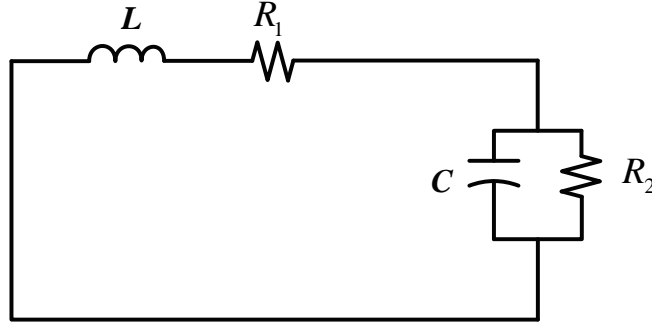


Figure 2.1 Circuit diagram.

The free response differential state equation is,

$$\begin{bmatrix} \dot{i}_L \\ \dot{v}_C \end{bmatrix} = \begin{bmatrix} a_{11} & a_{12} \\ a_{21} & a_{22} \end{bmatrix} \begin{bmatrix} i_L \\ v_C \end{bmatrix} \text{ or } \begin{bmatrix} \dot{i}_L \\ \dot{v}_C \end{bmatrix} = \begin{bmatrix} -\frac{R_1}{L} & -\frac{1}{L} \\ \frac{1}{C} & -\frac{1}{R_2 C} \end{bmatrix} \begin{bmatrix} i_L \\ v_C \end{bmatrix} \quad (2.46)$$

The eigenvalues of the model are,

$$\lambda_{1,2} = \frac{-(-a_{11} - a_{22}) \pm \left((-a_{11} - a_{22})^2 - 4(a_{11}a_{22} - a_{12}a_{21}) \right)^{\frac{1}{2}}}{2} \text{ or} \quad (2.47)$$

$$\lambda_{1,2} = \frac{-\left(\frac{R_1}{L} + \frac{1}{R_2 C} \right) \pm \left[\left(\frac{R_1}{L} + \frac{1}{R_2 C} \right)^2 - 4 \left(\frac{R_1}{R_2 CL} + \frac{1}{CL} \right) \right]^{\frac{1}{2}}}{2}$$

The sensitivity matrices of the second order model can be easily obtained using the partial derivatives,

$$S_1 = \begin{bmatrix} \frac{\partial \lambda_1}{\partial a_{11}} & \frac{\partial \lambda_1}{\partial a_{12}} \\ \frac{\partial \lambda_1}{\partial a_{21}} & \frac{\partial \lambda_1}{\partial a_{22}} \end{bmatrix} \quad S_2 = \begin{bmatrix} \frac{\partial \lambda_2}{\partial a_{11}} & \frac{\partial \lambda_2}{\partial a_{12}} \\ \frac{\partial \lambda_2}{\partial a_{21}} & \frac{\partial \lambda_2}{\partial a_{22}} \end{bmatrix} \quad (2.48)$$

which leads to the following expressions,

$$\frac{\partial \lambda_1}{\partial a_{11}} = \frac{1}{2} + \frac{1}{4} \left[\left(\frac{R_1}{L} + \frac{1}{R_2 C} \right)^2 - 4\alpha \right]^{-\frac{1}{2}} \left(\frac{2R_1}{L} - \frac{2}{R_2 C} \right) \quad (2.49)$$

$$\frac{\partial \lambda_1}{\partial a_{12}} = \left(\frac{1}{C} \right) \left[\left(\frac{R_1}{L} + \frac{1}{R_2 C} \right)^2 - 4\alpha \right]^{-1/2} \quad (2.50)$$

$$\frac{\partial \lambda_1}{\partial a_{21}} = - \left(\frac{1}{L} \right) \left[\left(\frac{R_1}{L} + \frac{1}{R_2 C} \right)^2 - 4\alpha \right]^{-1/2} \quad (2.51)$$

$$\frac{\partial \lambda_1}{\partial a_{22}} = \frac{1}{2} + \frac{1}{4} \left[\left(\frac{R_1}{L} + \frac{1}{R_2 C} \right)^2 - 4\alpha \right]^{-1/2} \left(\frac{2R_1}{L} - \frac{2}{R_2 C} \right) \quad (2.52)$$

$$\frac{\partial \lambda_2}{\partial a_{11}} = \frac{1}{2} - \frac{1}{4} \left[\left(\frac{R_1}{L} + \frac{1}{R_2 C} \right)^2 - 4\alpha \right]^{-1/2} \left(\frac{2R_1}{L} - \frac{2}{R_2 C} \right) \quad (2.53)$$

$$\frac{\partial \lambda_2}{\partial a_{12}} = - \left(\frac{1}{C} \right) \left[\left(\frac{R_1}{L} + \frac{1}{R_2 C} \right)^2 - 4\alpha \right]^{-1/2} \quad (2.54)$$

$$\frac{\partial \lambda_2}{\partial a_{21}} = \frac{1}{L} \left[\left(\frac{R_1}{L} + \frac{1}{R_2 C} \right)^2 - 4\alpha \right]^{-1/2} \quad (2.55)$$

$$\frac{\partial \lambda_2}{\partial a_{22}} = \frac{1}{2} - \frac{1}{4} \left[\left(\frac{R_1}{L} + \frac{1}{R_2 C} \right)^2 - 4\alpha \right]^{-1/2} \left(\frac{2R_1}{L} - \frac{2}{R_2 C} \right) \quad (2.56)$$

where

$$\alpha = \frac{R_1}{R_2 C L} + \frac{1}{C L} \quad (2.57)$$

Using the definition (2.29) for the solution of the second order model,

$$\begin{bmatrix} i_L \\ v_C \end{bmatrix} = \begin{bmatrix} \frac{\partial \lambda_1}{\partial a_{11}} e^{\lambda_1 t} + \frac{\partial \lambda_2}{\partial a_{11}} e^{\lambda_2 t} & \frac{\partial \lambda_1}{\partial a_{21}} e^{\lambda_1 t} + \frac{\partial \lambda_2}{\partial a_{21}} e^{\lambda_2 t} \\ \frac{\partial \lambda_1}{\partial a_{12}} e^{\lambda_1 t} + \frac{\partial \lambda_2}{\partial a_{12}} e^{\lambda_2 t} & \frac{\partial \lambda_1}{\partial a_{22}} e^{\lambda_1 t} + \frac{\partial \lambda_2}{\partial a_{22}} e^{\lambda_2 t} \end{bmatrix} \begin{bmatrix} i_L(0) \\ v_C(0) \end{bmatrix} \quad (2.58)$$

From (2.41) the participation factor matrix is,

$$P = \begin{bmatrix} \frac{\partial \lambda_1}{\partial a_{11}} & \frac{\partial \lambda_2}{\partial a_{11}} \\ \frac{\partial \lambda_1}{\partial a_{22}} & \frac{\partial \lambda_2}{\partial a_{22}} \end{bmatrix} \quad (2.59)$$

The approximated solution of the second order system according to the participation factors is,

$$\begin{bmatrix} i_L^* \\ v_c^* \end{bmatrix} = \begin{bmatrix} \left[\frac{\partial \lambda_1}{\partial a_{11}} e^{\lambda_1 t} + \frac{\partial \lambda_2}{\partial a_{11}} e^{\lambda_2 t} \right] i_L^*(0) \\ \left[\frac{\partial \lambda_1}{\partial a_{22}} e^{\lambda_1 t} + \frac{\partial \lambda_2}{\partial a_{22}} e^{\lambda_2 t} \right] v_c^*(0) \end{bmatrix} \quad (2.60)$$

where the initial conditions are equal to one for all state variables. In (2.60) the solution is composed of the diagonal elements of (2.58) which corresponds to the condition: A has to be diagonal dominant.

2.3.1 Change of basis

System state equations can have different representations depending on the choice of the state variables. However, the different representations of the equations do not change the intrinsic dynamics of the system.

Consider an arbitrary change of basis of matrix T , defined as

$$x(t) = T \cdot \tilde{x}(t) \quad (2.61)$$

It leads to a new form of state matrix A as

$$\tilde{A} = T^{-1} A T \quad (2.62)$$

Consider the transformation matrix T diagonal as

$$T = \begin{bmatrix} t_{11} & 0 & \cdots & 0 \\ 0 & t_{22} & \cdots & 0 \\ \vdots & \vdots & \ddots & \vdots \\ 0 & 0 & \cdots & t_{nn} \end{bmatrix} \quad (2.63)$$

The autonomous model represented by (2.1) and (2.2), becomes after basis change

$$\begin{bmatrix} \dot{\tilde{x}}_1(t) \\ \dot{\tilde{x}}_2(t) \\ \vdots \\ \dot{\tilde{x}}_n(t) \end{bmatrix} = \begin{bmatrix} a_{11} & t_{22} t_{11}^{-1} a_{12} & \cdots & t_{nn} t_{11}^{-1} a_{1n} \\ t_{11} t_{22}^{-1} a_{21} & a_{22} & \cdots & t_{nn} t_{22}^{-1} a_{2n} \\ \vdots & \vdots & \ddots & \vdots \\ t_{11} t_{nn}^{-1} a_{n1} & t_{22} t_{nn}^{-1} a_{n2} & \cdots & a_{nn} \end{bmatrix} \begin{bmatrix} \tilde{x}_1(t) \\ \tilde{x}_2(t) \\ \vdots \\ \tilde{x}_n(t) \end{bmatrix} \quad (2.64)$$

The linear transformation using (2.61) does not change the diagonal elements in (2.64). Therefore, the participation factor approximation does not change in the case of a diagonal transformation matrix.

A particular case of diagonal basis change will be discussed in the next section.

2.3.2 Per-unit representation

In power system analysis, it is usually convenient to use a per-unit model to normalize system units. Compared to the use of physical units (amperes, volts, ohms, webers, henrys,

etc.), the per-unit system offers computational simplicity by eliminating units and expressing system quantities as dimensionless ratios.

A well-chosen per-unit system can minimize computational effort, simplify evaluation and facilitate understanding of the characteristics. Some base quantities may be chosen independently and quite arbitrary, while others follow automatically depending on fundamental relationships between system variables. Normally, the base values are chosen so that the principal variables still be equal to one per-unit under the nominal condition.

The general representation can be,

$$\text{quantity in per unit} = \frac{\text{actual quantity}}{\text{base value of quantity}} \quad (2.65)$$

In a power electrical system, there are some relations for the common variables in the system and the choice of the base values is commonly as,

- P_b : power base,
- V_b : voltage base generally chosen as the nominal voltage of the electrical network under analysis.
- i_b : current base, related to the power base and voltage base defined as

$$i_b = \frac{P_b}{V_b} \quad (2.66)$$

- R_b : resistance base, calculated as,

$$R_b = \frac{V_b}{i_b} \quad (2.67)$$

- f_b : frequency base

This per-unit representation is very useful for simple variables like voltages and currents. However, with energy storage elements there are different units for the different energy domains. The DC case is only developed here.

Energy at the nominal point of operation can be chosen as base variable, using the normalized time constant H , defined for the mechanical inertia in (Kundur 2007) as

$$H(\text{seconds}) = \frac{\text{Kinetic co-energy in watts-seconds}}{P_b \text{ in watts}} \quad (2.68)$$

For example in rotatory machines, H is defined as,

$$H(\text{seconds}) = \frac{\frac{1}{2}(\text{moment of inertia})(\text{angular velocity})^2}{P_b} \quad (2.69)$$

For the DC elements, this constant is extended using the stored co-energy in inductors and capacitors.

For inductors this normalized constant is described as,

$$H_L = \frac{\frac{1}{2}L(i_b^2)}{P_b} \quad (2.70)$$

where L is the inductance value in henrys.

For the capacitances,

$$H_C = \frac{\frac{1}{2}C(V_b^2)}{P_b} \quad (2.71)$$

where the C is the capacitance value in Farads. H_C and H_L are in seconds.

- *Example of per unit representation for the DC circuits*

For the circuit presented in Figure 2.1, the state equation is(2.46),

$$\begin{bmatrix} \dot{i}_L \\ \dot{v}_C \end{bmatrix} = \begin{bmatrix} -\frac{R1}{L} & -\frac{1}{L} \\ \frac{1}{C} & -\frac{1}{R2C} \end{bmatrix} \begin{bmatrix} i_L \\ v_C \end{bmatrix}$$

The per unit representation of the capacitance and inductance are,

$$L = \frac{2H_L P_b}{i_b^2} \quad (2.72)$$

$$C = \frac{2H_C P_b}{V_b^2} \quad (2.73)$$

Substituting (2.72) in the first state equation in (2.46) gives,

$$\frac{2H_L P_b}{i_b^2} \left(\frac{di_L}{dt} \right) = -R1i_L - v_C \quad (2.74)$$

Rearranging, it yields,

$$2H_L \frac{d}{dt} \left(\frac{i_L}{i_b} \right) = \frac{-R1i_L - v_C}{\frac{P_b}{i_b}} \quad (2.75)$$

or

$$2H_L \frac{d}{dt} \left(\frac{i_L}{i_b} \right) = \left(\frac{-R1}{\frac{V_b}{i_b}} \right) \left(\frac{i_L}{i_b} \right) - \frac{v_C}{\frac{V_b i_b}{i_b}} \quad (2.76)$$

From the definitions of per-unit variables,

$$2H_L \frac{di_{L \text{ pu}}}{dt} = -R_{1 \text{ pu}} i_{L \text{ pu}} - v_{C \text{ pu}} \quad (2.77)$$

rearranging

$$\frac{di_{L \text{ pu}}}{dt} = \frac{-R_{1 \text{ pu}}}{2H_L} i_{L \text{ pu}} - \frac{1}{2H_L} v_{C \text{ pu}} \quad (2.78)$$

For the second differential equation, using equation (2.73) it gives,

$$\frac{2H_C P_b}{V_b^2} \left(\frac{dv_C}{dt} \right) = i_L - \frac{v_C}{R2} \quad (2.79)$$

Rearranging, it yields,

$$2H_C \left(\frac{dv_C}{dt} \right) = \frac{i_L - \frac{v_C}{R2}}{\frac{P_b}{V_b^2}} \quad (2.80)$$

$$2H_C \frac{d}{dt} \left(\frac{v_C}{V_b} \right) = \frac{i_L}{\frac{V_b i_b}{V_b}} - \left(\frac{v_C}{V_b} \right) \frac{R2}{\frac{i_b}{V_b}} \quad (2.81)$$

simplifying using the definitions of the per-unit values,

$$2H_C \frac{dv_{C \text{ pu}}}{dt} = i_{L \text{ pu}} - v_{C \text{ pu}} \frac{1}{R2_{\text{pu}}} \quad (2.82)$$

rearranging

$$\frac{d}{dt} \left(\frac{v_C}{V_b} \right) = \frac{i_{L \text{ pu}}}{2H_C} - v_{C \text{ pu}} \frac{1}{R2_{\text{pu}} 2H_C} \quad (2.83)$$

The system state equation (2.46) becomes in the new basis

$$\begin{bmatrix} \dot{i}_{L \text{ pu}} \\ \dot{v}_{C \text{ pu}} \end{bmatrix} = \begin{bmatrix} -\frac{R_{1 \text{ pu}}}{2H_L} & -\frac{1}{2H_L} \\ \frac{1}{2H_C} & -\frac{1}{R2_{\text{pu}} 2H_C} \end{bmatrix} \begin{bmatrix} i_{L \text{ pu}} \\ v_{C \text{ pu}} \end{bmatrix} \quad (2.84)$$

The transformation matrix T is,

$$T = \begin{bmatrix} i_b & 0 \\ 0 & V_b \end{bmatrix} \quad (2.85)$$

It is worth showing that the diagonal terms given here in pu have unchanged values

Remarks of the change of basis

This per unit representation is a common practice for the analysis and modeling of power electrical systems and particularly in the case of modal analysis.

When the per-unit representation is performed, the energy storage element parameters of the system have to be changed to a common unit.

Linear transformations using diagonal transformation matrices do not change the numerical value of the diagonal terms in the matrices and the eigenvalues of the matrix are the same in the per-unit system and the original one.

Moreover, the use of the PF in transformed pu models does not change its conclusions.

2.4 Usage and interpretation of sensitivity matrices and participation factors

The sensitivity matrices are a tool used for modal analysis. Their development responds to two objectives (Porter and Crossley 1972),

- i. The selection of system parameters such as the eigenvalues and their associated eigenvectors be as insensitive as possible to changes in such parameters.
- ii. The determination of good approximations of the eigenvalues and eigenvectors associated with various system components, without having to compute all the eigenvalues and eigenvectors.

Participation factor theory was developed to understand and reduce models with uncoupled dynamics; its use in the selective modal analysis is well justified and understood as presented in section 2.2.

The use of participation factors has changed since its first definition. For example in (Arabi et al. 1991), the PF matrix is used to show how important is a state variable for the eigenvalues or how important the eigenvalue is for the state variable. In (Hsu and Chen 1987) and (Ignacio J. Perez-Arriaga et al. 1990) they are used for the identification of the best location for stabilizers.

In both cases, for the PF theory to be applied some assumptions have to be verified. The following examples will present some cases where this approach can suffer of a lack of precision.

- *Example 2.2: RLC circuit: time response and participation factor approximation*

Three cases are considered with different values for the element parameters. In the first case, the values are chosen in order to have real eigenvalues with a non-diagonal dominant matrix. In the second case, the eigenvalues are complex and the state matrix is non-diagonal dominant. In the third one the values are chosen to have complex eigenvalues and diagonal dominant matrix. As outputs, the selected states are the current in the inductance and the voltage in the capacitor.

Case 1; Real eigenvalues, A non-diagonal dominant

Table 2.1 Parameters of the circuit

Parameter	Value	Parameter	Value
L	2 mH	C	1 μF
R_1	10 Ω	R_2	100 Ω

The free motion system is,

$$\begin{bmatrix} \dot{i}_L \\ \dot{v}_C \end{bmatrix} = \begin{bmatrix} -5000 & -500 \\ 10000 & -100 \end{bmatrix} \begin{bmatrix} i_L \\ v_C \end{bmatrix} \quad (2.86)$$

The eigenvalues are,

$$\lambda_1 = -3551.2 \quad \lambda_2 = -1548.7 \quad (2.87)$$

The modal matrices are,

$$V = \begin{bmatrix} -0.32 & 0.14 \\ 0.94 & -0.98 \end{bmatrix} \quad U = \begin{bmatrix} -5.28 & -5.04 \\ -0.75 & -1.74 \end{bmatrix} \quad (2.88)$$

Thus, the sensitivity matrices are,

$$S_1 = \begin{bmatrix} 1.7235 & -4.993 \\ 0.2497 & -0.7235 \end{bmatrix} \quad S_2 = \begin{bmatrix} -0.7235 & 4.993 \\ -0.2497 & 1.7235 \end{bmatrix} \quad (2.89)$$

The participation factor matrix is,

$$\begin{bmatrix} i_L \\ v_C \end{bmatrix} P = \begin{bmatrix} 1.72 & -0.72 \\ -0.72 & 1.72 \end{bmatrix} \quad (2.90)$$

Using the per-unit representation for DC circuits presented in (2.84) the transformed system has the same eigenvalues. Table 2.2 presents the base values for the transformation.

Table 2.2 Per unit base parameters

Parameter	Value
P_b	50 Watts
V_b	10 volts

The per unit representation is,

$$\begin{bmatrix} \dot{i}_{L \text{ pu}} \\ \dot{v}_{C \text{ pu}} \end{bmatrix} = \begin{bmatrix} -5000 & -1000 \\ -5000 & -100 \end{bmatrix} \begin{bmatrix} i_{L \text{ pu}} \\ v_{C \text{ pu}} \end{bmatrix} \quad (2.91)$$

The modal matrices for the per-unit base are,

$$V_{pu} = \begin{bmatrix} -0.56 & 0.27 \\ 0.82 & -0.96 \end{bmatrix} \quad U_{pu} = \begin{bmatrix} -3.03 & -2.59 \\ -0.87 & -1.79 \end{bmatrix} \quad (2.92)$$

thus, the sensitivity matrices are,

$$S_{1pu} = \begin{bmatrix} 1.7235 & -2.4969 \\ 0.4994 & -0.7235 \end{bmatrix} \quad S_{2pu} = \begin{bmatrix} -0.7235 & 2.4969 \\ -0.4994 & 1.7235 \end{bmatrix} \quad (2.93)$$

The participation factor matrix is unchanged as

$$\begin{matrix} & \boxed{\lambda_1 \quad \lambda_2} \\ \begin{bmatrix} i_{L_{pu}} \\ v_{C_{pu}} \end{bmatrix} P_{pu} = & \begin{bmatrix} 1.72 & -0.72 \\ -0.72 & 1.72 \end{bmatrix} \end{matrix} \quad (2.94)$$

From the elements in (2.94) it appears that the most important state for λ_1 is the current (in pu) in the inductance L and the most important state for λ_2 is the voltage in C .

To validate this statement free response approximated by the PF given in (2.60) has to be compared with the complete free response of equation (2.58).

The approximated free response solution using (2.60) is,

$$\begin{bmatrix} i_{L_{pu}}^*(t) \\ v_{C_{pu}}^*(t) \end{bmatrix} = \begin{bmatrix} \left[1.72e^{(-3551.2)t} - 0.72e^{(-1548.7)t} \right] i_{L_{pu}}^*(0) \\ \left[-0.72e^{(-3551.2)t} + 1.72e^{(-1548.7)t} \right] v_{C_{pu}}^*(0) \end{bmatrix} \quad (2.95)$$

The complete free response solution using (2.58) is

$$\begin{bmatrix} i_{L_{pu}}(t) \\ v_{C_{pu}}(t) \end{bmatrix} = \begin{bmatrix} 1.72e^{\lambda_1 t} - 0.72e^{\lambda_2 t} & 0.49e^{\lambda_1 t} - 0.49e^{\lambda_2 t} \\ -2.49e^{\lambda_1 t} + 2.49e^{\lambda_2 t} & -0.72e^{\lambda_1 t} + 1.72e^{\lambda_2 t} \end{bmatrix} \begin{bmatrix} i_{L_{pu}}(0) \\ v_{C_{pu}}(0) \end{bmatrix} \quad (2.96)$$

A comparison between the two solutions (2.95) and (2.96) is presented in Figure 2.2. The initial conditions are set to 1 ampere and 1 volt

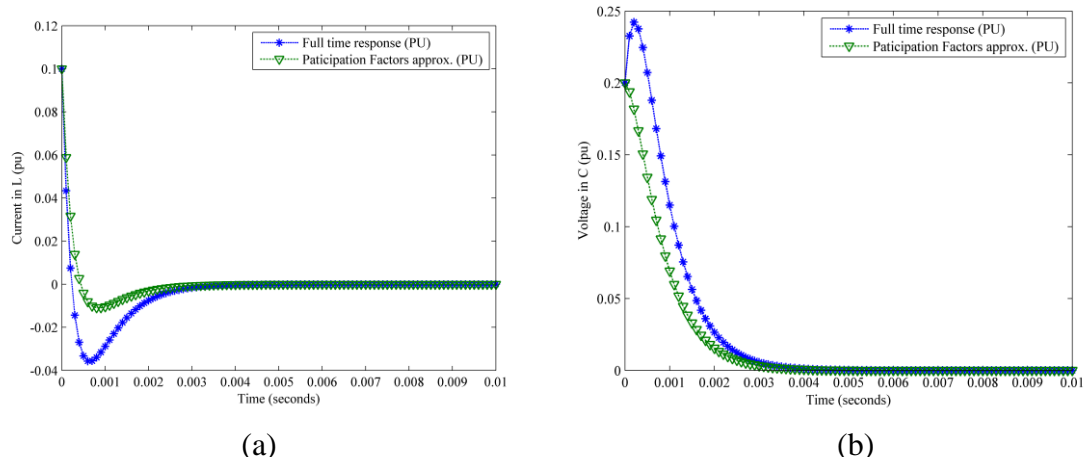


Figure 2.2 Current in L (a) and voltage in C (b).

Note the difference in the time responses and the peak amplitude.

Case 2; Complex conjugated eigenvalues, A non-diagonal dominant.

Table 2.3 Changes in the parameters.

Parameter	Value	Parameter	Value
L	2 mH	C	1×10^{-4} Farads
R1	1 Ohms	R2	100 Ohms

The per-unit representation is,

$$\begin{bmatrix} \dot{i}_{L_{pu}} \\ \dot{v}_{C_{pu}} \end{bmatrix} = \begin{bmatrix} -5000 & -100 \\ 50000 & -100 \end{bmatrix} \begin{bmatrix} i_{L_{pu}} \\ v_{C_{pu}} \end{bmatrix} \quad (2.97)$$

and the eigenvalues are,

$$\lambda_1 = -255 + 663.3i \quad \lambda_2 = -255 - 663.3i \quad (2.98)$$

The participation factor matrix is,

$$\begin{bmatrix} i_{L_{pu}} \\ v_{C_{pu}} \end{bmatrix} P_{pu} = \begin{bmatrix} 0.5 + 0.04i & 0.5 - 0.04i \\ 0.5 - 0.04i & 0.5 + 0.04i \end{bmatrix} \quad (2.99)$$

It is natural to have complex PF if the eigenvalues are complex. These complex values have no meaning for the analysis (I.J. Perez-Arriaga 1981), and it is a common practice to use the modulus of the complex numbers.

$$|P_{kl}| = \sqrt{\text{real}(P_{kl})^2 + \text{imaginary}(P_{kl})^2} \quad (2.100)$$

Using (2.100) in (2.99) yields

$$\begin{matrix} \lambda_1 & \lambda_2 \\ \begin{bmatrix} i_{L_{pu}} \\ v_{C_{pu}} \end{bmatrix} | P_{pu} | = \begin{bmatrix} 0.5020 & 0.5020 \\ 0.5020 & 0.5020 \end{bmatrix} \end{matrix} \quad (2.101)$$

It can be seen that (2.101) is not normalized.

The problematics of interpretation of the complex elements in the PF has been explored in (Abed, Hassouneh, and Hashlamoun 2009), where an extension of the definition is proposed for PF with complex elements.

The free response is (initial conditions are set to 1 ampere and 1 volt),

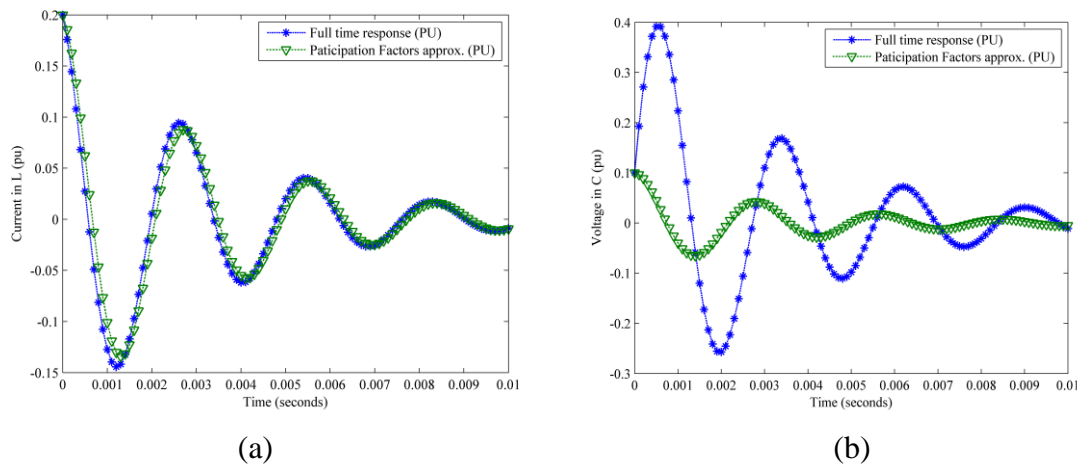


Figure 2.3 Response with complex eigenvalues

In this case the oscillatory response due to the complex eigenvalues is noticeable. The response for the voltage presents a difference with the PF approximation.

Case 3; Conjugated complex eigenvalues, diagonal dominant.

Table 2.4 Parameters

Parameter	Value	Parameter	Value
L	1 mH	C	1 mF
R_1	10 Ω	R_2	0.1 Ω

The system equations are

$$\begin{bmatrix} \dot{i}_L \\ \dot{v}_C \end{bmatrix} = \begin{bmatrix} -10000 & -1000 \\ 1000 & -10000 \end{bmatrix} \begin{bmatrix} i_L \\ v_C \end{bmatrix} \quad (2.102)$$

The participation factor matrix is,

$$\begin{matrix} & \boxed{\begin{matrix} \lambda_1 & \lambda_2 \end{matrix}} \\ \boxed{\begin{matrix} i_L \\ v_C \end{matrix}} P = \begin{bmatrix} 0.5 & 0.5 \\ 0.5 & 0.5 \end{bmatrix} \end{matrix} \quad (2.103)$$

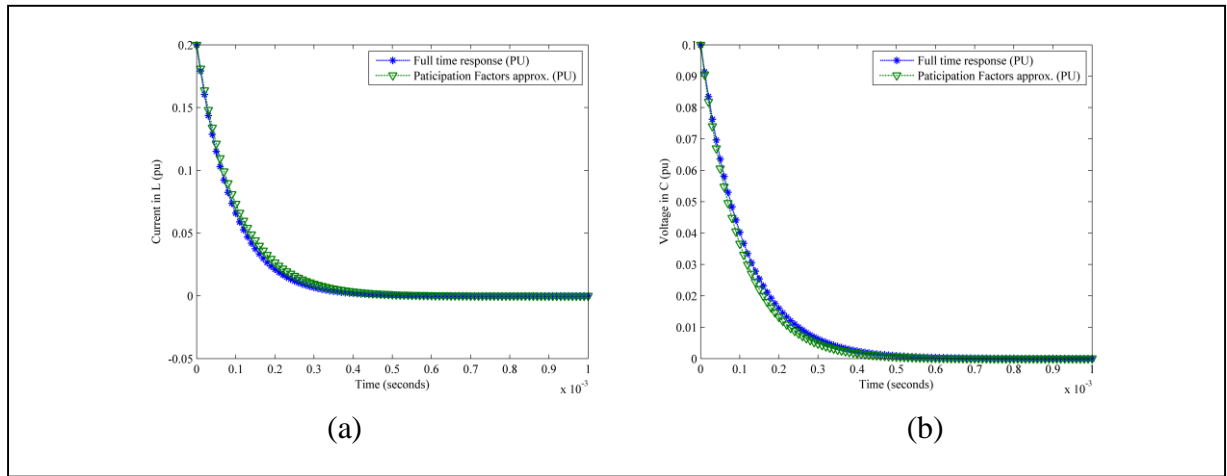
The per-unit representation is,

$$\begin{bmatrix} \dot{i}_{L\ pu} \\ \dot{v}_{C\ pu} \end{bmatrix} = \begin{bmatrix} -10000 & -2000 \\ 500 & -10000 \end{bmatrix} \begin{bmatrix} i_{L\ pu} \\ v_{C\ pu} \end{bmatrix} \quad (2.104)$$

Since they are equivalent systems, the eigenvalues for both representations are,

$$\lambda_1 = -10000 + 1000i \quad \lambda_2 = -10000 - 1000i \quad (2.105)$$

The time response is given in Figure 2.4. and the initial conditions are set to 1 ampere and 1



volt

Figure 2.4 Diagonal dominant response in pu.

Figure 2.4 shows that the approximation of the PF is close to the complete response.

Gershgorin theorem (Gershgorin 1931; D. Meyer and Veselić 1980), defines inclusion and exclusion regions for the location of the eigenvalues of a given matrix A .

A Gershgorin circle C_i drawn in the complex plane is centered in each a_{ii} -term of A , and

has a radius $R_i = \sum_{\substack{j=1 \\ j \neq i}}^n |a_{ij}|$.

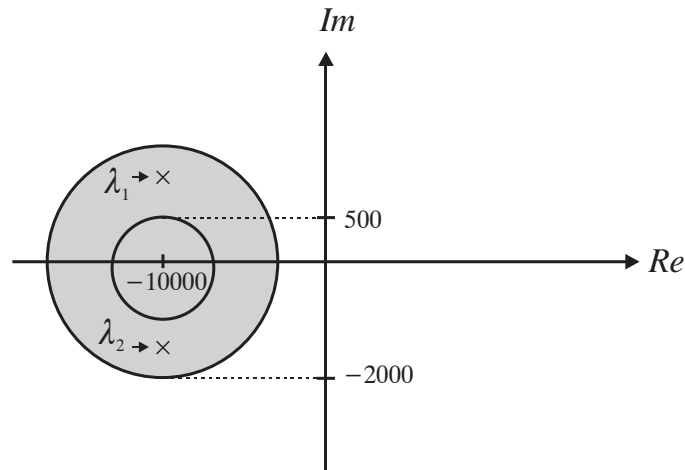


Figure 2.5 Gershgorin circles for equation (2.104).

The circles in Figure 2.5 corresponds to the inclusion region containing all eigenvalues.

When the system matrix is diagonal dominant, such regions of inclusion is relatively “small” and each of them can enclose are eigenvalue (Quarteroni, Sacco, and Saleri 2007; Varga 2000).

A diagonal basis change changes the radius of circles only.

2.5 Conclusions

The use of participation factors has to face some limitations as diagonal dominance the biggest restriction.

The didactic simple example was aimed at showing up the imprecisions involved in some cases where the limitation was not respected.

The role of the basis change has been discussed, and particularly in the case of per-unit representation.

Chapter 3 Sensitivity analysis

3.1 Introduction

The sensitivity analysis responds to the fundamental eigen-problem associated with the behavior of linear systems. Such problem relating changes in element parameters has been studied by numerous authors since the early work of Carl Gustav Jacob Jacobi (Jacobi 1856).

Parametric sensitivity analysis is used for the analysis of power electrical systems as in (Smed 1993) and (D'Arco, Suul, and Fosso 2014b). In (Smed 1993) a “new sensitivity analysis” is proposed, where the main purpose is to analyze large power systems. This methodology is used for the analysis of constrain of active and reactive modulation for a generator, analysis of static VAR compensators and the static model of a HVDC link.

More recently a workgroup in Norway has applied the parametric sensitivity analysis to the analysis of virtual synchronous machine (D'Arco, Suul, and Fosso 2015) for the control scheme voltage source converter (SCV) based HVDC grids (D'Arco, Suul, and Molinas 2014). This analysis deals with the sensitivity of the “most critical poles” A drawback of this methodology is that the parametric analysis is performed comparing elements with different units.

3.2 New definition of parametric sensitivity matrix

The analysis of electrical systems and electrical machinery using participation factors principally relates the state variables to the eigenvalues. However, as shown in the previous sections, there are some assumptions and limitations.

The objective of this section is to present a new form of sensitivity matrix relating the change in the eigenvalues with respect to the parameters.

Consider a model with n distinct eigenvalues and suppose that m parameters β_j ($\forall j = 1, 2, \dots, m$) could change.

The sensitivity of a given eigenvalue λ_i due to changes in the matrix elements is calculated as

$$S_i = \begin{bmatrix} \frac{\partial \lambda_i}{\partial a_{11}} & \frac{\partial \lambda_i}{\partial a_{12}} & \dots & \frac{\partial \lambda_i}{\partial a_{1n}} \\ \frac{\partial \lambda_i}{\partial a_{21}} & \frac{\partial \lambda_i}{\partial a_{22}} & \dots & \frac{\partial \lambda_i}{\partial a_{2n}} \\ \vdots & \vdots & \ddots & \vdots \\ \frac{\partial \lambda_i}{\partial a_{n1}} & \frac{\partial \lambda_i}{\partial a_{n2}} & \dots & \frac{\partial \lambda_i}{\partial a_{nn}} \end{bmatrix} \quad (i = 1, 2, \dots, m) \quad (3.1)$$

Each element of S_i is the sensitivity of the eigenvalue λ_i to an element of matrix A . Here we propose to consider the sensitivity of the eigenvalues to the physical parameters of the system.

Consider a small change in the parameter β_j . Then the change in the eigenvalue λ_i can be approximated by,

$$\delta\lambda_i \approx \frac{\partial\lambda_i}{\partial\beta_j} \delta\beta_j \quad (3.2)$$

The partial derivative in (3.2) of an eigenvalue with respect to the parameter β_j is,

$$\frac{\partial\lambda_i}{\partial\beta_j} = \frac{\partial\lambda_i}{\partial a_{11}} \frac{\partial a_{11}}{\partial\beta_j} + \dots + \frac{\partial\lambda_i}{\partial a_{kl}} \frac{\partial a_{kl}}{\partial\beta_j} + \dots + \frac{\partial\lambda_i}{\partial a_{mm}} \frac{\partial a_{mm}}{\partial\beta_j} \quad \text{for all } k, l, i = 1, 2, \dots, n \quad (3.3)$$

Using equation(2.27), it leads to

$$\frac{\partial\lambda_i}{\partial a_{kl}} \frac{\partial a_{kl}}{\partial\beta_j} = u_{ik} v_{il} \frac{\partial a_{kl}}{\partial\beta_j} \quad (3.4)$$

We propose the following definition of a new sensitivity matrix of the eigenvalues with respect to a parameter.

Definition 3.1: Consider a system model with n distinct eigenvalues and suppose that m parameters could change. The following matrix called Parametric Sensitivity Matrix (PSM) is proposed, containing by rows the sensitivity of each eigenvalue to one parameter β_j $j = 1, 2, \dots, m$.

$$Sp = \begin{bmatrix} \frac{\partial\lambda_1}{\partial\beta_1} & \frac{\partial\lambda_2}{\partial\beta_1} & \frac{\partial\lambda_3}{\partial\beta_1} & \dots & \frac{\partial\lambda_n}{\partial\beta_1} \\ \vdots & \vdots & \vdots & \dots & \vdots \\ \frac{\partial\lambda_1}{\partial\beta_j} & \frac{\partial\lambda_2}{\partial\beta_j} & \frac{\partial\lambda_3}{\partial\beta_j} & \dots & \frac{\partial\lambda_n}{\partial\beta_j} \\ \vdots & \vdots & \vdots & \dots & \vdots \\ \frac{\partial\lambda_1}{\partial\beta_m} & \frac{\partial\lambda_2}{\partial\beta_m} & \frac{\partial\lambda_3}{\partial\beta_m} & \dots & \frac{\partial\lambda_n}{\partial\beta_m} \end{bmatrix} \quad (3.5)$$

The organization of the parameters and the eigenvalues can help to understand the results. We recommend having a prior knowledge of the dynamics and the characteristics of the system to help in this organization task.

- *Repeated eigenvalues*

Parametric sensitivity matrix (PSM) is based on the hypothesis of distinct eigenvalues. The case of repeated eigenvalues is problematic, However, there are some alternatives for the numeric calculation of the partial derivatives in the matrix Sp .

As presented in (Paraskevopoulos, Tsonis, and Tzafestas 1974), the characteristic polynomial helps to calculate the different sensitivities. With higher order systems this methodology can be difficult to implement. Alden and Qureshy in 1985 presented a second order approximation of the sensitivity for the repeated eigenvalues. This approximated value can help but it is difficult to prove its efficacy.

More recently, the use of parametric sensitivity for mechanical damped systems has brought the problem of the calculation of eigenvalue sensitivities when there are repeated eigenvalues. In (Choi et al. 2004) adjacent eigenvectors and orthonormal conditions are used to compose an algebraic equation. The algebraic equation developed can be used to compute derivatives of eigenvalues and eigenvectors. In (Li et al. 2013) a normalization of the eigenvalues is proposed as a first step to find the sensitivities; then a particular numeric solution is proposed, under the assumption of a damped system. In both cases the fact that the system is damped helps to make assumptions for the solution.

This problematics of repeated eigenvalues is not solved yet for this thesis. It is important to assure always if the analyzed model has distinct eigenvalues for the use of the PSM.

3.2.1 Example 3.1: Simple Circuit sensitivity of the eigenvalues to the elements

Considering the circuit in Figure 2.1, the objective is to find the sensitivity of the eigenvalues to the parameters L and C

The matrix of the model given in (2.46),

$$\begin{bmatrix} \dot{i}_L \\ \dot{v}_C \end{bmatrix} = \begin{bmatrix} -\frac{R_1}{L} & -\frac{1}{L} \\ \frac{1}{C} & -\frac{1}{R_2 C} \end{bmatrix} \begin{bmatrix} i_L \\ v_C \end{bmatrix}$$

The eigenvalues are,

$$\lambda_{1,2} = \frac{(a_{11} + a_{22}) \pm \left[(-a_{11} - a_{22})^2 - 4(a_{11}a_{22} - a_{12}a_{21}) \right]^{1/2}}{2}$$

or

$$\lambda_{1,2} = \frac{-\left(\frac{R_1}{L} + \frac{1}{R_2 C}\right) \pm \left[\left(\frac{R_1}{L} + \frac{1}{R_2 C}\right)^2 - 4\left(\frac{R_1}{R_2 CL} + \frac{1}{CL}\right) \right]^{1/2}}{2}$$

The sensitivity of λ_1 with respect to L calculated directly is

$$\frac{\partial \lambda_1}{\partial L} = \frac{R_1}{2L^2} + \left[\left(\frac{R_1}{L} + \frac{1}{R_2 C}\right)^2 - 4\left(\frac{R_1}{R_2 CL} + \frac{1}{CL}\right) \right]^{-1/2} \left(\frac{1}{CL^2} - \frac{R_1^2}{2L^3} + \frac{R_1}{2R_2 CL^2} \right) \quad (3.6)$$

It can also be derived using equation (3.3)

$$\frac{\partial \lambda_1}{\partial L} = \frac{\partial \lambda_1}{\partial a_{11}} \frac{\partial a_{11}}{\partial L} + \frac{\partial \lambda_1}{\partial a_{12}} \frac{\partial a_{12}}{\partial L} + \frac{\partial \lambda_1}{\partial a_{21}} \frac{\partial a_{21}}{\partial L} + \frac{\partial \lambda_1}{\partial a_{22}} \frac{\partial a_{22}}{\partial L} \quad (3.7)$$

Thus, the sensitivity of λ_2 to L is,

$$\frac{\partial \lambda_2}{\partial L} = \frac{R_1}{2L^2} + \left[\left(\frac{R_1}{L} + \frac{1}{R_2 C} \right)^2 - 4 \left(\frac{R_1}{R_2 CL} + \frac{1}{CL} \right) \right]^{-1/2} \left(\frac{R_1^2}{2L^3} - \frac{R_1}{2R_2 CL^2} - \frac{1}{CL^2} \right) \quad (3.8)$$

In this second order system, the sensitivities are easy to derive, but it becomes more difficult for higher order models.

From the sensitivity matrix S_i ($i = 1, \dots, n$) in terms of the eigenvalues, (from equation 2.28)

$$S_1 = \begin{bmatrix} \frac{\partial \lambda_1}{\partial a_{11}} & \frac{\partial \lambda_1}{\partial a_{12}} \\ \frac{\partial \lambda_1}{\partial a_{21}} & \frac{\partial \lambda_1}{\partial a_{22}} \end{bmatrix} = \begin{bmatrix} u_{11}v_{11} & u_{11}v_{12} \\ u_{12}v_{11} & u_{12}v_{12} \end{bmatrix} \quad (3.9)$$

$$S_2 = \begin{bmatrix} \frac{\partial \lambda_2}{\partial a_{11}} & \frac{\partial \lambda_2}{\partial a_{12}} \\ \frac{\partial \lambda_2}{\partial a_{21}} & \frac{\partial \lambda_2}{\partial a_{22}} \end{bmatrix} = \begin{bmatrix} u_{21}v_{21} & u_{21}v_{22} \\ u_{22}v_{21} & u_{22}v_{22} \end{bmatrix}$$

it gives

$$\frac{\partial \lambda_2}{\partial L} = u_{21}v_{21} \frac{\partial a_{11}}{\partial L} + u_{21}v_{22} \frac{\partial a_{12}}{\partial L} \quad (3.10)$$

Using Definition 3.1, the sensitivity matrix with respect to L and C is derived as,

$$Sp = \begin{bmatrix} \frac{\partial \lambda_1}{\partial L} & \frac{\partial \lambda_2}{\partial L} \\ \frac{\partial \lambda_1}{\partial C} & \frac{\partial \lambda_2}{\partial C} \end{bmatrix} = \begin{bmatrix} u_{11}v_{11} \frac{\partial a_{11}}{\partial L} + u_{11}v_{12} \frac{\partial a_{12}}{\partial L} & u_{21}v_{21} \frac{\partial a_{11}}{\partial L} + u_{21}v_{22} \frac{\partial a_{12}}{\partial L} \\ u_{12}v_{11} \frac{\partial a_{21}}{\partial C} + u_{12}v_{12} \frac{\partial a_{22}}{\partial C} & u_{22}v_{21} \frac{\partial a_{21}}{\partial C} + u_{22}v_{22} \frac{\partial a_{22}}{\partial C} \end{bmatrix} \quad (3.11)$$

It can be derived in analytical form. This clearly reduces the complexity of deriving the analytical expressions of the eigenvalues directly.

The objective is to compare the contribution of each term of the PSM.

The PSM shows up several properties:

- It is not normalized
- It is unit dependent
- There is no restriction of diagonal dominance matrices.

It is possible to measure the sensitivity of the eigenvalues to any parameter in matrix A (explicit or implicit)

Since the PSM is unit dependent, each element in the matrix can be any real or complex number. Comparing the contributions of the parameter to the eigenvalues with elements in a normalized base could help to understand its values.

3.2.2 Normalization

Consider the parameter sensitivity matrix Sp given in equation (3.5) of a system with n eigenvalues and m parameters of interest.

A. Normalization by rows

The influence of the parameter β_j in the eigenvalues is represented by the j^{th} row of Sp

$$Sp_j = \begin{bmatrix} \frac{\partial \lambda_1}{\partial \beta_j} & \frac{\partial \lambda_2}{\partial \beta_j} & \frac{\partial \lambda_3}{\partial \beta_j} & \dots & \frac{\partial \lambda_n}{\partial \beta_j} \end{bmatrix} \quad (3.12)$$

To make it possible to compare the different parameter contributions, a normalization is proposed using different norms.

- **Using norm L1 or grid norm,**

The norm L1 (C. D. Meyer 2000) of Sp_j is defined as

$$\|Sp_j\|_1 = \sum_{i=1}^n |Sp_{ji}| \quad (3.13)$$

where Sp_{ji} is the i^{th} element of Sp_j . Thus the normalized vector is

$$Spn_j = \begin{bmatrix} \frac{Sp_{j1}}{\|Sp_j\|_1} & \frac{Sp_{j2}}{\|Sp_j\|_1} & \frac{Sp_{j3}}{\|Sp_j\|_1} & \dots & \frac{Sp_{jn}}{\|Sp_j\|_1} \end{bmatrix} \quad (3.14)$$

The norm L1 of Spn_j is equal to 1.

- **Using norm L2 or Euclidean norm,**

The norm L2 of Sp_j is defined (C. D. Meyer 2000) as,

$$\|Sp_j\|_2 = \left(\sum_{i=1}^n |Sp_{ji}|^2 \right)^{1/2} \quad (3.15)$$

Similarly, the normalized vector is

$$Sp_{nrj} = \begin{bmatrix} \frac{Sp_{j1}}{\|Sp_j\|_2} & \frac{Sp_{j2}}{\|Sp_j\|_2} & \frac{Sp_{j3}}{\|Sp_j\|_2} & \dots & \frac{Sp_{jn}}{\|Sp_j\|_2} \end{bmatrix} \quad (3.16)$$

The normalized vector Sp_{nrj} has the characteristic that if the original vector Sp_j is complex, the normalized Sp_{nrj} is also complex.

B. Normalization by columns, using the norm L2

The influence of a set of parameters β_j $j=1,2,\dots,m$ in all eigenvalues, for λ_i is represented for the i^{th} column of Sp .

$$Sp^i = \begin{bmatrix} \frac{\partial \lambda_i}{\partial \beta_1} & \frac{\partial \lambda_i}{\partial \beta_2} & \frac{\partial \lambda_i}{\partial \beta_3} & \dots & \frac{\partial \lambda_i}{\partial \beta_m} \end{bmatrix}^T \quad (3.17)$$

By columns, the normalization represents the change of the eigenvalues when several parameters change of the same quantity; this normalization can only be performed for parameters with the same unit.

The normalization using the L2-norm (3.18) is defined as,

$$\|Sp^i\|_2 = \left(\sum_{j=1}^n |Sp_{ji}|^2 \right)^{1/2} \quad (3.18)$$

The normalized column is

$$Sp_{nc}^i = \begin{bmatrix} \frac{Sp_{1i}}{\|Sp^i\|_2} & \frac{Sp_{2i}}{\|Sp^i\|_2} & \frac{Sp_{3i}}{\|Sp^i\|_2} & \dots & \frac{Sp_{mi}}{\|Sp^i\|_2} \end{bmatrix}^T \quad (3.19)$$

Hereafter, some examples present the application of the parameter sensitivity matrix PSM using the simple circuit from Figure 2.1 for different dynamic characteristics

3.2.3 Example 3.2: Simple Circuit with real eigenvalues

Consider the simple circuit of Figure 2.1 and the equations in per-unit presented in (2.84),

$$\begin{bmatrix} \dot{i}_{L\ pu} \\ \dot{v}_{C\ pu} \end{bmatrix} = \begin{bmatrix} -\frac{R_{lpu}}{2H_L} & -\frac{1}{2H_L} \\ \frac{1}{2H_C} & -\frac{1}{R_{2pu}2H_C} \end{bmatrix} \begin{bmatrix} i_{L\ pu} \\ v_{C\ pu} \end{bmatrix}$$

Using the following parameters,

Table 3.1 Parameters of the circuit

Parameter	Value	Parameter	Value	Parameter	Value
L	2 mH	C	100 μF	P_b	50 W
R_l	10 Ω	R_2	100 Ω	V_b	10 V

the system equations in per-unit from equation (2.91)

$$\begin{bmatrix} \dot{i}_{H_L} \\ \dot{v}_{H_C} \end{bmatrix} = \begin{bmatrix} -5000 & -1000 \\ 5000 & -100 \end{bmatrix} \begin{bmatrix} i_{H_L} \\ v_{H_C} \end{bmatrix}$$

the eigenvalues are,

$$\lambda_1 = -3551.2, \quad \lambda_2 = -1548.7$$

The right and left eigenvectors from equation (2.92) are

$$\begin{aligned} \begin{bmatrix} v_1 & v_2 \end{bmatrix}_{pu} &= \begin{bmatrix} -0.56 & 0.27 \\ 0.82 & -0.96 \end{bmatrix} \\ \begin{bmatrix} u_1 & u_2 \end{bmatrix}_{pu} &= \begin{bmatrix} -3.03 & -2.59 \\ -0.87 & -1.79 \end{bmatrix} \end{aligned}$$

Using the definition (3.1)

$$Sp_{H_c} = \begin{bmatrix} \frac{\partial \lambda_1}{\partial H_c} & \frac{\partial \lambda_2}{\partial H_c} \end{bmatrix} = \begin{bmatrix} u_{11}v_{12} \frac{\partial a_{21}}{\partial H_c} + u_{12}v_{12} \frac{\partial a_{22}}{\partial H_c} & u_{21}v_{22} \frac{\partial a_{21}}{\partial H_c} + u_{22}v_{22} \frac{\partial a_{22}}{\partial H_c} \end{bmatrix} \quad (3.20)$$

Using the parameters in Table 3.1, the sensitivity to the per-unit value of the capacitor is

$$\begin{aligned} \frac{\partial \lambda_1}{\partial H_c} &= \frac{(-3.03)(0.27)}{2H_c^2} + \frac{(-2.59)(0.27)}{(50)2H_c^2} \\ \frac{\partial \lambda_2}{\partial H_c} &= \frac{(-0.87)(-0.96)}{2H_c^2} + \frac{(-1.79)(-0.96)}{(50)2H_c^2} \end{aligned} \quad (3.21)$$

The sensitivity to the per-unit value of the inductor H_L is,

$$Sp_{H_L} = \begin{bmatrix} \frac{\partial \lambda_1}{\partial H_L} & \frac{\partial \lambda_2}{\partial H_L} \end{bmatrix} = \begin{bmatrix} u_{11}v_{11} \frac{\partial a_{11}}{\partial H_L} + u_{21}v_{11} \frac{\partial a_{12}}{\partial H_L} & u_{12}v_{12} \frac{\partial a_{11}}{\partial H_L} + u_{22}v_{12} \frac{\partial a_{12}}{\partial H_L} \end{bmatrix} \quad (3.22)$$

Using the associated eigenvectors it yields,

$$\begin{aligned} \frac{\partial \lambda_1}{\partial H_L} &= \frac{(5)(-3.03)(-0.56)}{H_L^2} + \frac{(-0.87)(-0.56)}{H_L^2} \\ \frac{\partial \lambda_2}{\partial H_L} &= \frac{(5)(-2.59)(0.27)}{H_L^2} + \frac{(-1.79)(0.27)}{H_L^2} \end{aligned} \quad (3.23)$$

The sensitivity to the energy storage elements using equation (3.21) and (3.23) is,

$$Sp_{pu} = \begin{bmatrix} \frac{\partial \lambda_1}{\partial H_L} & \frac{\partial \lambda_2}{\partial H_L} \\ \frac{\partial \lambda_1}{\partial H_c} & \frac{\partial \lambda_2}{\partial H_c} \end{bmatrix} = \begin{bmatrix} 12240954.4 & -2240954.4 \\ -25692280.08 & 26692280 \end{bmatrix} \quad (3.24)$$

A. Normalization by rows

Normalizing by rows, the L2-norm of the first row of Sp_{pu} is,

$$\|Sp_{pu1}\|_2 = \sqrt{(12240954.4)^2 + (-2240954.4)^2} = 12444390 \quad (3.25)$$

The L2 norm for the second row Sp is,

$$\|Sp_{pu2}\|_2 = \sqrt{(-25692280.08)^2 + (26692280)^2} = 37048226.3 \quad (3.26)$$

The normalized by rows sensitivity matrix $Sp_{nr pu}$ is,

$$\begin{bmatrix} H_L \\ H_c \end{bmatrix} Sp_{nr pu} = \begin{bmatrix} \lambda_1 & \lambda_2 \\ 0.98365 & 0.3551 \\ -0.69348 & 0.72047 \end{bmatrix} \quad (3.27)$$

where each row represents the change in the eigenvalues with respect to each parameter in per-unit H_L and H_C . To demonstrate the validity of the results in (3.27), a small change in H_L and H_C is performed.

A change of $\pm 10\%$ from the nominal value of H_L produces the following eigenvalue trajectories in Figure 3.1 and Figure 3.2

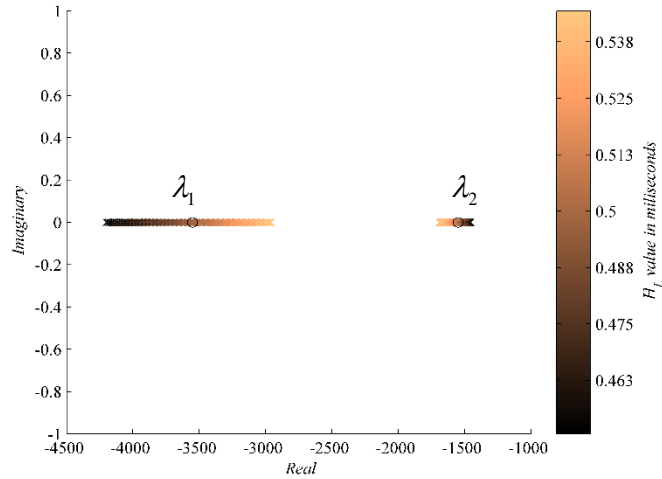


Figure 3.1 Eigenvalue trajectories for a small change in H_L .

A H_C change of $\pm 10\%$ from the nominal value in H_C produces,

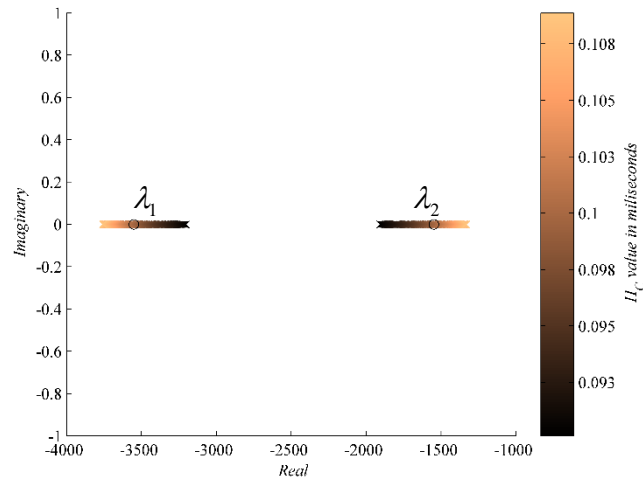


Figure 3.2 Eigenvalue trajectories for small change in H_C .

The eigenvalues remain real and negative thus stable.

B. Normalization by columns

The first column Sp_{pu}^1 ,

$$Sp_{pu}^1 = \begin{bmatrix} 12240954.4 \\ -25692280.08 \end{bmatrix} \quad (3.28)$$

using L2-norm (3.15) as

$$\|Sp_{pu}^1\|_2 = \sqrt{(12240954.4)^2 + (-25692280.08)^2} = 28459343.3 \quad (3.29)$$

and the second column Sp_{pu}^2

$$Sp_{pu}^2 = \begin{bmatrix} -2240954.4 \\ 26692280 \end{bmatrix} \quad (3.30)$$

using L2 norm (3.15) as,

$$\|Sp_{pu}^2\|_2 = \sqrt{(-2240954.4)^2 + (26692280)^2} = 26786184.74 \quad (3.31)$$

lead to the normalized sensitivity matrix $Sp_{nc\ pu}$

$$\begin{bmatrix} H_L \\ H_C \end{bmatrix} Sp_{nc\ pu} = \begin{bmatrix} \lambda_1 & \lambda_2 \\ 0.4810 & -0.083 \\ -0.8766 & 0.9964 \end{bmatrix} \quad (3.32)$$

The matrix $Sp_{nc\ pu}$ represents the relative contribution of each parameter changing of the same value. The eigenvalue evolution for an equal change (0.01 milliseconds) of the parameters H_L and H_C is presented in Figure 3.3.

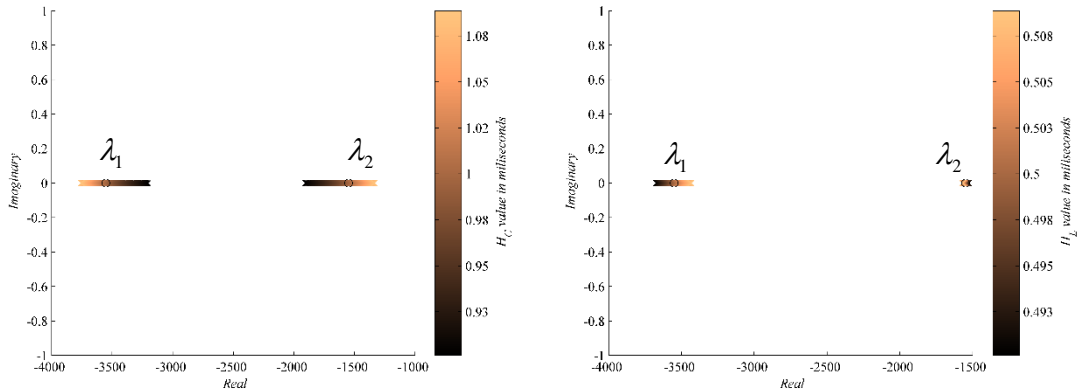


Figure 3.3 Comparison for an equal change.

The change in H_C and H_L produce a change in λ_1 and λ_2 in the same proportion shown in each column of $Sp_{nc\ pu}$.

3.2.4 Example 3.3: Simple Circuit zero in a diagonal element

Considering a change in a resistance R1 to zero,

Table 3.2 Parameters for a zero in the diagonal

Parameter	Value	Parameter	Value	Parameter	value
L	2 mH	C	$100 \text{ } \mu\text{F}$	P_b	50 W
R_1	$0 \text{ } \Omega$	R_2	$100 \text{ } \Omega$	V_b	10 V

The system equations in per unit are,

$$A_{pu} = \begin{bmatrix} 0 & -1000 \\ 5000 & -100 \end{bmatrix} \quad (3.33)$$

The eigenvalues are,

$$\lambda_1 = -50 + 2235.5i, \quad \lambda_2 = -50 - 2235.5i \quad (3.34)$$

The modal matrices are,

$$\begin{aligned} V_{pu} &= \begin{bmatrix} 0.00912 + 0.4081i & 0.00912 - 0.4081i \\ 0.9128 & 0.9128 \end{bmatrix} \\ U_{pu} &= \begin{bmatrix} -1.225051i & 1.225051i \\ 0.5477 + 0.01225i & 0.5477 + 0.01225i \end{bmatrix} \end{aligned} \quad (3.35)$$

The participation factor matrix is,

$$P_{pu} = \begin{bmatrix} 0.5 - 0.0112i & 0.5 + 0.0112i \\ 0.5 - 0.0112i & 0.5 - 0.0112i \end{bmatrix} \quad (3.36)$$

and the modulus of P_{pu} is,

$$|P_{pu}| = \begin{bmatrix} 0.5001 & 0.5001 \\ 0.5001 & 0.5001 \end{bmatrix} \quad (3.37)$$

The sensitivity with respect to the parameters is,

$$Sp_{pu} = \begin{bmatrix} \frac{\partial \lambda_1}{\partial H_L} & \frac{\partial \lambda_2}{\partial H_L} \\ \frac{\partial \lambda_1}{\partial H_C} & \frac{\partial \lambda_2}{\partial H_C} \end{bmatrix} = \begin{bmatrix} -2236627.2i & 2236627.2i \\ 500000 - 11171952.8i & 500000 + 11171952.8i \end{bmatrix} \quad (3.38)$$

Normalizing by rows using the L2 norm gives

$$\begin{array}{c} \begin{array}{cc} \lambda_1 & \lambda_2 \end{array} \\ \begin{bmatrix} H_L \\ H_C \end{bmatrix} Sp_{nr pu} = \begin{bmatrix} -0.7071i & 0.7071i \\ 0.031614 - 0.70639i & 0.031614 + 0.70639i \end{bmatrix} \end{array} \quad (3.39)$$

In equation (3.39), it is shown up that changes in the per-unit value of the inductance H_L produce only changes in the imaginary part of the eigenvalues. It is with the matrix $Sp_{nr pu}$ gives more information using its complex representation.

Figure 3.4 shows the eigenvalue trajectories with a change of $\pm 10\%$ from the nominal value of H_L . Clearly, the eigenvalues variate only on the imaginary axis, as the matrix $Sp_{nr pu}$ predicts

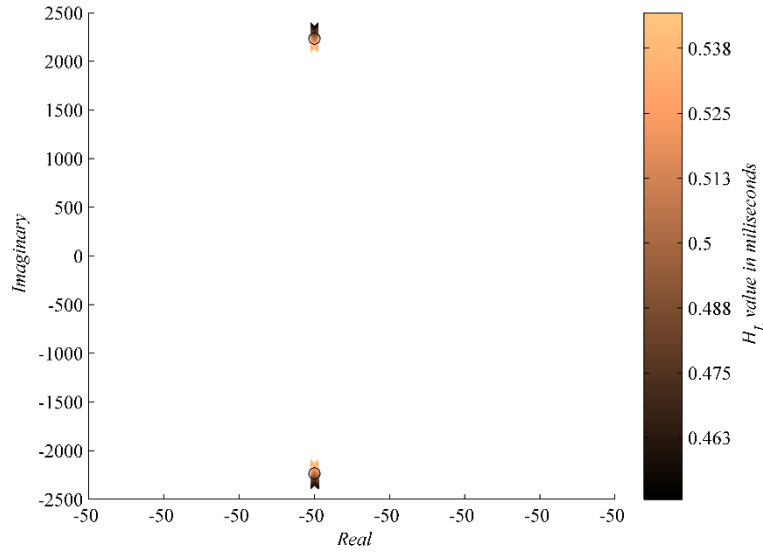


Figure 3.4 Eigenvalue trajectories for L

3.2.5 Example 3.4: Simple Circuit with diagonal dominant elements

Consider the parameters in Table 3.3. (case 3 in Chapter 2)

Table 3.3 Parameters in diagonal dominant case

Parameter	Value	Parameter	Value
L	1 mH	C	1 mF
R_1	10 Ω	R_2	0.1 Ω

and the model calculated in (2.104),

$$\begin{bmatrix} \dot{i}_{L_{pu}} \\ \dot{v}_{C_{pu}} \end{bmatrix} = \begin{bmatrix} -10000 & -2000 \\ 500 & -10000 \end{bmatrix} \begin{bmatrix} i_{L_{pu}} \\ v_{C_{pu}} \end{bmatrix}$$

The eigenvalues in (2.105),

$$\lambda_1 = -10000 + 1000i, \quad \lambda_2 = -10000 - 1000i$$

The modal matrices are,

$$\begin{aligned} V_{pu} &= \begin{bmatrix} 0.8944 & 0.8944 \\ -0.4472i & 0.4472i \end{bmatrix} \\ U_{pu} &= \begin{bmatrix} 0.559 & 1.118i \\ 0.559 & -1.118i \end{bmatrix} \end{aligned} \quad (3.40)$$

The participation factor matrix is,

$$P_{pu} = \begin{bmatrix} 0.5 & 0.5 \\ 0.5 & 0.5 \end{bmatrix} \quad (3.41)$$

The sensitivity with respect to the parameters in this case is,

$$Sp_{pu} = \begin{bmatrix} \frac{\partial \lambda_1}{\partial H_L} & \frac{\partial \lambda_2}{\partial H_L} \\ \frac{\partial \lambda_1}{\partial H_C} & \frac{\partial \lambda_2}{\partial H_C} \end{bmatrix} = \begin{bmatrix} 5000000 - 5000000i & 5000000 + 5000000i \\ 5000000 - 5000000i & 5000000 + 5000000i \end{bmatrix} \quad (3.42)$$

the normalized matrix $Sp_{nr pu}$ is,

$$\begin{bmatrix} H_L \\ H_C \end{bmatrix} Sp_{nr pu} = \begin{bmatrix} 0.703 - 0.0703i & 0.703 + 0.0703i \\ 0.703 - 0.0703i & 0.703 + 0.0703i \end{bmatrix} \quad (3.43)$$

Comparing with the previous examples this is the only case where the sensitivity and the participation factors lead to the same conclusions. Both parameters contribute in similar amount to the dynamics of the system.

3.3 Remarks and uses.

From the different scenarios in the examples, some remarks are established.

As said before the use of participation factors is limited to the models with diagonal dominant state matrices.

Advantages of the proposed PSM matrix

- Using the PSM more information can be retrieved as
 - The sign of the elements represents the direction in the change of the eigenvalues.
 - The complex values in the PSM elements give information of how the contribution of the parameters affects the imaginary and the real part.
 - The normalization by rows gives the contribution of a parameter to all eigenvalues.
 - The normalization by columns gives the comparative contribution of the parameters for each eigenvalue. For this comparison, it is necessary to choose parameters with the same unit without exceptions.
 - The analysis of the parameters is not limited to the dynamic elements or explicit elements in the matrix A.

Drawbacks

- The need of the partial derivatives of the matrix A with respect to the elements is clear. Depending on the equations, they could be difficult to derive.
- The eigenvalues are assumed to be distinct.

The information given by the PSM can be useful in different application scenarios as:

- For the selection of parameters: clearly, the methodology shows its importance in this area by understanding the effect of the system parameters.

- For the tuning of control parameters: the use of the PSM is not restricted to open loop models but may be applied also to closed loop systems, where in many cases the tuning of parameters is a big issue.
- For stability analysis: by knowing the general direction of trajectories in the eigenvalues for small changes in the parameters it is possible to determine which parameters participate the most in the eigenvalues close to be unstable.

Table 3.4 presents the differences between the participation factor matrix and the parametric sensitivity of (D'Arco, Suul, and Fosso 2014a) and (Barrera-Gallegos, Dauphin-Tanguy, and Guillaud 2016).

Table 3.4 Comparison of different approaches

	Participation factors (I.J. Perez-Arriaga, Verghese, and Schweppe 1982)	Parameter Sensitivity (D'Arco, Suul, and Fosso 2014a)	PSM (Barrera et al 2016)
Formulation	$P = \begin{bmatrix} \frac{\partial \lambda_1}{\partial a_{11}} & \frac{\partial \lambda_2}{\partial a_{11}} & \dots & \frac{\partial \lambda_n}{\partial a_{11}} \\ \frac{\partial \lambda_1}{\partial a_{22}} & \frac{\partial \lambda_2}{\partial a_{22}} & \dots & \frac{\partial \lambda_n}{\partial a_{22}} \\ \vdots & \vdots & \ddots & \vdots \\ \frac{\partial \lambda_1}{\partial a_{nn}} & \frac{\partial \lambda_2}{\partial a_{nn}} & \dots & \frac{\partial \lambda_n}{\partial a_{nn}} \end{bmatrix}$	$\frac{\partial \lambda_i}{\partial \beta_k} = \frac{u_{ik} \frac{\partial A}{\partial \beta_j} v_{il}}{v_{il} u_{ik}}$	$Sp = \begin{bmatrix} \frac{\partial \lambda_1}{\partial \beta_1} & \frac{\partial \lambda_2}{\partial \beta_1} & \frac{\partial \lambda_3}{\partial \beta_1} & \dots & \frac{\partial \lambda_n}{\partial \beta_1} \\ \vdots & \vdots & \vdots & \dots & \vdots \\ \frac{\partial \lambda_1}{\partial \beta_j} & \frac{\partial \lambda_2}{\partial \beta_j} & \frac{\partial \lambda_3}{\partial \beta_j} & \dots & \frac{\partial \lambda_n}{\partial \beta_j} \\ \vdots & \vdots & \vdots & \dots & \vdots \\ \frac{\partial \lambda_1}{\partial \beta_m} & \frac{\partial \lambda_2}{\partial \beta_m} & \frac{\partial \lambda_3}{\partial \beta_m} & \dots & \frac{\partial \lambda_n}{\partial \beta_m} \end{bmatrix}$
Applied to	All modes of the system and states	Critical modes, and critical parameters	All modes of the system and parameters
Normalization	Normalized by definition	Not normalized	Normalized by <ul style="list-style-type: none"> • Rows • Columns
Objective of analysis	The relative contribution of states in mode.	<ul style="list-style-type: none"> • Sensitivity analysis of critical modes • Stability analysis • Tuning parameters 	<ul style="list-style-type: none"> • Relative contribution of parameters in modes. • Sensitivity analysis • Stability analysis • Tuning parameters
Complex numbers interpretation	No interpretation given	Meaningful in the sign of each part real and imaginary but not scaled (not normalized)	Meaningful in the sign of each part real and imaginary and scaled to all elements (normalized)
Diagonal dominance	Yes	No	No

3.4 Conclusions

The participation factor matrix as analysis tool has shown up some limitations which makes it interesting to propose a new tool of analysis more general and rich in information on the dynamics of the system.

The new methodology for analysis has the advantage of having normalized elements, where the information is organized, clear and useful.

The interpretation of the elements in the PSM is not limited to real elements but also to complex variations of eigenvalues. Each element of the matrix describes the first order sensitivity of the eigenvalue, this can be understood as the general direction of the eigenvalue with respect to changes of the parameters.

The new matrix can give a measurement of the change of the eigenvalues for changes of the parameters, and it can be used for different purposes as,

- Stability analysis
- Tuning of control parameters
- Analysis and selection of new parameters
- Analysis of coupling in different subsystems and parameters

Chapter 4 State-space modeling of HVDC systems

4.1 Introduction

The previous chapters it is presented the analysis of the tools used till now on the classical AC power system and proposed another methodology more general but a little bit more complex to use. This approach will be applied on the specific domain of the HVDC grids. The presentation of this analysis is divided in two parts. The chapter 4 presents the modelling of the power electronics converter. It starts with the Voltage Source Converter, a very well-known topology, to follow on the Modular Multilevel converter which is now used for all the new projects in HVDC grid. The different control loops (current and voltage) are explained and some linearized models are proposed. In HVDC applications, two (HVDC link) ore more converters (MTDC grid) may be connected via cables or lines. A simplified model of these systems is also proposed. The same approach is proposed with MMC.

4.2 Context of the HVDC development

Chapter 1 presents the problematics of the dynamic analysis methods applied for the AC electrical networks in the high voltage DC networks. The difference in its fundamental dynamics makes the systems with power electronics different from the systems analyzed in (I.J. Perez-Arriaga et al. 1988) for this reason the present chapter is a brief presentation on the modeling of the HVDC systems.

The electrical networks have been growing in size since the first power plants installed in big cities. The growing capability of the electrical network also evolved into a system with different ways of producing electrical energy from converting oil and gas, potential energy stored in dams, power from nuclear reactions, from the sun with photovoltaic panels from the wind with wind turbine. All these actual characteristics in the electrical systems bring new problems for controlling the electrical network.

Nowadays the production of energy could be organized in two different kinds of production means of electrical energy, as non-renewable energy sources and renewable energy sources. A renewable source is a naturally recovered energy that could be extracted from nature without affecting its natural process of recovering. As an example of renewable energy source it could be rain, wind, sunlight, geothermal heat, tides and waves of the ocean. As a consequence a non-renewable energy source is where the energy extracted from this source cannot be recovered as a natural process of the system.

Electrical power systems are composed of different elements as generators that convert the mechanical power to electrical one, transformers that allow changing the voltage values in order to transmit this electricity by efficient means, lines of transmission and elements of consumption and storage. Synchronous machines used for generation of electricity transform the mechanical power from primary sources prime mover (oil, gas, nuclear, hydraulic) into electrical power.

The structure of electrical power systems varies in size and structure, however they all have the same basic characteristics; they are three-phase AC (alternating current) operating essentially at a constant voltage.

Generation and transmission facilities use three-phase equipment.

The transmission of the electrical power over significant distance to consumers spread over a wide area requires a transmission system comprising subsystems operating at different voltage levels (Kundur 2007). The voltage in the AC system has a particular wave form for each phase,

$$\begin{aligned} v_a &= V \sin(\omega t) = V\sqrt{2} \sin(\omega t) \\ v_b &= V \sin\left(\omega t - \frac{2}{3}\pi\right) = V\sqrt{2} \sin\left(\omega t - \frac{2}{3}\pi\right) \\ v_c &= V \sin\left(\omega t + \frac{2}{3}\pi\right) = V\sqrt{2} \sin\left(\omega t + \frac{2}{3}\pi\right) \end{aligned} \quad (4.1)$$

where V is the root mean square (RMS) voltage, t is time, ω is the base pulsation of the electrical system and each phase (v_a, v_b, v_c) is dephased 120° from the other. If the voltage is represented as a vector with an amplitude and a phase with respect to v_a , we can plot the vectors of the three-phase voltage as shown in Figure 4.1.

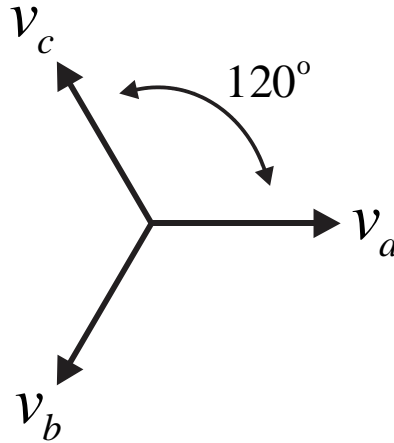


Figure 4.1 Phasorial representation of the three-phase voltage.

The previous mentioned characteristics are very important for the interconnection between the different generation systems. The connection between different system is regulated to avoid congestion in the interconnections.

For example in Figure 4.2, the generation of each side could have different levels of voltage and frequencies.

These differences between systems are common in the transmission lines connecting different generation systems. There are some ways to overcome this problematics, from the use of transformers, to the application of specific control methodologies.

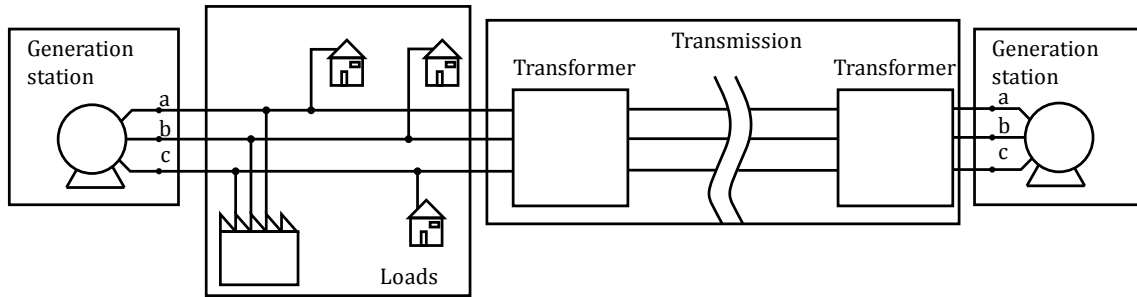


Figure 4.2 Two generation systems connected

Another option for connecting two different AC systems is by using the conversion to high voltage direct current (HVDC). With the grown market of renewable energy, the AC to DC conversion is used to connect this kind of systems. The power levels for the renewable sources may change depending on the conditions of the transmission and the associated energy sources, making the DC grids a very good option to connect such energy sources.

The conversion is accomplished by means of power electronics using thyristors, insulated gate bipolar transistors (IGBT), or other power electronic components like integrated gate-commutated thyristor (IGCT).

It has been studied and proved that HVDC interconnections have less losses and better performance (Kundur 2007; Chapman 2010; Krause, Wasynczuk, and Sudhoff 2002). This performance also depends on the control architecture of the system.

In some cases, the preferred way of power transmission from wind farms to AC systems is by using the HVDC connections (Gao et al. 2013; Bernal-Perez et al. 2012; Perveen, Kishor, and Mohanty 2014). HVDC also helps in the connection between power networks with different control systems and energy policies and connection between countries (Ismunandar 2010).

From different perspectives, the installation of power electronic technologies such as HVDC transmission and flexible alternating current transmission system (FACTS) devices will help improving the degree of flexibility of the grid. This means that those technologies support the increasing usable capacity without harming secure operation of the grid (Liang, Gomis-Bellmunt, and Hertem 2016).

This involves changes on the grid from the traditional dynamic of the system governed by the dynamic of the synchronous generators to the dynamics of the power electronics used in the DC converters. Among the different converter technologies, in this thesis the analysis is focused

on the voltage source converters (VSC) and the modular multi-level converters (MMC), which are the more currently used nowadays.

4.3 Voltage source converter

The interconnection between two or more substations requires the control of power, voltage, and current in each substation to regulate the way the energy is transmitted from one or more sources to the loads. Because of that, the control is designed to act on all the variables.

4.3.1 General control scheme

Figure 4.3 presents the general control architecture of a station interconnecting an AC network to a DC grid (Rault et al. 2012; Cole et al. 2010).

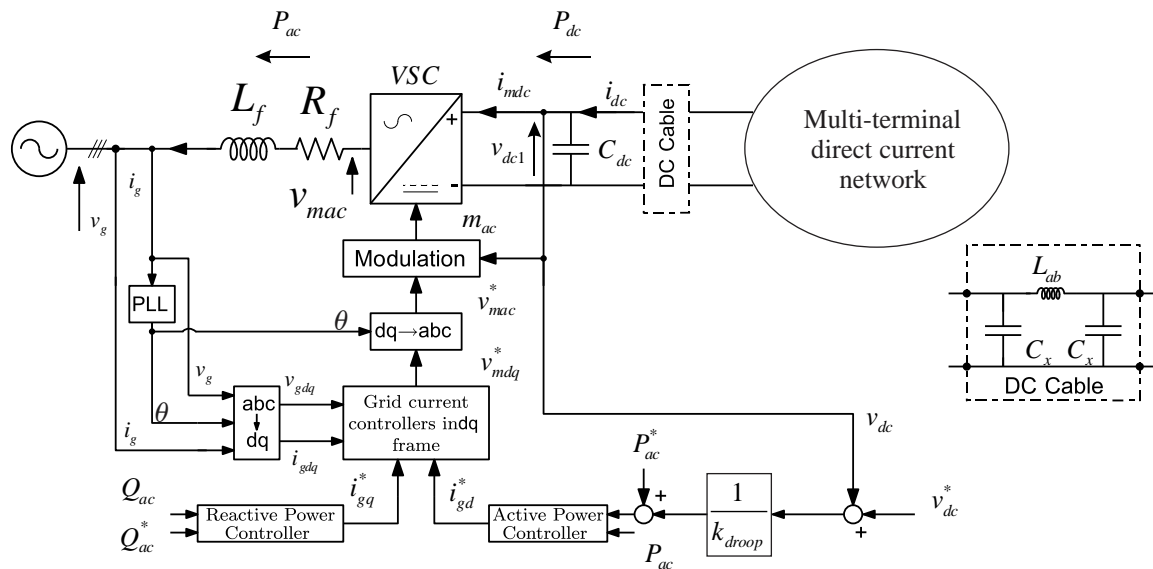


Figure 4.3 Voltage source station control diagram.

In Figure 4.3, P_{dc} is the power provided by the DC network, P_{ac} is the power at the AC side of the substation. Power transferred to the AC side of the converter, is considered as positive.

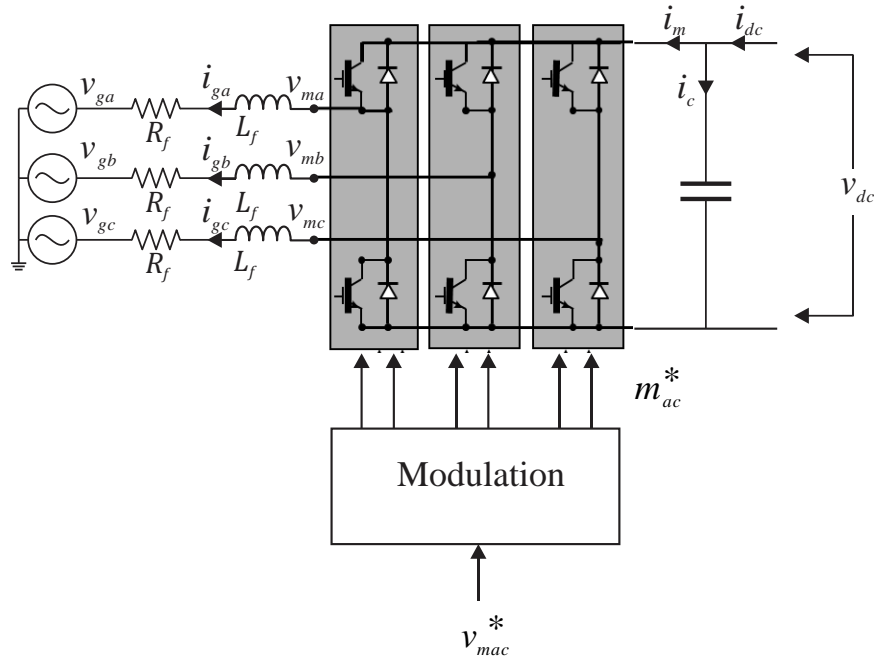


Figure 4.4 VSC converter

Figure 4.4 presents a configuration of Insulated Gate Bipolar Transistors (IGBT) used in the structure of an inverter. The modulation signals to the IGBT devices allow to open or close the switching devices in the converter and control the voltages v_{ma} , v_{mb} and v_{mc} at the AC side of the converter. This process is well known and described in literature (Mohan, Undeland, and Robbins 2003; Shen et al. 2012; Wu et al. 2014; Yazdani and Iravani 2010).

The DC side terminals of a VSC are typically connected in parallel with a relatively large capacitor that behaves as a voltage source

The VSC is a non-linear system, the model in Yazdani and Iravani 2010 presents a simplification of the VSC model for simulation and analysis of large scale systems.

A. Average VSC model

Under the hypothesis that the switching devices are fast, the average value model can be used (Peralta, Saad, Denetiere, et al. 2012; K. Wang et al. 2014). Figure 4.5 shows this simplification, the switching devices are replaced by three-phase voltage sources v_m and a current source i_m .

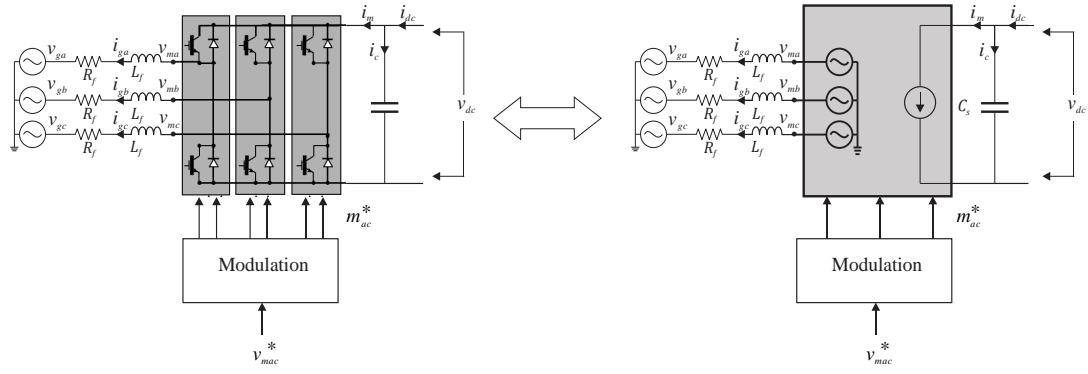


Figure 4.5 Reduced model of a VSC

The power conservation principle, means that the power on the AC side must be equal to the power on the DC.

$$v_{ma}i_{ga} + v_{mb}i_{gb} + v_{mc}i_{gc} = v_{dc}i_m \quad (4.2)$$

which becomes in the dq0 frame,

$$v_{md}i_{gd} + v_{mq}i_{gq} = v_{dc}i_m \quad (4.3)$$

The dq0 reduced diagram is presented in Figure 4.6, where each axis has its modulation signal m_q and m_d . The capacitance C_{dc} is the equivalent capacitance of the converter.

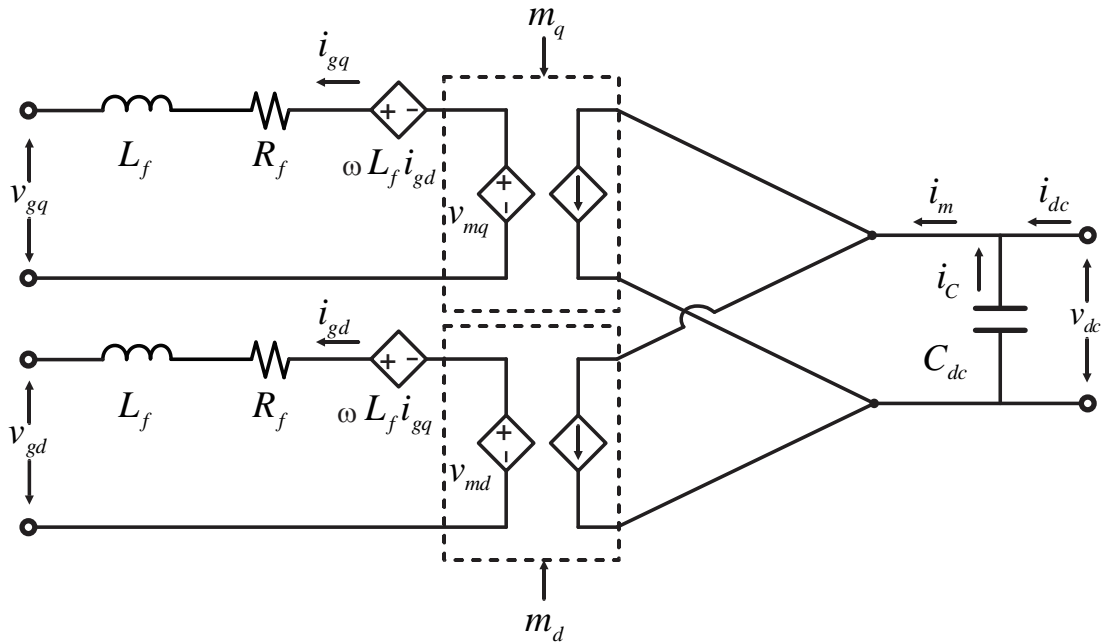


Figure 4.6 dq0 model of a VSC

The equations describing the circuit in the dq0 frame at the AC side are.

$$\begin{aligned} v_{md} &= v_{gd} + R_f \cdot i_{gd} + L_f \frac{d(i_{gd})}{dt} + \omega \cdot L_f \cdot i_{gq} \\ v_{mq} &= v_{gq} + R_f \cdot i_{gq} + L_f \frac{d(i_{gq})}{dt} + \omega \cdot L_f \cdot i_{gd} \end{aligned} \quad (4.4)$$

In the frequency domain equations (4.4) are,

$$\begin{aligned} (L_f s + R_f) i_{gd} &= v_{md}^* - L_f \omega i_{gq} \\ (L_f s + R_f) i_{gq} &= v_{mq}^* + L_f \omega i_{gd} \end{aligned} \quad (4.5)$$

where,

$$\begin{aligned} v_{mq}^* &= v_{mq} - v_{gq} \\ v_{md}^* &= v_{md} - v_{gd} \end{aligned} \quad (4.6)$$

and ω is the frequency of oscillation at the AC side. In practice, the frequency is reconstructed using Phase Lock Loop (PLL). In the following, the frequency value ω is assumed to be constant.

B. Current loop

The control of the current using power electronics is widely used for high voltage source converters. The objective is to produce a sinusoidal AC output in which amplitude and frequency and phase can be controlled in order to fix the current of the AC side of the VSC.

The control of the current through the converter is necessary to control the transferred power. A common methodology is using the rotating reference frame dq0 instead of the three-phase stationary coordinated system; by decoupling the signals from the d and q axis the control is independently controlling active and reactive power.

Derived from (4.5) and (4.6) the block diagram of the physical AC system in dq0 is shown in Figure 4.7. It shows up the coupling between i_{gd} and i_{gq} . This coupling has been related to the transfer of active power and reactive power through each axis. If the coupling between the axis is compensated by the control, it is possible to have a decoupled control for active and reactive power.

Neglecting the switching devices, the current loop presented in Figure 4.7 is a common strategy to control the current through the converter.

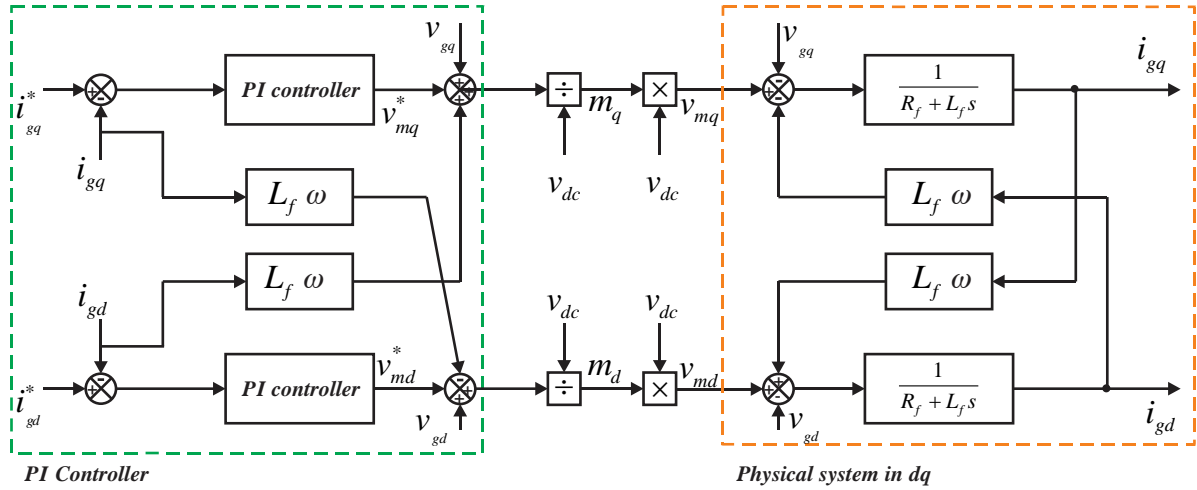


Figure 4.7 Current loop

Figure 4.7 shows up the coupling between the currents i_{gd} and i_{gq} .

The effects of the terms $L_f \omega i_{gq}$ and $L_f \omega i_{gd}$ are compensated

The transfer function of the decoupled physical system is,

$$\frac{i_{gq}}{v_{mq}^*} = \frac{i_{gd}}{v_{md}^*} = \frac{\frac{1}{L_f}}{s + \frac{R_f}{L_f}} \quad (4.7)$$

and the current loop PI controller transfer function is,

$$H(s) = k_p \left(1 + \frac{1}{T_i s} \right) \quad (4.8)$$

k_p is the proportional gain of the PI controller, and T_i is the integral time of the controller. The two current loops have exactly the same parameters for the PI controllers. In a decoupled form each control loop is independent as presented in Figure 4.8, the closed loop equation of each loop is,

$$G(s) = \frac{\frac{k_p}{L_f} s + \frac{k_p}{L_f T_i}}{s^2 + \left(\frac{R_f}{L_f} + \frac{k_p}{L_f} \right) s + \left(\frac{k_p}{L_f T_i} \right)} \quad (4.9)$$

The desired behavior of the closed loop is settled by fixing the damping coefficient $\xi = 0.7$ and the undamped natural frequency ω_n set to achieve a settling time t_s of 10 milliseconds

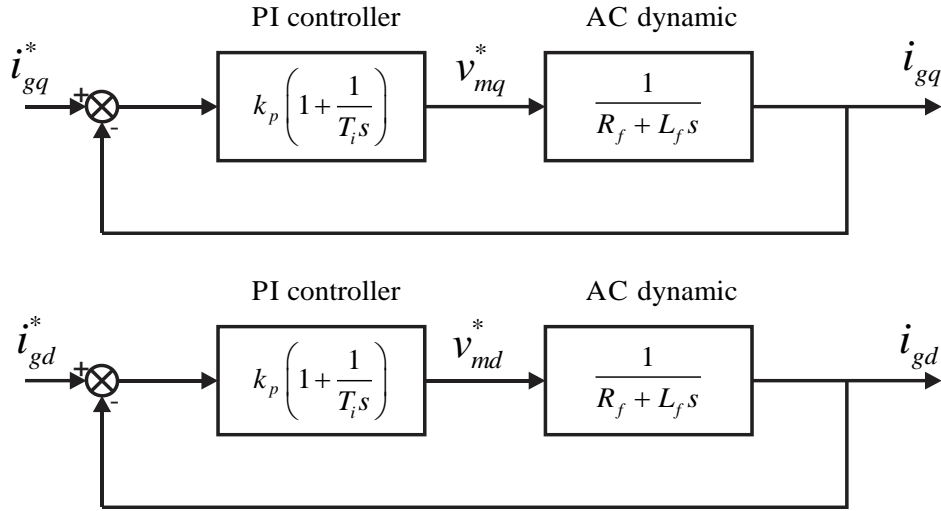


Figure 4.8 Decoupled current loops

Due to the choice on the PLL, the active power is related to the d-axis current magnitude and the reactive power with the q-axis current. If the reference of the q-axis current is set to zero, the possibility of repeated poles reduces and the dynamic analysis is straight forward.

C. Voltage droop control

For the control of the voltage, there are different approaches in the literature (Thams et al. 2015; Wenyuan et al. 2014). In Figure 4.3 the voltage control is presented with a proportional block (droop control). This type of control is used in Multi-terminal DC grid since it allows sharing the balance effort in case of large variations of power.

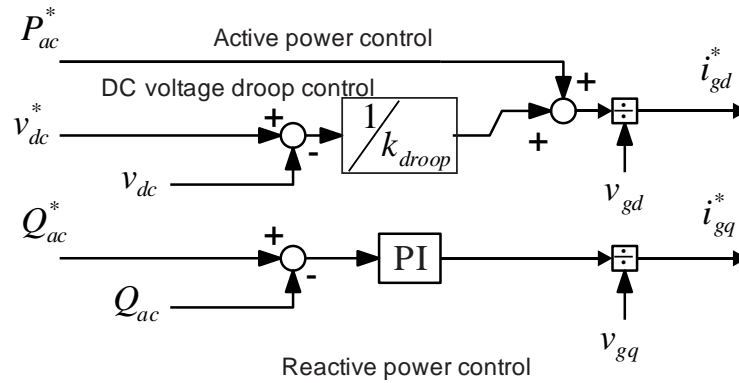


Figure 4.9 Voltage and power control.

The constant parameter $1/k_{droop}$ shown in Figure 4.9 defines the drop of the voltage when there is a change of power in the system between certain limits. This characteristic is presented in Figure 4.10, where the x-axis of the graph corresponds to the power range of an AC system connected to the DC grid with a voltage range of change. In the point of desired operation P_{aci} the voltage in the DC grid will be v_{dci} .

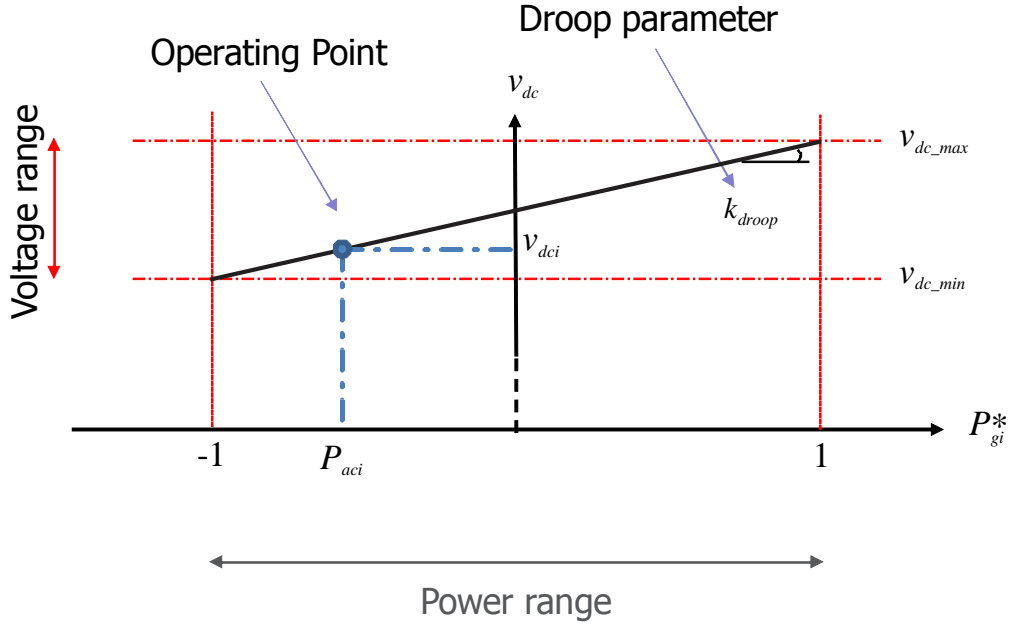


Figure 4.10 Voltage droop characteristic.

The response time of the system depends on the k_{droop} value. For a small k_{droop} the voltage droop is small.

The changes of the power are considered from 1 to -1 in per unit. For a positive value the power will be consumed by the AC system.

D. Linearization of the model

Equation (4.3) presents nonlinear characteristics. For the modal analysis, a linearization is necessary.

The linear equations of the model are,

$$\Delta i_{gd} V_{md0} + \Delta V_{md} I_{gd0} = \Delta i_m V_{dc0} + \Delta v_{dc} I_{mdc0} \quad (4.10)$$

The station linearized model is presented in Figure 4.11 as a block diagram (Rault et al. 2012)

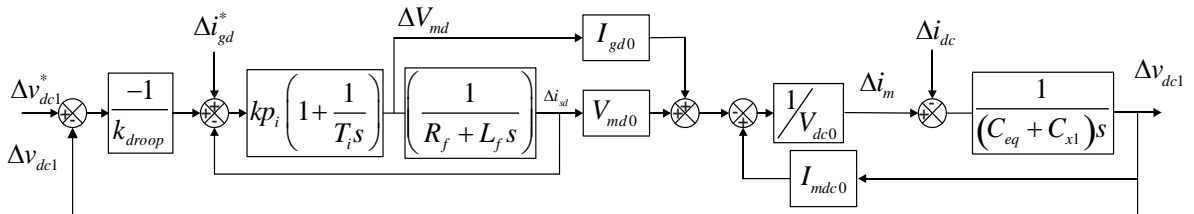


Figure 4.11 Linear model.

The sub index 0 refers to the operating point. This model is simplified but represents the major dynamics of the system: the DC bus voltage dynamics and grid current dynamics.

Clearly, this model neglects the inner controls of phase locked loop and the switching controls. The purpose of this simplification is to have a model simple enough to begin the analysis.

4.3.2 Per-unit in HVDC grids

As mentioned in section 2.3.2, the per-unit representation has its advantages for the use of manageable magnitudes of the variables.

The use of the base values of an AC system into the HVDC network has become a standard (Yazdani and Iravani 2010).

- *Ac per-unit representation*

For the systems involving AC to DC conversions, the use of the AC per-unit representation involves AC base values corresponding to the oscillatory behavior of the system. When applied, the DC side of the converter is presented in terms of the AC base values including the oscillatory variables (oscillation frequency ω in rad).

Consider the following base values for a HVDC with a VSC station.

Table 4.1 Base values for a VSC station

Base value	Description
S_b	Base value of the apparent power of the AC side, in VA
$P_b = S_b \cos(\phi_n)$	Base active value that depends on the phase angle ϕ_n
U_{ln}	Nominal line to line voltage in volts
$V_b = V_{ln} = \frac{U_{ln}}{\sqrt{3}}$	Nominal line to neuter voltage in volts
f_b	Frequency base in hertz
ω_b	Frequency base in radians per second
V_{dcb}	Nominal voltage of the AC side

Using the fundamental values of Table 4.1 the following relationships are developed for the AC side,

$$\begin{aligned}
 I_b &= \frac{S_b}{3V_b} [\text{A}]; & Z_b &= \frac{V_b}{I_b} = \frac{3V_b^2}{S_b} [\Omega] \\
 L_b &= \frac{Z_b}{\omega_b} [\text{H}]; & C_b &= \frac{1}{Z_b \omega_b} [\text{F}]
 \end{aligned}
 \tag{4.11}$$

The base value of the energy storage elements depends on the impedance base Z_b and the oscillation frequency ω_b .

The DC per unit is based on a strong assumption (Yazdani and Iravani 2010)

$$V_{dcb} = 2U_{1n} = 2\sqrt{3}V_b \text{ and } \cos(\phi_n) = 1 \quad (4.12)$$

the fundamental relations the current base and the resistance base are,

$$I_{dcb} = \frac{\sqrt{3}I_b}{2} [\text{A}]; \quad R_{dcb} = 4Z_b [\Omega] \quad (4.13)$$

remembering that,

$$S_b = V_{dcb} \cdot I_{dcb} \quad (4.14)$$

For example, consider the following state equation for a capacitor in a DC network in per unit

$$C \frac{dv_C}{dt} = i_{dc} \quad (4.15)$$

Considering (4.11), (4.15) yields,

$$C_{pu} C_b V_{dcb} \frac{dv_{C,pu}}{dt} = i_{dc,pu} I_{dcb} \quad (4.16)$$

replacing C_b and rearranging

$$C_{pu} \frac{1}{Z_b \omega_b} \frac{V_{dcb}}{I_{dcb}} \frac{dv_{C,pu}}{dt} = i_{dc,pu} \quad (4.17)$$

Since $Z_b = \frac{R_{dcb}}{4}$ hence

$$C_{pu} \frac{4}{R_{dcb} \omega_b} \frac{V_{dcb}}{I_{dcb}} \frac{dv_{C,pu}}{dt} = i_{dc,pu} \quad (4.18)$$

The state equation becomes,

$$\frac{dv_{C,pu}}{dt} = \frac{\omega_b}{4C_{pu}} i_{dc,pu} \quad (4.19)$$

The capacitor in per-unit is

$$C_{pu} = \frac{C}{C_b} = \frac{C}{\frac{1}{Z_b \omega_b}} = CZ_b \omega_b \quad (4.20)$$

The capacitance C_{pu} depends on the value of the base impedance, which depends on the voltage of the AC side.

The per-unit values depend on the base values of the AC side. Thus, the following consequences apply.

- The parametric analysis of a model with bigger order of magnitude in the AC (in pu) side this could lead wrong conclusions.
- On the contrary, if the elements of the AC side (in pu) are smaller than the elements of the DC side this could lead to consider that the elements of the DC side are too important for certain modes.

The per-unit representation has a scaling effect on the per-unit value of the elements. If the base of scaling is not well chosen, the results can lead to different conclusions. Those will be valid in the context of the per-unit representation but not in the physical units of the system.

It also opens the opportunity to discuss under which circumstances this method is not viable.

Another alternative is to use the per-unit based on the stored energy of the DC elements as presented in section 2.3.2. This basis has the advantage of having elements that represent in a way the stored energy of each element in a uniform unit (seconds for the energy storage elements and per-unit for resistive elements).

4.3.3 Reduced linear equivalent

Consider the system of Figure 4.12, It

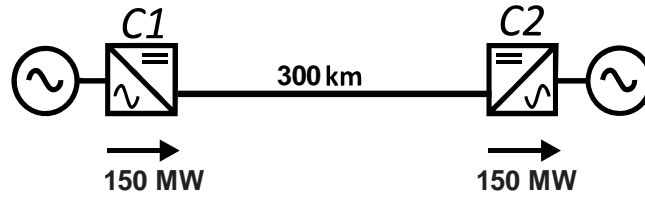


Figure 4.12 HVDC link with two stations.

For didactic reasons, let us assume that the changes of the operating point have no influence on the dynamics of the system. In addition, the dynamic of the current loop is supposed to be infinite.

Therefore, the equivalent circuit in Figure 4.13 represent such reduced model.

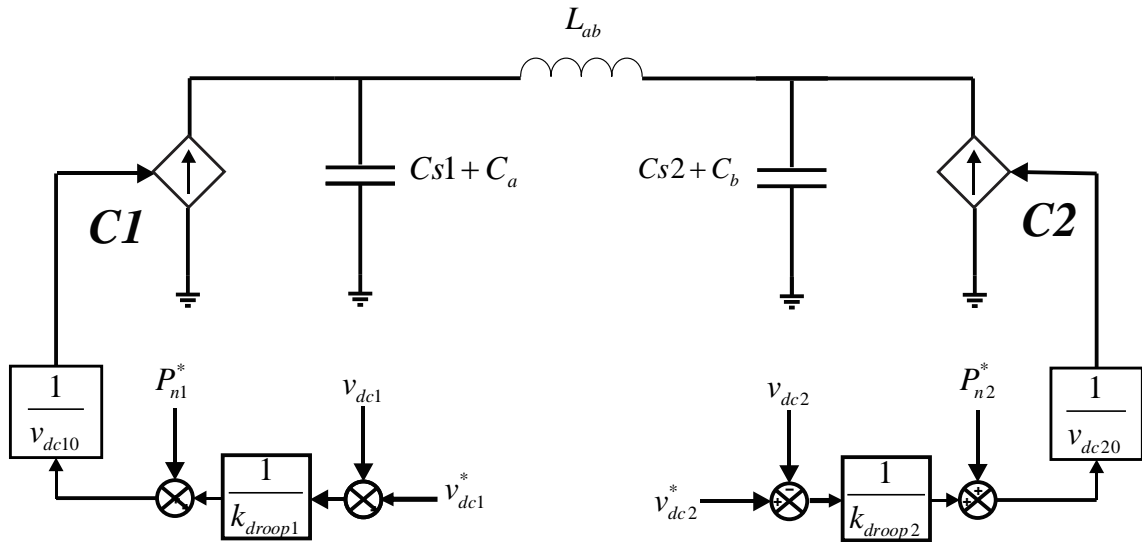


Figure 4.13 HVDC link equivalent circuit.

The two stations $C1$ and $C2$ are connected through a cable modeled by an inductor with two capacitors in each extremities, and a droop control scheme.

- v_{dc1} and v_{dc2} : voltages in each station measured in the capacitor in per-unit.
- v_{dc1}^* and v_{dc2}^* : reference voltages in each station in per-unit.
- v_{dc10} and v_{dc20} : Voltage in the point of operation.
- i_{dc10} and i_{dc20} : current in the point of operation.
- P_1^* and P_2^* : power reference for the equivalent sources in per-unit.
- $C_{eq1} = Cs1 + C_a$ and $C_{eq2} = Cs2 + C_b$: equivalent capacitances composed by the capacitance of the station and the capacitance of each side of the equivalent model of the cable.
- L_{ab} : equivalent inductance of the cable.
- k_{droop1} and k_{droop2} : voltage droop controllers.

The equations of the model in per-unit are,

$$\begin{bmatrix} \dot{v}_{dc1\ pu} \\ \dot{v}_{dc2\ pu} \\ \dot{i}_{L_{ab}\ pu} \end{bmatrix} = \begin{bmatrix} \alpha_1 & 0 & \frac{\omega_b}{4C_{eq1}} \\ 0 & \alpha_2 & \frac{-\omega_b}{4C_{eq2}} \\ \frac{-4\omega}{L_{ab}} & \frac{4\omega}{L_{ab}} & 0 \end{bmatrix} \begin{bmatrix} v_{dc1\ pu} \\ v_{dc2\ pu} \\ i_{L_{ab}\ pu} \end{bmatrix} \quad (4.21)$$

where,

$$\begin{aligned} \alpha_1 &= -\left(\frac{\omega}{4C_{eq1}}\right) \left(\frac{i_{dcpu01}k_{droop1} + 1}{k_{droop1}v_{dcpu10}}\right) \\ \alpha_2 &= -\left(\frac{\omega}{4C_{eq2}}\right) \left(\frac{-i_{dcpu02}k_{droop2} + 1}{k_{droop2}v_{dcpu20}}\right) \end{aligned} \quad (4.22)$$

The objective of this example is to measure the parametric sensitivity with respect to the capacitances in the stations and the inductance of the cable.

This reduced model has no means to reproduce the complete dynamics of the systems but under the right circumstances can help to reproduce a large scale MTDC grid (Cole et al. 2010).

- *First order equivalent model*

Under the hypothesis of having $L_{ab} = 0$ the model in Figure 4.13 is reduced to a first order system with lumped capacitance.

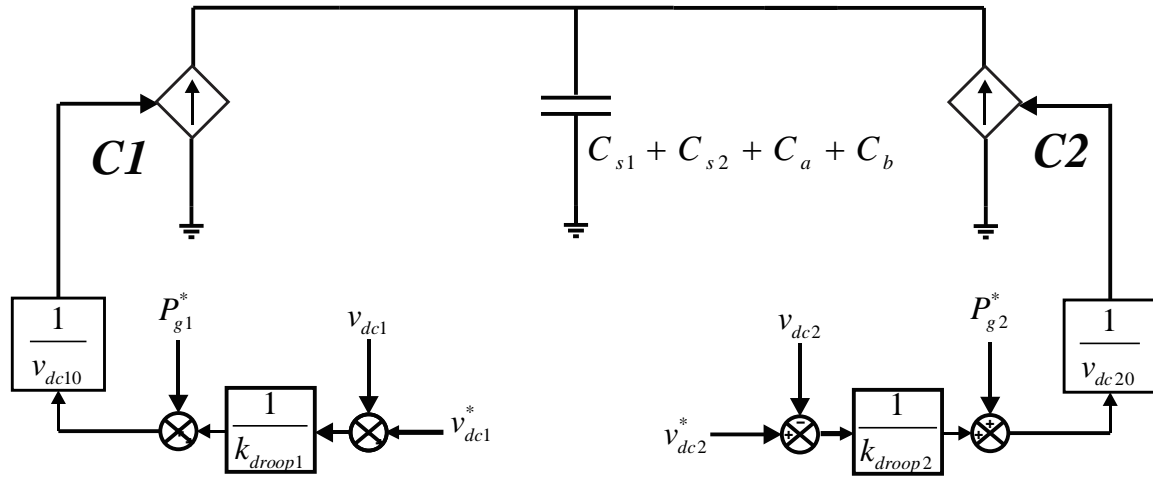


Figure 4.14 HVDC link equivalent circuit.

The equivalent linear block diagram is presented in

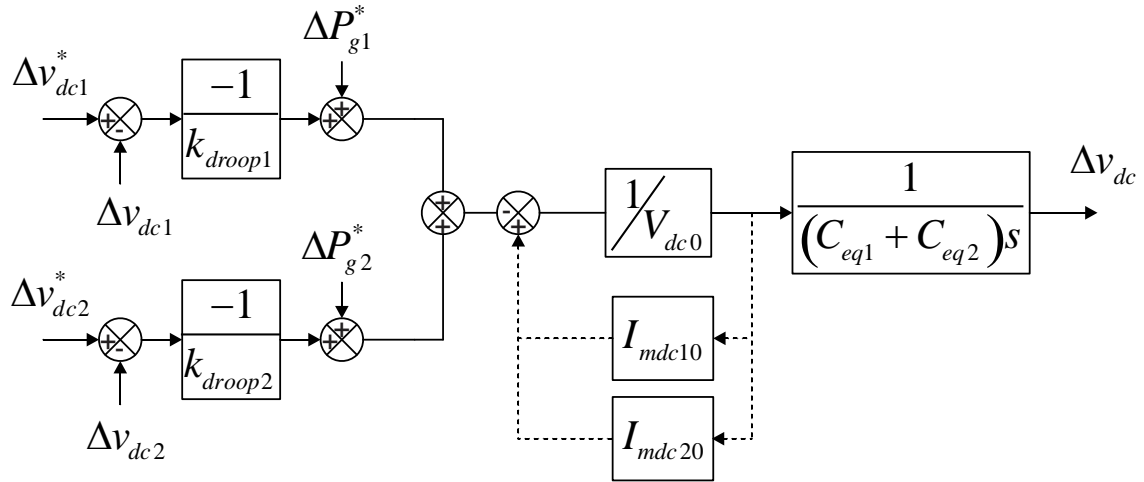


Figure 4.15 Block diagram of the equivalent HVDC link.

From which the first order fundamental polynomial is derived as

$$\frac{\Delta v_{dc}}{\Delta v_{dc}^*} = \frac{\frac{1}{\frac{1}{k_{droop1}} + \frac{1}{k_{droop2}}}}{1 + \frac{V_{dc0} v_{dc} (C_{eq1} + C_{eq2})}{1 + \frac{1}{\frac{1}{k_{droop1}} + \frac{1}{k_{droop2}}}} s} \quad (4.23)$$

in which the eigenvalue is,

$$\lambda = \frac{\frac{1}{k_{droop1}} + \frac{1}{k_{droop2}}}{V_{dc0} v_{dc} (C_{eq1} + C_{eq2})} \quad (4.24)$$

This first order transfer function is simple, describes the DC voltage behavior.

4.3.4 Three terminal DC grid model

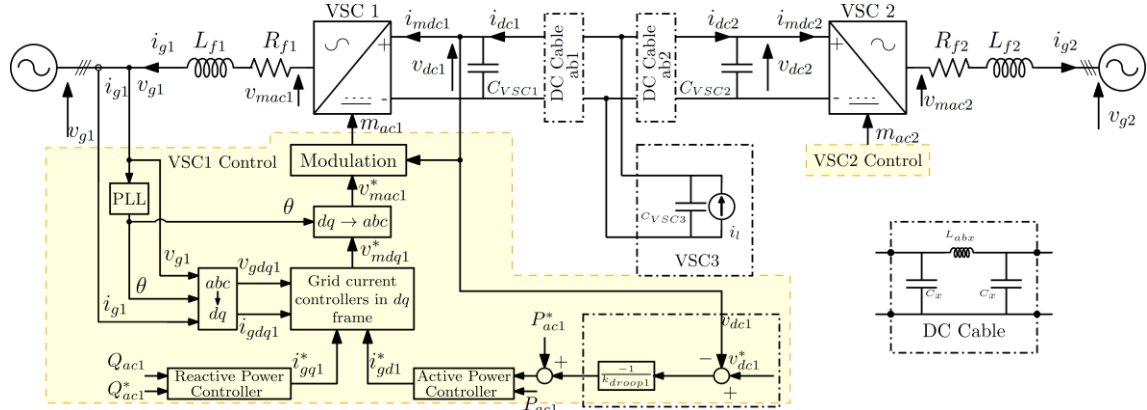


Figure 4.16 illustrates the overall scheme of the studied three terminals MTDC. Converters 1 and 2 are modeled with a classical two level droop-controlled VSC average models. The third terminal is only modeled with a current source i_l and its associated DC capacitor. The power of each station is supposed to be 1 GW. The DC grid is modeled with two PI sections of DC cable, *ab1* connecting the VSC 1 with VSC 3 and *ab2* for the connection of VSC 2 with VSC 3 (section *ab1* : 150km and *ab2* : 300km)

A. MTDC model

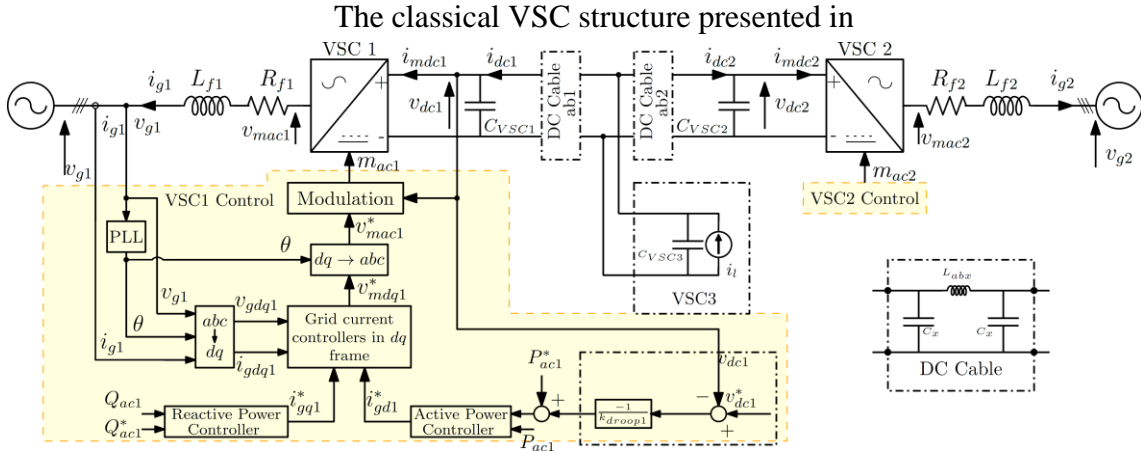


Figure 4.16 is composed of a three-phase reactor AC filter L_{f1} , R_{f1} . The capacitor C_{vsc1} , directly connected on the DC side, is lumped in parallel with the end-point capacitor of the DC cable C_x resulting in an equivalent capacitance expressed as :

$$\begin{aligned} C_{eq1} &= C_{vsc1} + C_{x1} \\ C_{eq2} &= C_{vsc2} + C_{x2} \end{aligned} \quad (4.25)$$

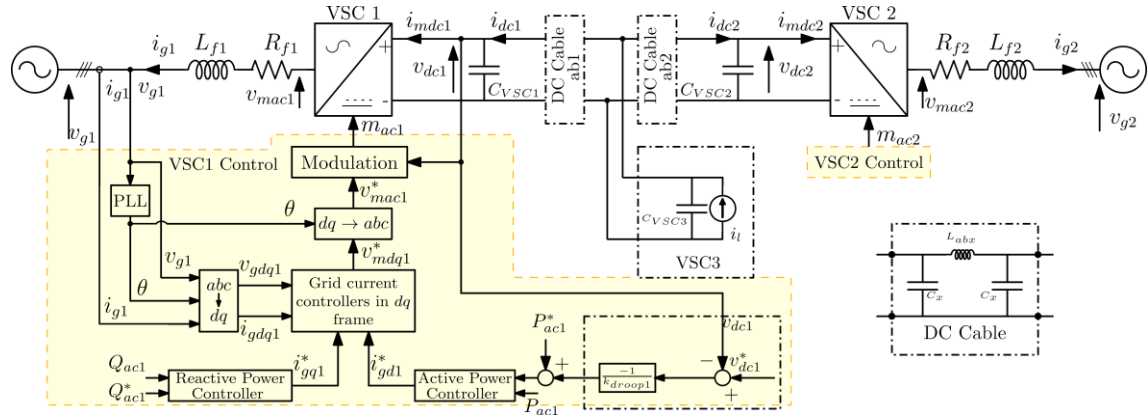
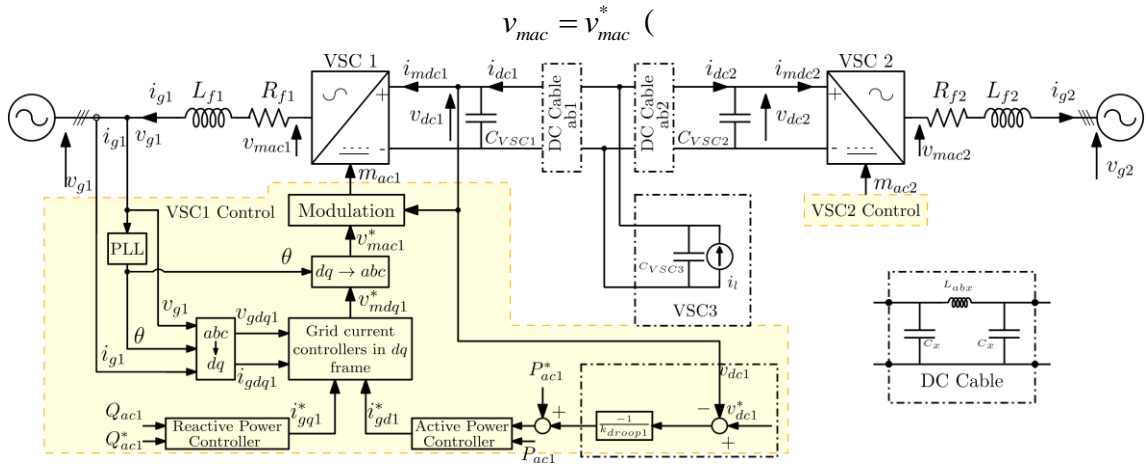


Figure 4.16 Three terminal MTDC grid with droop controlled VSC.

Some considerations are taken into account regarding the station dynamic equivalent:

The particular dynamic of the low level control and the switching devices are neglected:



- Figure 4.16).
- The system is considered under balanced conditions.
- Since the AC voltage source is considered here as perfect, the dynamic of the PLL is not taken into account.

For simplifying the model, i_{gq} is supposed to be null.

All the other equations are linear so, there are included in the same form as in the linearized model of the VSC. The complete block diagram of the linearized MTDC system is presented in Figure 4.17.

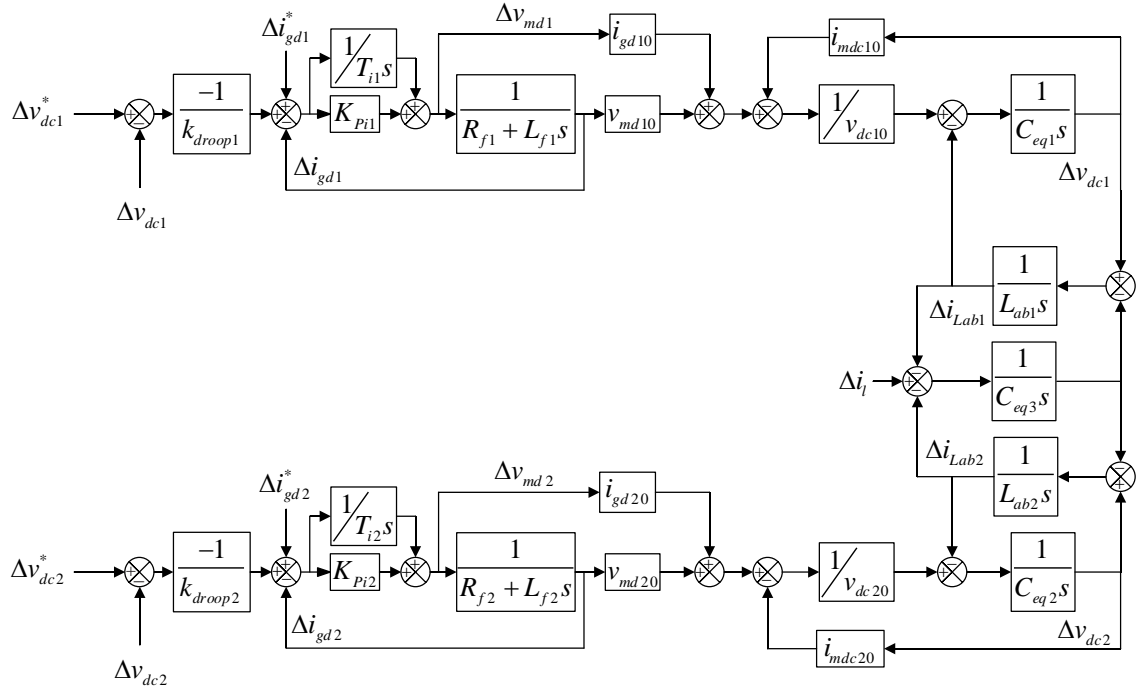


Figure 4.17 Block diagram of the MTDC system

where the variables in upper case and with the subscript 0 are the operating point, and the variables with the Greek symbol Δ refer to the deviation variables.

A. Model in per unit

As explained in Chapter 3, an accurate conclusion from the use of parametric sensitivity matrix supposes to have quantities without any unit. It is the reason why the use of per unit is mandatory in this type of analysis. With a linear model, the equations in per unit are the same as for the original ones. In the new model, all the per-unit elements are represented with a subscript “pu” for this section. The system in per unit can be expressed in a state-space form as follows:

$$\begin{bmatrix} \dot{v}_{dc1} \\ \dot{i}_{L_{ab1}} \\ \dot{i}_{L_{f1}} \\ v_{dc2} \\ \dot{i}_{L_{ab2}} \\ \dot{i}_{L_{f2}} \\ v_{dc3} \\ \dot{Int}_1 \\ \dot{Int}_2 \end{bmatrix} = \begin{bmatrix} \alpha_1 & \frac{-\omega_b}{4C_{eq1pu}} & \beta_1 & \frac{i_{gd10}k_{p1}\omega_b}{4C_{eq1pu}v_{dc10}} & 0 & 0 & 0 & 0 & 0 \\ \frac{2\omega_b}{L_{ab1pu}} & 0 & 0 & 0 & 0 & 0 & 0 & 0 & \frac{-2\omega_b}{L_{ab1pu}} \\ \frac{-k_{p1}}{k_{droop1}L_{f1pu}} & 0 & \frac{-k_{p1}-R_{s1pu}}{L_{f1pu}} & \frac{k_{p1}+R_{s1pu}}{L_{f1pu}} & 0 & 0 & 0 & 0 & 0 \\ \frac{-1}{k_{droop1}T_{i1}} & 0 & \frac{-1}{T_{i1}} & 0 & 0 & 0 & 0 & 0 & 0 \\ 0 & 0 & 0 & 0 & \alpha_2 & \frac{-\omega_b}{4C_{eq2pu}} & \beta_2 & \frac{i_{gd20}k_{p2}\omega_b}{4C_{eq2pu}v_{dc20}} & 0 \\ 0 & 0 & 0 & 0 & \frac{-2\omega_b}{L_{ab2pu}} & 0 & 0 & 0 & \frac{2\omega_b}{L_{ab2pu}} \\ 0 & 0 & 0 & 0 & \frac{-k_{p2}}{k_{droop2}L_{f2pu}} & 0 & \frac{-k_{p2}-R_{s2pu}}{L_{f2pu}} & \frac{k_{p2}+R_{s2pu}}{L_{f2pu}} & 0 \\ 0 & 0 & 0 & 0 & \frac{-1}{k_{droop2}T_{i2}} & 0 & \frac{-1}{T_{i2}} & 0 & 0 \\ 0 & \frac{-\omega_b}{4C_{eq3pu}} & 0 & 0 & 0 & \frac{-\omega_b}{4C_{eq3pu}} & 0 & 0 & 0 \end{bmatrix} \begin{bmatrix} v_{dc1} \\ i_{L_{ab1}} \\ i_{L_{f1}} \\ v_{dc2} \\ i_{L_{ab2}} \\ i_{L_{f2}} \\ v_{dc3} \\ Int_1 \\ Int_2 \end{bmatrix} \quad (4.26)$$

where,

$$\begin{aligned} \alpha_1 &= \frac{\omega_b (i_{mdc10}k_{droop1} - i_{gd10}k_{p1})}{4C_{eq1pu}k_{droop1}v_{dc10}} \\ a_2 &= \frac{\omega_b (i_{mdc20}k_{droop2} - i_{gd20}k_{p2})}{4C_{eq2pu}k_{droop2}v_{dc20}} \end{aligned} \quad (4.27)$$

$$\begin{aligned} \beta_1 &= \frac{\omega_b \left(v_{gd10} - \frac{i_{gd10}k_{p1}}{v_{dc10}} \right)}{4C_{eq1pu}} \\ \beta_2 &= \frac{\omega_b \left(v_{gd20} - \frac{i_{gd20}k_{p2}}{v_{dc20}} \right)}{4C_{eq2pu}} \end{aligned} \quad (4.28)$$

B. Analysis of the solution of the free-motion model

From the free motion system equations, prior knowledge of the system can be interpreted. The use prior knowledge of the system helps for the modal analysis. For example, the diagonal elements with zero in (4.26) assure that there is no strict diagonal dominance. Nevertheless, the few diagonal elements can have a strong importance for the solution of the system.

Consider the parameters in Table 4.2

Table 4.2 Parameters of the HVDC system

Element	Value in SI	Value in pu
C_{eq1}	2.3236×10^{-4} F	7.4749 pu
C_{eq2}	2.1383×10^{-4} F	6.8790 pu
C_{eq3}	2.5088×10^{-4} F	8.707pu
L_{ab1}	1.122 H	3.4422 pu
L_{ab2}	0.5610 H	1.7211 pu
L_f	0.0978 H	0.3pu
R_f	0.05 Ohm	1.221×10^{-4} pu

Two different conditions are considered for the free-motion system

- For $k_{droop}=0.5$

The matrix of the system is

$$A = \begin{bmatrix} -5.25 & -10.51 & 10.51 & 0 & 0 & 0 & 0 & 0 & 0 \\ 182.53 & 0 & 0 & 0 & 0 & 0 & -182.53 & 0 & 0 \\ -839.99 & 0 & -420 & 0 & 0 & 0 & 0 & 420 & 0 \\ 0 & 0 & 0 & 5.708 & 11.417 & 11.417 & 0 & 0 & 0 \\ 0 & 0 & 0 & -365.069 & 0 & 0 & 365.069 & 0 & 0 \\ 0 & 0 & 0 & -839.99 & 0 & -420 & 0 & 0 & 420 \\ 0 & 9.7314 & 0 & 0 & 9.7314 & 0 & 0 & 0 & 0 \\ -428.57 & 0 & -214.28 & 0 & 0 & 0 & 0 & 0 & 0 \\ 0 & 0 & 0 & -428.57 & 0 & -214.28 & 0 & 0 & 0 \end{bmatrix} \quad (4.29)$$

The eigenvalues are presented in Table 4.3.

Table 4.3 Eigenvalues for $k_{droop} = 0.5$

Eigenvalues	Frequency (Hz)	Damping ratio
$\lambda_{1,2} = -4.20 \pm 94.01i$	14.97	0.044
$\lambda_{3,4} = -11.03 \pm 48.1i$	7.85	0.223
$\lambda_5 = -14.37$	0	-
$\lambda_{6,7} = -198.05 \pm 225.26i$	47.73	0.66
$\lambda_{8,9} = -199.31 \pm 225.16i$	47.85	0.662

The solution of the system is derived from definition (2.29)

$$x(t) = \left[\sum_{i=1}^n e^{\lambda_i t} S_i^T \right] x(0)$$

For the current i_{Lab1} the solution is

$$[i_{Lab1}] = \left[\left(\frac{\partial \lambda_1}{\partial a_{12}} e^{\lambda_1 t} + \dots + \frac{\partial \lambda_9}{\partial a_{12}} e^{\lambda_9 t} \right) \left(\frac{\partial \lambda_1}{\partial a_{22}} e^{\lambda_1 t} + \dots + \frac{\partial \lambda_9}{\partial a_{22}} e^{\lambda_9 t} \right) \dots \left(\frac{\partial \lambda_1}{\partial a_{n2}} e^{\lambda_1 t} + \dots + \frac{\partial \lambda_9}{\partial a_{n2}} e^{\lambda_9 t} \right) \right] [x_0] \quad (4.30)$$

Each term of (4.30) corresponds to the elements of the sensitivity matrices, x_0 represent the initial conditions vector.

The first four terms of the solution equation (4.30) the elements of multiplu

$$\begin{aligned} t_1 &= \left((0.02 - 0.17i) e^{\lambda_1 t} + (0.02 + 0.17i) e^{\lambda_2 t} + (0.2 + 1.5i) e^{\lambda_3 t} + (0.2 - 1.5i) e^{\lambda_4 t} + (-0.43) e^{\lambda_5 t} + \right. \\ &\quad \left. (-0.02 + 0.02) e^{\lambda_6 t} + (-0.02 - 0.02) e^{\lambda_7 t} \right) \\ t_2 &= \left((0.09 - 0.01i) e^{\lambda_1 t} + (0.09 + 0.01i) e^{\lambda_2 t} + (0.42 - 0.7i) e^{\lambda_3 t} + (0.42 + 0.7i) e^{\lambda_4 t} + (-0.02) e^{\lambda_5 t} + \right. \\ &\quad \left. (-0.01 + 0.0) e^{\lambda_6 t} + (-0.02 - 0.00) e^{\lambda_7 t} \right) \\ t_3 &= \left((0.01 - 0.00i) e^{\lambda_1 t} + (0.01 + 0.00i) e^{\lambda_2 t} + (0.01 + 0.0i) e^{\lambda_3 t} + (0.01 - 0.0i) e^{\lambda_4 t} + (-0.02) e^{\lambda_5 t} + \right. \\ &\quad \left. (-0.01 + 0.0) e^{\lambda_6 t} + (-0.01 - 0.00) e^{\lambda_7 t} \right) \\ t_4 &= \left((0.05 - 0.54i) e^{\lambda_1 t} + (0.05 + 0.54i) e^{\lambda_2 t} + (0.13 + 1.06i) e^{\lambda_3 t} + (0.13 - 1.06i) e^{\lambda_4 t} + (-0.36) e^{\lambda_5 t} \right) \end{aligned} \quad (4.31)$$

The circled elements are the elements with greater contribution to the dynamics of the state.

The complete solution of the state is difficult to present, nevertheless the comparison between them gives interesting results.

- The term t_3 has small participation in the solution.
- The terms t_1 , t_2 and t_4 have an important contribution to the solution for the exponential terms $e^{\lambda_3 t}$ and $e^{\lambda_4 t}$

For the PF analysis, it is necessary that t_2 has to be more important, looking at the numbers of the exponential terms $e^{\lambda_3 t}$ and $e^{\lambda_4 t}$ it is clear that t_1 and t_4 have a bigger contribution to the solution.

4.4 Modular Multi-level Converter reduced model

The use of modular multilevel converter (MMC) is a real breakthrough compared with the classical 2 and 3 level converters. All new HVDC links are now using this kind of topology. The advantages are, low losses, modularity, scalability and low harmonic distortion (Abildgaard and Molinas 2012). The dynamic analysis is an important task to understand its behavior, control its dynamics, and avoid stability problems in the systems using MMC stations.

The Figure 4.18 shows the topology of a three phase Modular Multilevel Converter. It has three legs, one per phase, and each leg has two arms (upper and lower arm). N submodules connected in series compose the arms. The number of submodules can vary depending on the desired output voltage level and expected redundancy. For a 401-Level MMC-HVDC system N could be in the order of 400 up to 440 (Peralta, Saad, Denetiere, et al. 2012)

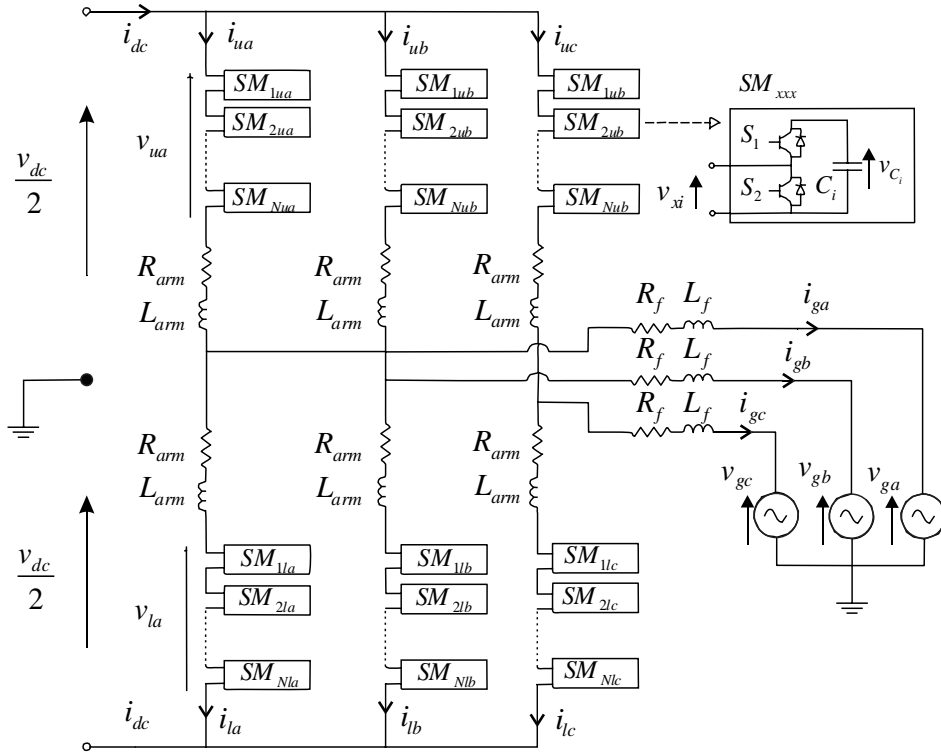


Figure 4.18 diagram of the modular multilevel converter

The MMC has the upper and lower arms composed by a series of blocks SM_{xxx} with two switches S_1 and S_2 . Each arm is connected to each phase of the AC sources (v_{ga} , v_{gb} , v_{gc}) and the upper and lower sides of the arms connected to the DC side of the converter.

The arm inductances (L_{arm}) limit the DC fault current gradients and support the voltage difference caused by the insertion and disconnection of the submodules. For limiting the current in case of AC fault, there are the inductances L_f in the AC side; they also help to control the grid current and limit the rise of current in the case of AC short circuit. The resistive part of the arm inductances and the output filter are noted as R_{arm} and R_f respectively.

This model can be very complex; its control has to be fast to provide the signals for each switch submodule. For this thesis as presented for the VSC converter the switching dynamics are not taken into account for simplification purposes. Nevertheless the simplification of this model has been developed in different forms (Bergna Diaz, Suul, and D'Arco 2015; Beddard and Barnes 2015; H Saad et al. 2014; Peralta, Saad, Denetière, et al. 2012)

The four different models in reduced complexity are presented in (H Saad et al. 2014) in the following form,

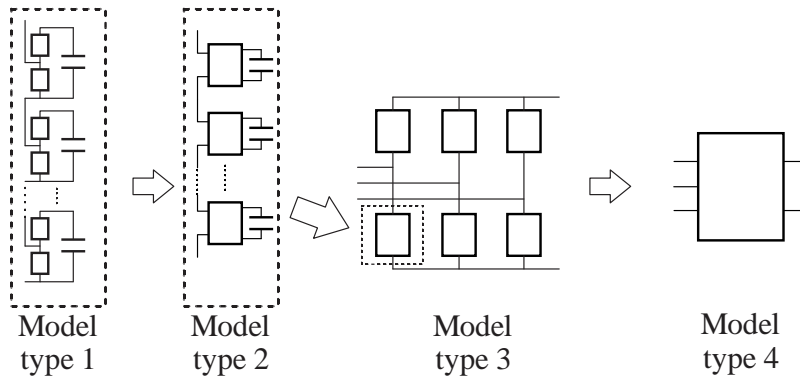


Figure 4.19 MMC models in decreasing complexity.

- Model 1: This model considers a detailed representation of power switches. The model presented uses an ideal controlled switch, two nonlinear (series and anti-parallel) diodes, and two snubber circuits.
- Model 2: This model replaces the power switches with ON/OFF resistors. This allows performing a Norton equivalent of the whole arm at each simulation step time, reducing the number of nodes of the circuit considerably.
- Model 3: In this model each MMC arm is averaged using the switching function concept of a half-bridge converter based on the assumption that all SM capacitor voltages are balanced (Delarue, Gruson, and Guillaud 2013).
- Model 4: Here the IGBT's and their diodes are not explicitly represented and the MMC behavior is modeled using controlled voltage and current sources.

The model type 3 represent a good dynamic behavior, it can still be simplified with reasonable assumptions (Freytes et al. 2016). In order to reduce the number of state variables and reduce dynamic complexity. Figure 4.20 depicts the MMC with arm average model (AAM),

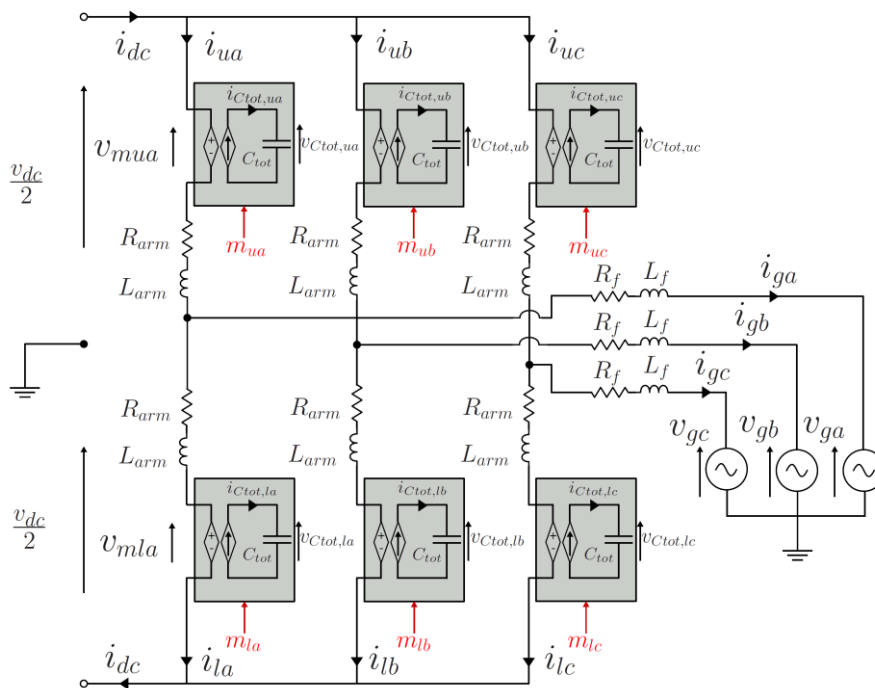


Figure 4.20 Model type 3.

This model assumes that the voltages of all the submodule capacitors are maintained in a close range, thus allowing to replace them by an equivalent one. Therefore, each arm includes an arm inductance L_{arm} , an arm resistance R_{arm} and an equivalent capacitor C_{tot} in parallel with a chopper.

The voltages $v_{m_{u_j}}$, $v_{m_{l_j}}$ and the currents i_{u_j} , i_{l_j} of each arm ($j = a, b, c$) are described as follows,

$$\begin{aligned} v_{m_{u_j}} &= m_{u_j} v_{C_{tot,u_j}} \\ v_{m_{l_j}} &= m_{l_j} v_{C_{tot,l_j}} \\ i_{C_{tot,u_j}} &= m_{u_j} i_{u_j} \\ i_{C_{tot,l_j}} &= m_{l_j} i_{l_j} \end{aligned} \quad (4.32)$$

where,

- $v_{C_{tot,u_j}}$ and $v_{C_{tot,l_j}}$ are the voltages across the capacitors in the upper and lower arms
- m_{u_j} and m_{l_j} are the corresponding instantaneous duty cycle
- $i_{C_{tot,u_j}}$ and $i_{C_{tot,l_j}}$ are the currents through capacitors of the upper and lower arms.

The Kirchhoff's law for each arm gives,

$$\begin{aligned} \frac{v_{dc}}{2} - v_{m_{u_j}} - L_{arm} \frac{di_{u_j}}{dt} - R_{arm} i_{u_j} - L_f \frac{di_{g_j}}{dt} - R_f i_{g_j} - v_{g_j} &= 0 \\ \frac{v_{dc}}{2} - v_{m_{l_j}} - L_{arm} \frac{di_{l_j}}{dt} - R_{arm} i_{l_j} - L_f \frac{di_{g_j}}{dt} - R_f i_{g_j} - v_{g_j} &= 0 \end{aligned} \quad (4.33)$$

The addition of the upper and lower parts yields,

$$v_{vj} - v_{g_j} = L_{eq}^{ac} \frac{di_{g_j}}{dt} + R_{eq}^{ac} i_{g_j} \quad (4.34)$$

where:

$$\begin{aligned} i_{g_j} &= i_{u_j} - i_{l_j} \\ v_{vj} &= \frac{v_{m_{u_j}} - v_{m_{l_j}}}{2} \\ R_{eq}^{ac} &= \frac{(R_{arm} + 2R_f)}{2} \\ L_{eq}^{ac} &= \frac{(L_{arm} + 2L_f)}{2} \end{aligned} \quad (4.35)$$

Equation (4.34) describes the AC side dynamics of the AAM.

For the DC side, the following equations are defined,

$$v_{dc} - v_{diff_j} = 2L_{arm} \frac{di_{diff_j}}{dt} + 2R_{arm} i_{diff_j} \quad (4.36)$$

where,

$$i_{diff_j} = \frac{i_{u_j} + i_{l_j}}{2} \quad (4.37)$$

$$v_{diff_j} = v_{m_{lj}} + v_{m_{uj}}$$

The relation of AC and the DC side (4.34) and (4.36) define the dynamics of the lower and upper parts of the arms. At this point, the model has three arms, each one with upper and lower part.

4.4.1 Simplification of the AAM

Considering that under controlled operation, the upper and lower voltages are equal,

$$v_{C_{tot_{uj}}} = v_{C_{tot_{lj}}} \approx \bar{v}_{C_{tot_j}} \quad (4.38)$$

where $\bar{v}_{C_{tot_j}}$ is the average voltage of the capacitor in the j arm.

$$\bar{v}_{C_{tot_j}} = \frac{v_{C_{tot_{uj}}} + v_{C_{tot_{lj}}}}{2} \quad (4.39)$$

With this assumption, each arm relationship becomes,

$$2C_{tot} \frac{d\bar{v}_{C_{tot}}}{dt} = m_{dc} i_{diff} - m_{ac} i_g = i_{mdc} - i_{mac} \quad (4.40)$$

where,

$$m_{ac} = \frac{(m_l - m_u)}{2} \quad (4.41)$$

$$m_{dc} = (m_u + m_l)$$

Then each phase of the AAM is reduced as shown in Figure 4.21.

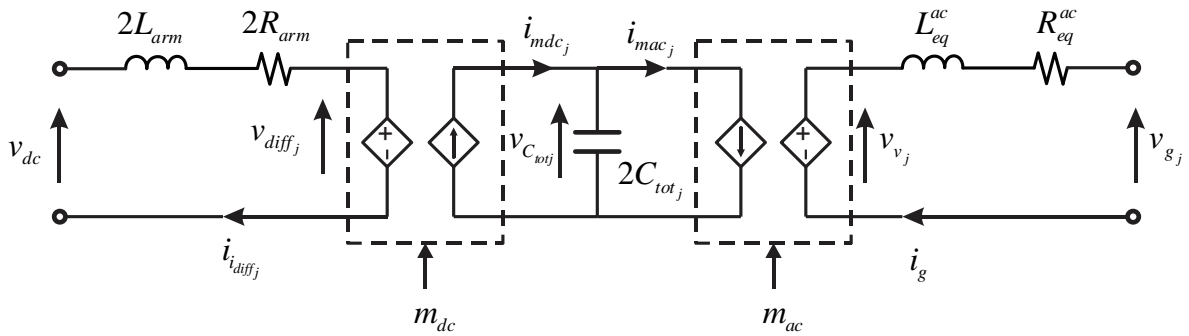


Figure 4.21 Reduced phase-arm circuit.

Under balanced conditions, each arm has the same amount of energy stored. Therefore in order to further simplify the model for a balanced AC system, it is reasonable to assume.

$$\bar{v}_{C_{tot_a}} = \bar{v}_{C_{tot_b}} = \bar{v}_{C_{tot_c}} \quad (4.42)$$

Following this assumption, it follows that,

$$2C_{tot^*} \frac{d\bar{v}_{C_{tot}}}{dt} = \sum_{j=a,b,c} i_{mdc_j} - \sum_{j=a,b,c} i_{mac_j} \quad (4.43)$$

This assumption allows to replace the six capacitors of the arms by a capacitor six times bigger.

$$C_{tot*} = 2C_{tot_a} + 2C_{tot_b} + 2C_{tot_c} \quad (4.44)$$

Moreover, it allows saying that the current is equally distributed among the arms. Thus, the modulation signals become,

$$m_{dc} = m_{dc_a} = m_{dc_b} = m_{dc_c} \quad (4.45)$$

This model is suitable when the focus is on the AC and DC current dynamics and the total energy stored in each arm. Finally, this allows comes up with the model in Figure 4.22.

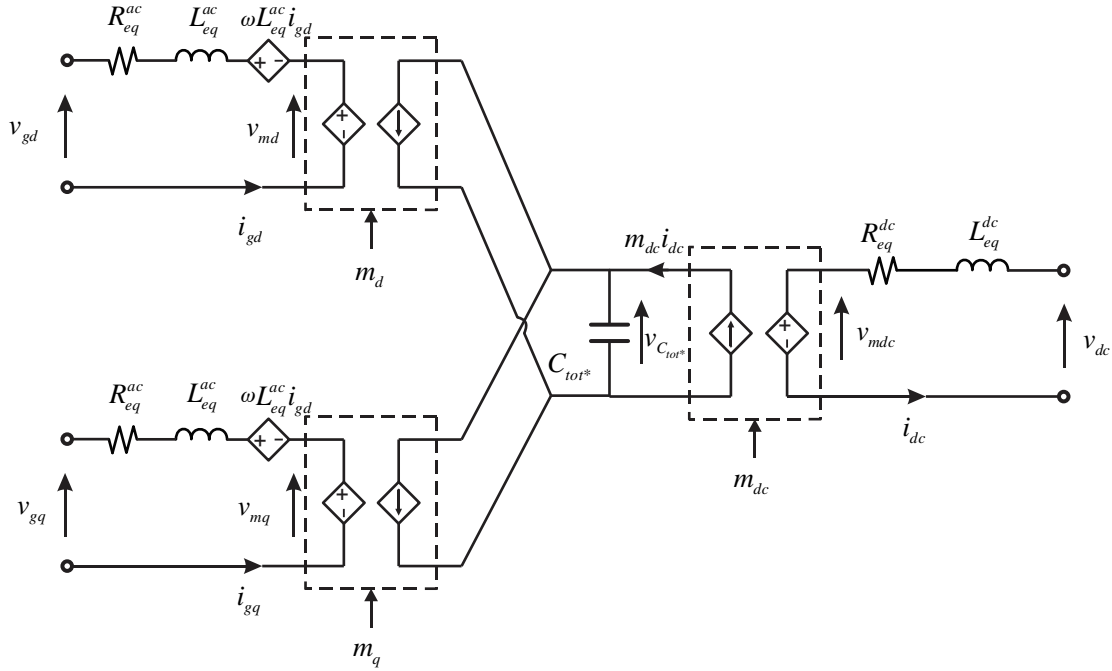


Figure 4.22 Equivalent dq0 MMC average model.

The equations of the average model for the AC side are

$$\begin{aligned} L_{eq}^{ac} \frac{di_{gd}}{dt} &= v_{md} - v_{gd} - R_{eq}^{ac} i_{gd} + \omega L_{eq}^{ac} i_{gq} \\ L_{eq}^{ac} \frac{di_{gq}}{dt} &= v_{mq} - v_{gq} - R_{eq}^{ac} i_{gq} - \omega L_{eq}^{ac} i_{gd} \end{aligned} \quad (4.46)$$

For the DC side

$$\begin{aligned} L_{eq}^{dc} \frac{di_{dc}}{dt} &= v_{mdc} - v_{dc} - R_{eq}^{dc} i_{dc} \\ C_{tot*} \frac{d\bar{v}_{C_{tot*}}}{dt} &= i_{mdc} - i_{mac} \end{aligned} \quad (4.47)$$

where the equivalent resistance and inductance are,

$$\begin{aligned} L_{eq}^{dc} &= \frac{2L_{arm}}{3} \\ R_{eq}^{dc} &= \frac{2R_{arm}}{3} \end{aligned} \quad (4.48)$$

The AC voltages and currents are

$$\begin{aligned} v_{md} &= m_d \bar{v}_{Ctot}, \quad v_{mq} = m_q \bar{v}_{Ctot} \\ i_{mac} &= m_d i_{gd} + m_q i_{gq} \end{aligned} \quad (4.49)$$

The DC side voltages and currents are

$$\begin{aligned} v_{mdc} &= m_{dc} \bar{v}_{Ctot} \\ i_{mdc} &= m_{dc} i_{dc} \end{aligned} \quad (4.50)$$

Choosing the energy in the MMC as the state variable its derivative is

$$\frac{dW_{tot}}{dt} = v_{mdc} i_{dc} - (v_{md} i_{gd} + v_{mq} i_{gq}) \quad (4.51)$$

which is non-linear

As it can be seen, this simplified MMC model is very similar to the VSC model. One more modulation is added between the capacitor C_{tot}^* and the DC bus.

4.4.2 Control strategy

The MMC control is much more complex than VSC control. It exists many possibilities to achieve this control. One solution is briefly presented here. More details can be find in (Samimi 2015)

As mentioned before, the MMC equivalent on the AC side is similar to the VSC station, The additional inductance and its proper capacitance in the DC side makes the MMC station different to control. As in the two-level VSC, a control strategy based on two cascaded loops (namely inner and outer loops) is applied.

A. Inner controllers

Figure 4.23 presents the inner controls for the MMC. The AC side presents a classical current controller. The DC side has a controller for the current i_{dc}

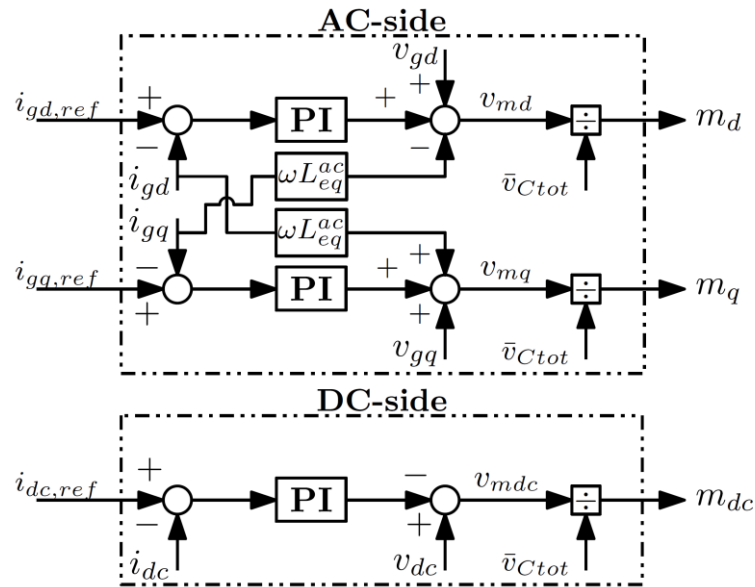


Figure 4.23 Inner controllers.

The blocks marked as PI are classical proportional and integral controllers. Inner control loops are required to be the fastest.

As the AC side in the MMC is similar to the VSC the control of the current is practically equal with the considerations required for this converter. In addition, in the MMC station a control of the differential currents in the arms is needed for the DC side.

B. Outer controllers

The outer loops correspond to the control of the voltage in the DC side and the total energy stored in the station (Hani Saad et al. 2015). Figure 4.25 presents the control blocks in the loops. The AC side controls the AC current in the inner control and the power of the AC side or the voltage in the DC side. The DC side controls the DC current and the total energy stored in the MMC. The control of the energy is based in the conservation of the energy exchanged in the converter.

The power controllers (P_{ac} control and Q_{ac} control) are the outer controllers of the AC side. Similarly, to the inner controllers, they use a structure of PI controllers.

If the energy reference of the controller is a constant value, as considered in (Hani Saad et al. 2015), then the equivalent capacitor C_{tot}^* is completely decoupled from the DC grid. However, if the energy reference is associated with the square of the DC voltage v_{dc}^2 , the equivalent capacitor may consider as if it were connected to the DC bus

To sum up, there are two alternatives for the control of the energy:

- Including the energy on in the cable capacitance in the DC grid.
- Excluding the energy on in the cable capacitance in the DC grid.

If the stored energy of the MMC is shared with the DC bus. The MMC behaves as if the C_{tot}^* were connected to the DC bus.

• Voltage control

If the converter is regulating the DC voltage, the d-axis current reference is generated by a DC voltage control loop equipped with a controller to ensure there is no static error on the slack-bus. In this case, an IP controller is used to limit the overshoot when changing the DC bus voltage reference.

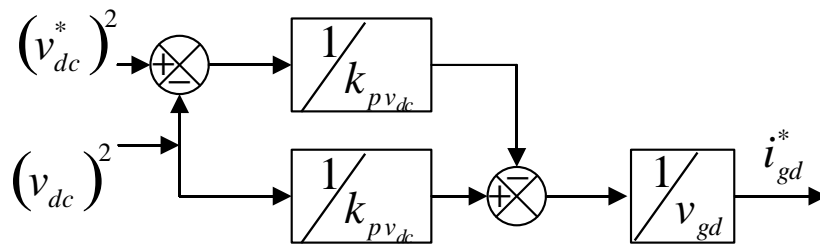


Figure 4.24 v_{dc} voltage controller.

- *Energy control*

The control of the total energy W_{tot} is based on the regulation of the exchanged energy between AC and DC sides (Hani Saad et al. 2015). For this control, a classic PI control is used.

Figure 4.25 presents the complete nonlinear system with its control (Akkari 2016).

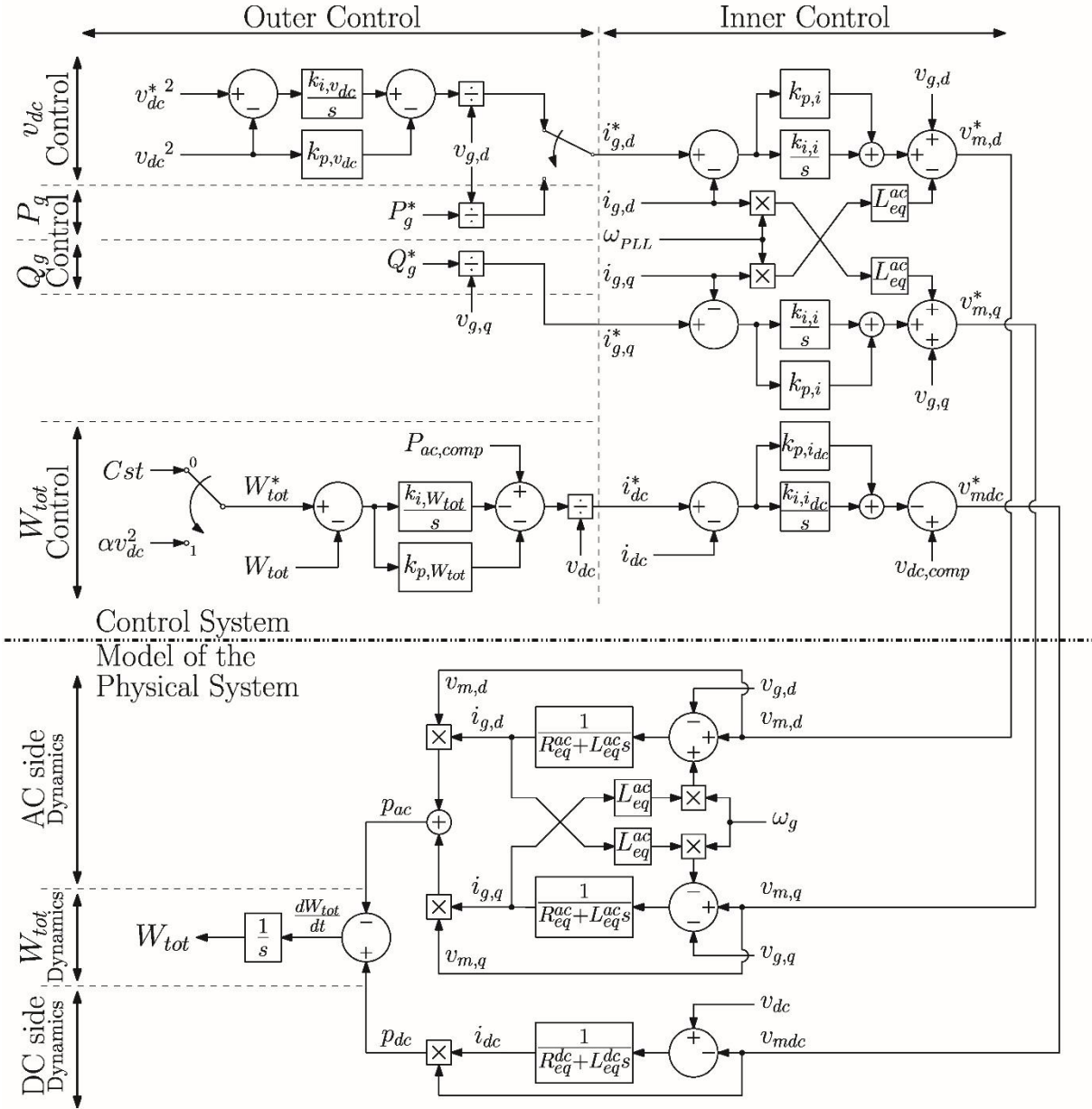


Figure 4.25 Block diagram of the complete non-linear system.

4.4.3 Linearization

As for the VSC, a linearized model proposed for the MMC.

The linearization of the energy equation (4.51) is,

$$\frac{d\Delta W_{tot}}{dt} = i_{dc0}\Delta v_{mdc} + v_{dc0}\Delta i_{dc} - (v_{md0}\Delta i_{gd} + v_{mq0}\Delta i_{gq} + i_{gq0}\Delta v_{mq} + i_{gd0}\Delta v_{md}) \quad (4.52)$$

Figure 4.26 presents the block diagram of the linear MMC station.

Figure 4.26 Linearized physical system.

4.4.4 One station MMC in a MTDC network

Consider the model given in Figure 4.27,

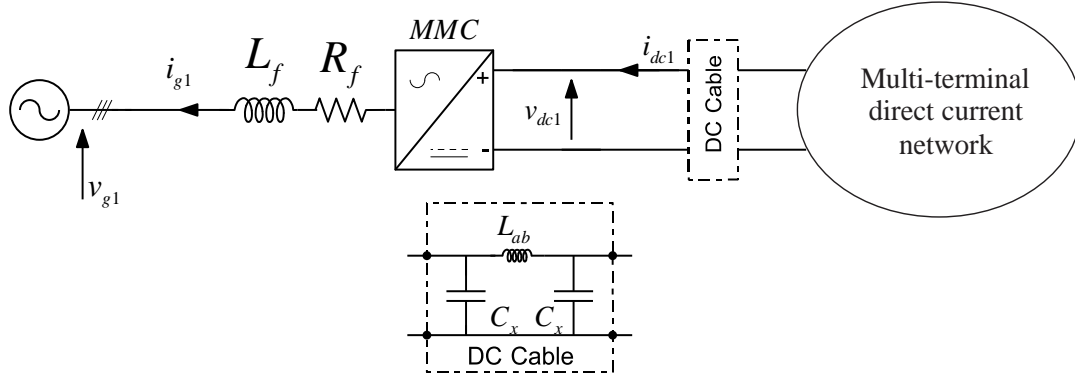


Figure 4.27 MMC station connected to a MTDC network.

This model is composed by a MMC station connected through a cable to a multi-terminal direct current network.

A. Power Control

Figure 4.28 presents the block diagram of the MMC station controlling the power.

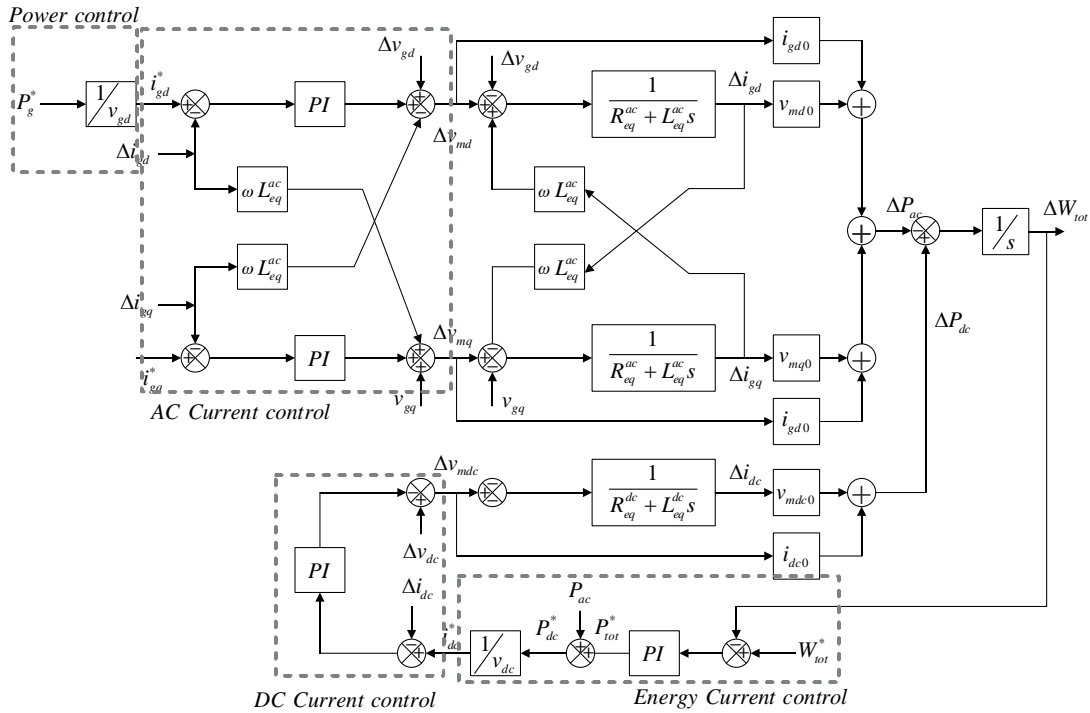


Figure 4.28 Block diagram of a power controlled MMC.

This model has the following state variables

Table 4.4 State variables of the MMC power controlled in a MTDC

State variable	description
Δi_{gd}	Current of the d-axis in the AC side
Δi_{gq}	Current of the q-axis in the AC side
Δi_{dc}	Current of the DC side
ΔW_{tot}	Total energy in the station
Int, i_{gd}	State of the controller of the AC current (d-axis)
Int, i_{gq}	State of the controller of the AC current (q-axis)
Int, i_{dc}	State of the controller of current in the DC side
Int, W_{tot}	State of the controller of energy

B. Voltage control

For the control of the voltage in the DC

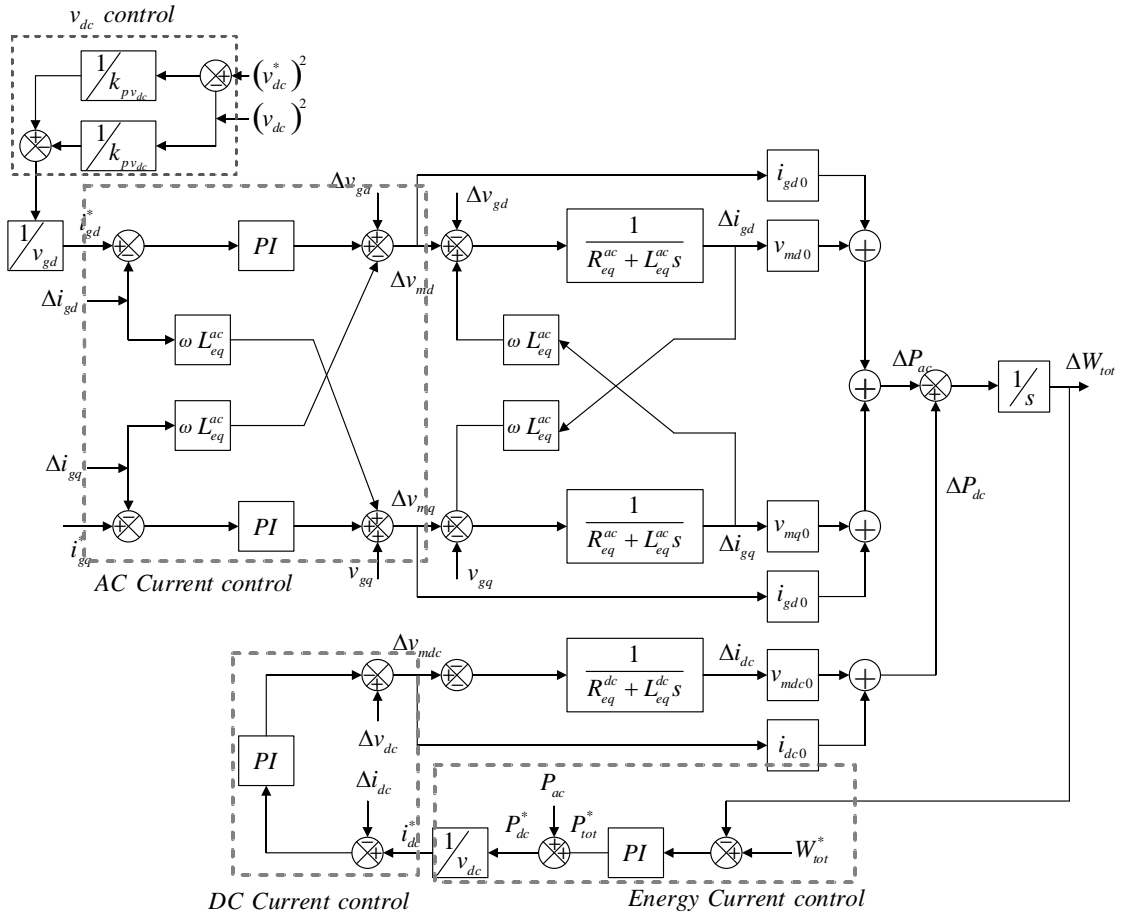


Figure 4.29 Block diagram of a voltage controlled MMC

Table 4.5 State variables of the MMC voltage controlled in a MTDC

State variable	description
Δi_{gd}	Current of the d-axis in the AC side
Δi_{gq}	Current of the q-axis in the AC side
Δi_{dc}	Current of the DC side
ΔW_{tot}	Total energy in the station
Int, i_{gd}	State of the controller of the AC current (d-axis)
Int, i_{gq}	State of the controller of the AC current (q-axis)
Int, i_{dc}	State of the controller of current in the DC side
Int, v_{dc}	State of the controller of voltage in the DC side
Int, W_{tot}	State of the controller of energy

4.4.5 Two stations MMC in a HVDC

Consider the diagram of the system in Figure 4.30, it presents an HVDC link using the

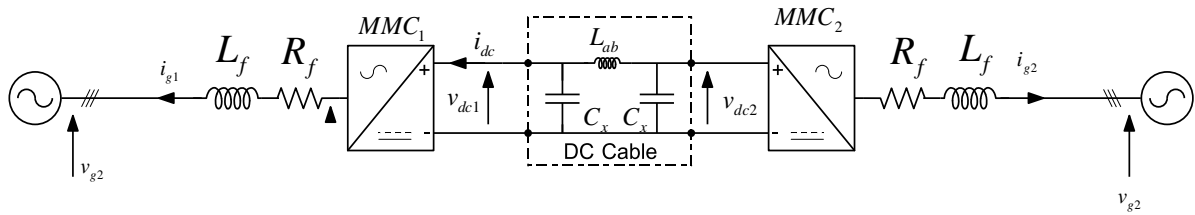


Figure 4.30 HVDC link with MMC stations.

This model has one station (MMC1) controlling the transferred power ΔP_{tot} and the other (MMC2) controlling the voltage v_{dc2} , the same structures of as in Figure 4.28 and Figure 4.29 respectively.

In total having 20 state variables,

Table 4.6 State variables of the MMC1

State variable	description
Δi_{gd}	Current of the d-axis in the AC side
Δi_{gq}	Current of the q-axis in the AC side
Δi_{dc}	Current of the DC side
ΔW_{tot}	Total energy in the station
Int, i_{gd}	State of the controller of the AC current (d-axis)

Int, i_{gq}	State of the controller of the AC current (q-axis)
Int, i_{dc}	State of the controller of current in the DC side
Int, W_{tot}	State of the controller of energy

Table 4.7 State variables of the MMC2

State variable	description
Δi_{gd}	Current of the d-axis in the AC side
Δi_{gq}	Current of the q-axis in the AC side
Δi_{dc}	Current of the DC side
ΔW_{tot}	Total energy in the station
Int, i_{gd}	State of the controller of the AC current (d-axis)
Int, i_{gq}	State of the controller of the AC current (q-axis)
Int, i_{dc}	State of the controller of current in the DC side
Int, v_{dc2}	State of the controller of voltage in the DC side
Int, W_{tot}	State of the controller of energy

Table 4.8 State variables of the cable

v_{dc1}	Voltage in the output of the MMC
v_{dc2}	Voltage in the side of the MTDC
i_{Lab}	Current in the inductance of the cable

4.5 Conclusions

The knowledge of the systems before the parametric analysis is important to understand the relationships between the parameters and the eigenvalues.

The VSC is one of the most studied converters, therefore its importance for using a new tool of analysis.

The model describing the MMC is a new model developed by the team of the L2EP, in a collaborative work leaded by Julian Freytes and others. The description of the Models and validations is made in a form that allows having automatically the linearized time invariant equations.

An automatic analysis tool was implemented for these models in the MATLAB ® environment. Appendix A describes the routine of parametric sensitivity analysis for the models described in this chapter. This computational tool adjusts to any LTI system automatically, having the appropriated inputs, it gives the PSM and the analysis tables.

Next chapter presents the results of the analysis performed in the systems detailed in the present chapter.

Chapter 5 Modal analysis on HVDC systems

5.1 Objectives of the analysis

Chapter 4 has presented the basic topologies used in HVDC application. In this chapter, the methodology of sensitivity parametric matrix is applied and compared with the participation factor. Different examples are chosen to illustrate this methodology. The simple system presented in section 4.3.3 is first analyzed. Due to the simplicity of the model, it cannot be considered as very realistic but since it is simple, it is possible to compare the obtain results with analytical results to confirm the accuracy of the method.

The second example is an elementary Multi Terminal DC grid connected to AC system with Voltage Source Converter. This example shows clearly the limit of the participation factor method.

The third example is focused on MMC: the converter by itself first and then in a HVDC link.

5.2 Simplified equivalent DC link

In a first step, a simplified HVDC link is analyzed. Figure 5.1 recalls the structure of this system.

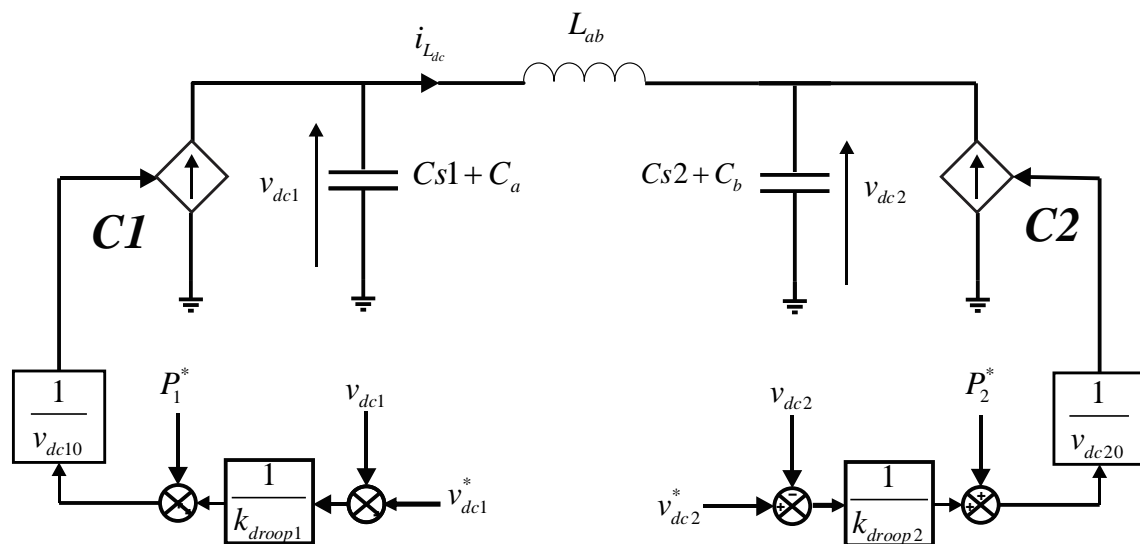


Figure 5.1 Topology of the simplified HVDC

For this model the following parameters are considered

Table 5.1 Parameters of the HVDC network

Element	Value	Element	Value
$Cs1$	195.31 μF	L_{ab}	2.2439 H
$Cs2$	195.31 μF	Ca	37.044 μF
$k_{droop1,2}$	0.2	Cb	37.044 μF
V_b	640 kV	Cable length l	300 km
P_b	1 MW		

As it can be seen in equation (4.21), the coefficient of the matrix are not symmetric while we could expect a symmetry due to the topology of the studied system. Looking at equation (4.22) the coefficients α_1 and α_2 depend on the operating points $i_{dc\ pu01}$ and $i_{dc\ pu02}$ which have the same magnitude but with opposite sign.

The AC per unit has been chosen, the numerical value of the state matrix is then deduced,

$$\begin{bmatrix} \dot{u}_{s1,pu} \\ \dot{u}_{s2,pu} \\ \dot{i}_{L_{ab},pu} \end{bmatrix} = \begin{bmatrix} -42.02 & 0 & 10.507 \\ 0 & -63.04 & -10.507 \\ -182.53 & 182.53 & 0 \end{bmatrix} \begin{bmatrix} u_{s1,pu} \\ u_{s2,pu} \\ i_{L_{ab},pu} \end{bmatrix} \quad (5.1)$$

The eigenvalues are

Table 5.2 Eigenvalues

Eigenvalues (rad/s)	Frequency (Hz)	Damping coefficient
$\lambda_{1,2} = -25.51 + 55.47i$	9.71	0.41
$\lambda_3 = -54.06$	–	1

The first pair of eigenvalues $\lambda_{1,2}$ can be associated to the coupling between the elements in the cable: equivalent capacitances C_{eq1} , C_{eq2} , and the inductance L_{ab} . Indeed, considering only the PI filter CLC the theoretical natural resonance frequency is

$$f_n \approx \frac{1}{2\pi} \sqrt{\frac{1}{L_{ab}} \left(\frac{1}{C_{eq1}} + \frac{1}{C_{eq2}} \right)} \approx 9.85 \text{ Hz} \quad (5.2)$$

As it can be noticed, the theoretical frequency is very similar to the calculated one.

The second pole λ_3 , can be calculated when neglecting the effect of the inductance (see section 4.3.3). The real eigenvalue on this first order model is,

$$1 + \frac{v_{dc0\ pu} v_{dcpu}}{\frac{P_1}{k_{droop1}} + \frac{P_2}{k_{droop2}}} \frac{4(C_{eq1\ pu} + C_{eq2\ pu})}{\omega_b s}$$

the theoretical eigenvalue is

$$s = -52.53 \text{ rad/s} \quad (5.3)$$

which is close to $\lambda_3 = -54.06 \text{ rad/s}$.

For change of reference of voltage in the station 2 v_{dc2}^* the dynamic response of the system is presented in Figure 5.2.

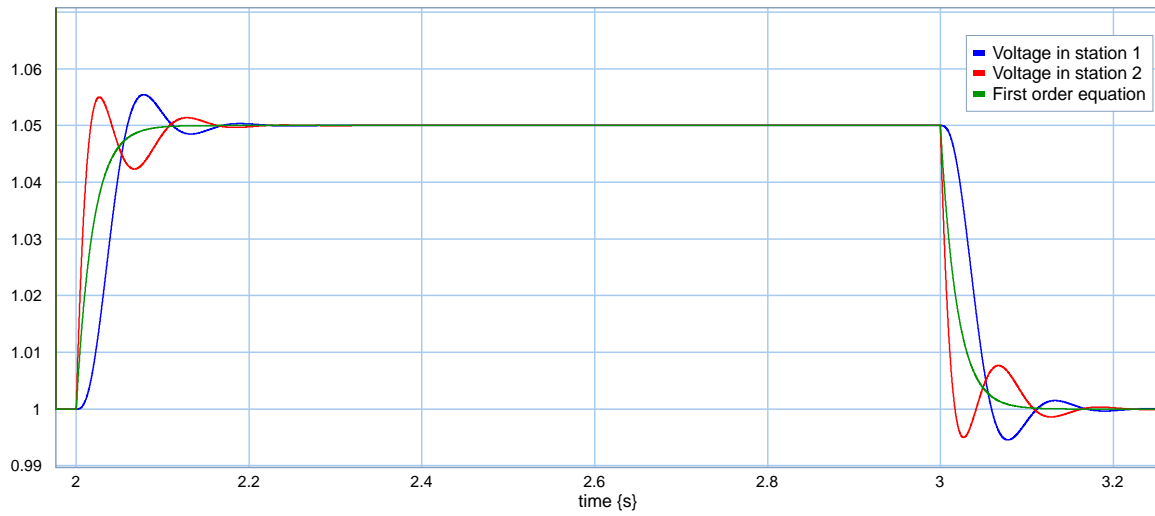


Figure 5.2 Dynamic response of the voltage in the link for a change of 0.1pu in the voltage reference.

the participation factor matrix is,

$$P = \begin{bmatrix} 0.32 - 0.05i & 0.32 + 0.05i & 0.368 \\ 0.17 - 0.17i & 0.17 + 0.17i & 0.659 \\ 0.51 + 0.22i & 0.51 - 0.22i & -0.02 \end{bmatrix} \quad (5.4)$$

the modulus of each element of P are,

$$\begin{bmatrix} v_{dc1} \\ v_{dc2} \\ i_{Lab} \end{bmatrix} |P| = \begin{bmatrix} \lambda_1 & \lambda_2 & \lambda_3 \\ 0.3206 & 0.3206 & 0.368 \\ 0.2394 & 0.2394 & 0.659 \\ 0.5601 & 0.5601 & 0.027 \end{bmatrix} \quad (5.5)$$

To each state variable, it is possible to associate a parameter

Table 5.3 Association between state variables and parameters

v_{dc1}	v_{dc2}	i_{Lab}
C_{eq1}	C_{eq2}	L_{ab}

$$Sp = \begin{bmatrix} \frac{\partial \lambda_1}{\partial (C_{eq1,pu})} & \frac{\partial \lambda_2}{\partial (C_{eq1,pu})} & \frac{\partial \lambda_3}{\partial (C_{eq1,pu})} \\ \frac{\partial \lambda_1}{\partial (C_{eq2,pu})} & \frac{\partial \lambda_2}{\partial (C_{eq2,pu})} & \frac{\partial \lambda_3}{\partial (C_{eq2,pu})} \\ \frac{\partial \lambda_1}{\partial L_{ab1,pu}} & \frac{\partial \lambda_2}{\partial L_{ab1,pu}} & \frac{\partial \lambda_3}{\partial L_{ab1,pu}} \end{bmatrix} = \begin{bmatrix} 2.369 - 2.007i & 2.369 + 2.007i & 3.695 \\ 1.3529 - 1.161i & 1.3529 + 1.161i & 2.916 \\ 0.218 - 9.9321i & 0.218 + 9.9321i & -0.436 \end{bmatrix} \quad (5.6)$$

Normalizing by rows using the L2 norm,

$$\begin{bmatrix} C_{eq1,pu} \\ C_{eq2,pu} \\ L_{ab1,pu} \end{bmatrix} Sp_{nr} = \begin{array}{c} \begin{matrix} \lambda_1 & \lambda_2 & \lambda_3 \end{matrix} \\ \begin{bmatrix} 0.41 + 0.35i & 0.41 - 0.35i & 0.64 \\ 0.35 + 0.3i & 0.35 - 0.3i & 0.76 \\ 0.02 + 0.71i & 0.02 - 0.71i & -0.03 \end{bmatrix} \end{array} \quad (5.7)$$

At this stage, an important remark has to be done about the elements of both matrices. In P , the numerical values have no physical meaning whereas in Sp_{nr} , it is possible to draw some information from these values.

From (5.6) and (5.7), small changes in the inductance L_{ab} produce changes in the imaginary part of λ_1 and λ_2 . As graphical illustration, Figure 5.3 presents the eigenvalue trajectories subject to a modification of $\pm 10\%$ for L_{ab} from its nominal value.

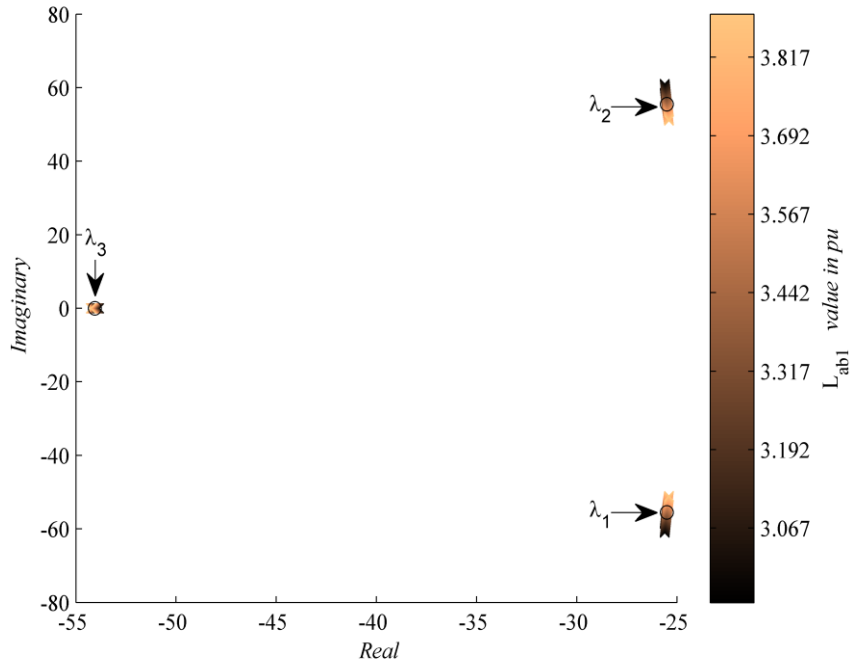


Figure 5.3 Eigenvalue trajectories changing L_{ab} .

In Figure 5.3, the circle in the trajectories represent the eigenvalues for the nominal parameter values.

Changing the value of the equivalent capacitance C_{eq1} in $\pm 10\%$ the eigenvalue trajectories are presented in Figure 5.4,

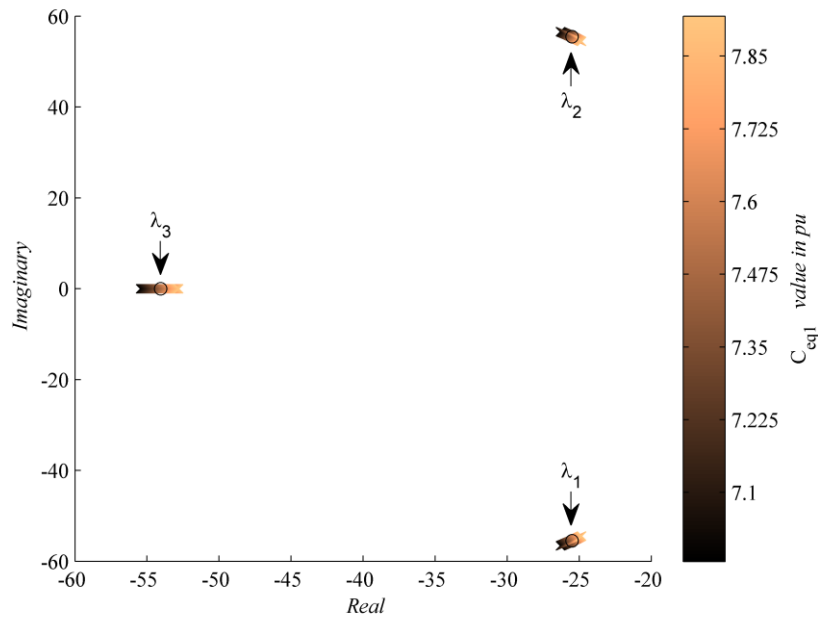


Figure 5.4 Eigenvalue trajectories changing the equivalent capacitance C_{eq1} .

Considering the normalization by columns,

$$\begin{matrix} & \lambda_1 & \lambda_2 & \lambda_3 \\ \begin{bmatrix} C_{eq1,pu} \\ C_{eq2,pu} \\ L_{ab1,pu} \end{bmatrix} S_{p_{nc}} = & \begin{bmatrix} 0.22+0.19i & 0.22-0.19i & 0.78 \\ 0.13+0.11i & 0.13-0.11i & 0.62 \\ 0.02+0.94i & 0.02-0.94i & -0.09 \end{bmatrix} \end{matrix} \quad (5.8)$$

Equation (5.8) reveals that $\lambda_{1,2}$ are sensitive to $C_{eq1,pu}$, $C_{eq2,pu}$ and $L_{ab1,pu}$ which is normal since this poles are linked with the natural resonance frequency of the CLC filter. As also expected λ_3 mainly depends on $C_{eq1,pu}$ and $C_{eq2,pu}$.

Consider variations in parameters k_{droop1} and k_{droop2} in the state equations, the parametric sensitivity matrix becomes,

$$S_p = \begin{bmatrix} \frac{\partial \lambda_1}{\partial k_{droop1}} & \frac{\partial \lambda_2}{\partial k_{droop1}} & \frac{\partial \lambda_3}{\partial k_{droop1}} \\ \frac{\partial \lambda_1}{\partial k_{droop2}} & \frac{\partial \lambda_2}{\partial k_{droop2}} & \frac{\partial \lambda_3}{\partial k_{droop2}} \end{bmatrix} \quad (5.9)$$

using the parameter values of Table 5.1 and the equation (3.3), the PSM normalized by columns is,

$$\begin{matrix} & \lambda_1 & \lambda_2 & \lambda_3 \\ \begin{bmatrix} k_{droop1} \\ k_{droop2} \end{bmatrix} S_{p_{nc}} = & \begin{bmatrix} 0.789-0.135i & 0.789+0.135i & 0.487 \\ 0.425-0.421i & 0.425+0.421i & 0.873 \end{bmatrix} \end{matrix} \quad (5.10)$$

A change of 0.02 in k_{droop1} and k_{droop2} produces the trajectories in Figure 5.5. It can be seen that λ_3 is more sensitive to a variation on k_{droop2} than on a variation on k_{droop1} .

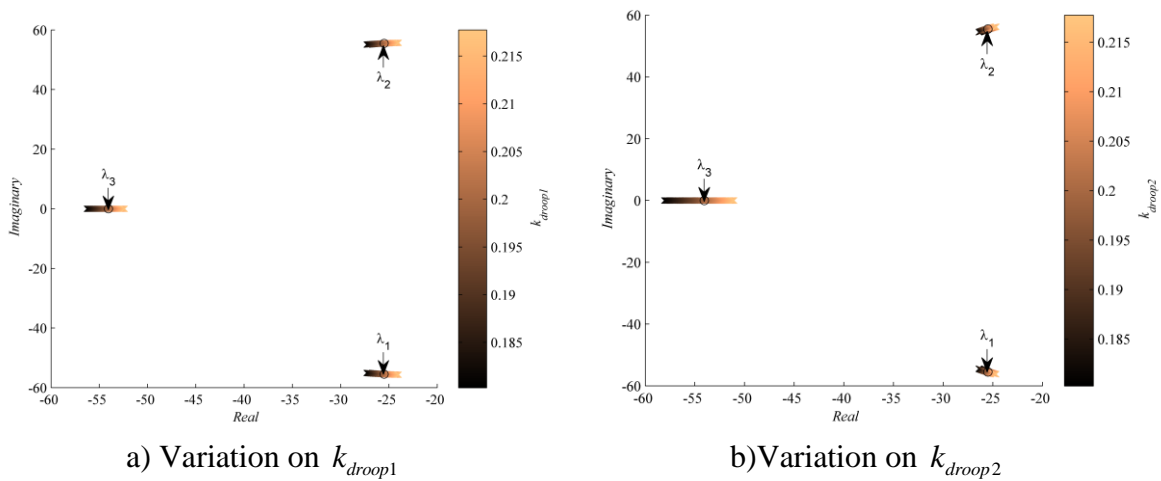


Figure 5.5 Eigenvalue Trajectories with a change on k_{droop1} and k_{droop2} .

From the analysis presented in (5.10), the eigenvalue λ_3 is mostly controlled by the k_{droop2} parameter. The integration of the control parameters to the Sp_{nc} matrix is possible only when the control parameters and the physical parameters have the same units. In this case the parameters k_{droop1} and k_{droop2} are linked to the power units.

Additionally, the integration of the control parameters in the analysis may hide some properties since the modes seems only sensitive to the control parameters. In the following examples, both results will be presented: either the parameters of the control and the power part in the same matrix or two different matrixes. This remark highlights that the conclusion drawn from the analysis of this matrix highly depends on the choice of the parameters integrated in the matrix.

5.3 Dynamic analysis of a three terminal MTDC

After the study of a simplified HVDC link model, the three points HVDC system define in section 4.3.4 is analyzed. The main parameters of the control and the system are given, the dynamics of this system is studied with respect to the variation of the droop value. In (Rault et al. 2013), a clear connection between the droop value and the response time of a simplified VSC MTDC system has been demonstrated. 3 decreasing values are analyzed: 0.5, 0.2 and 0.1 which means decreasing time response of the voltage control.

Since participation factors link eigenvalues to state variable and sensitivity matrix eigenvalue to parameters, a strict comparison is not straightforward. Hence, only physical parameters relative to state variables have been placed in the sensitivity matrix.

Table 5.4 Association between state variables and parameters

v_{dc1}	$i_{L_{ab1}}$	$i_{L_{f1}}$	v_{dc2}	$i_{L_{ab2}}$	$i_{L_{f2}}$	v_{dc3}
C_{eq1}	L_{ab1}	L_{f1}	C_{eq2}	L_{ab2}	L_{f2}	C_{eq3}

A. High droop value

The numerical values has already been presented in section 4.3.4. for a droop value set to 0.5.

The system has the nine eigenvalues presented in Table 5.5

Table 5.5 Eigenvalues for $k_{droop} = 0.5$

Eigenvalues	Frequency (Hz)	Damping ratio
$\lambda_{1,2} = -4.20 \pm 94.01i$	14.97	0.044
$\lambda_{3,4} = -11.03 \pm 48.1i$	7.85	0.223
$\lambda_5 = -14.37$	-	1

$\lambda_{6,7} = -198.05 \pm 225.26i$	47.73	0.66
$\lambda_{8,9} = -199.31 \pm 225.16i$	47.85	0.662

Figure 5.6 presents the time domain simulation for the system subject to a change of power in the third station of 0.1 pu. The signal shows a first order response combined with a slightly damped second order response. The frequency of the pseudo oscillation approximately corresponds to $\lambda_{1,2}$

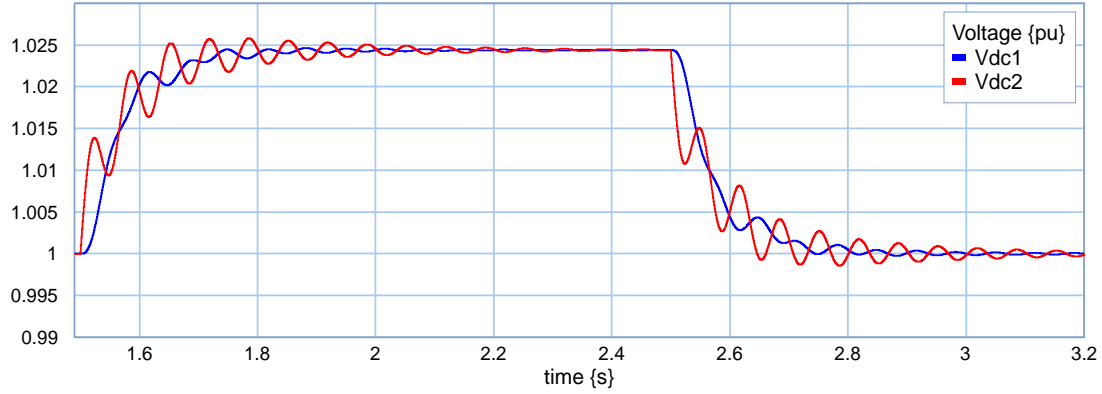


Figure 5.6 Voltage response.

Before analyzing the participation factor and the sensitivity matrix, some intuitive considerations may be done:

- λ_5 corresponds to the first order pole found in (Rault et al. 2013) assuming a simple DC network only composed of capacitors the theoretical value is -14 rad/s .
- $\lambda_{6,7}$ and $\lambda_{8,9}$ are relative to the current loop. Since the chosen time response is 10 ms with a damping of 0.7, the theoretical natural frequency is: 47.7 Hz.

Looking only to the physical elements chosen in (5.11), the matrix Sp_{nc} is:

	λ_1	λ_2	λ_3	λ_4	λ_5	λ_6	λ_7	λ_8	λ_9
C_{eq1}	ε	ε	$0.18 + 0.23i$	$0.18 - 0.23i$	0.64	ε	ε	ε	ε
L_{ab1}	ε	ε	$0.04 + 0.85i$	$0.04 - 0.85i$	ε	ε	ε	ε	ε
L_{f1}	ε	ε	ε	ε	ε	ε	ε	$0.99 + 0.07i$	$0.99 - 0.05i$
C_{eq2}	ε	ε	$0.03 + 0.16$	$0.03 - 0.16i$	0.54	ε	ε	ε	ε
L_{ab2}	$0.01 + 0.97i$	$0.01 - 0.97i$	$-0.04 + 0.38i$	$-0.04 - 0.38i$	ε	ε	ε	ε	ε
L_{f2}	ε	ε	ε	ε	ε	$0.99 + 0.07i$	$0.99 - 0.07i$	ε	ε
C_{eq3}	$-0.01 + 0.15i$	$-0.01 - 0.15i$	ε	ε	0.53	ε	ε	ε	ε

(5.11)

The participation factors are:

$$P = \begin{matrix} & \lambda_1 & \lambda_2 & \lambda_3 & \lambda_4 & \lambda_5 & \lambda_6 & \lambda_7 & \lambda_8 & \lambda_9 \\ \begin{matrix} v_{dc1} \\ i_{Lab1} \\ i_{Lf1} \\ v_{dc2} \\ i_{Lab2} \\ i_{Lf2} \\ v_{dc3} \\ Int_1 \\ Int_2 \end{matrix} & \begin{bmatrix} \varepsilon & \varepsilon & 0.29 - 0.14i & 0.29 + 0.14i & 0.38 & \varepsilon & \varepsilon & \varepsilon & \varepsilon \\ \varepsilon & \varepsilon & 0.42 + 0.08i & 0.42 - 0.08i & \varepsilon & \varepsilon & \varepsilon & \varepsilon & \varepsilon \\ \varepsilon & \varepsilon & \varepsilon & \varepsilon & \varepsilon & \varepsilon & \varepsilon & 0.50 - 0.49i & 0.50 + 0.49i \\ 0.18 - 0.06i & 0.18 + 0.06i & 0.17 + 0.01i & 0.17 - 0.01i & 0.30 & \varepsilon & \varepsilon & \varepsilon & \varepsilon \\ 0.41 + 0.01i & 0.41 - 0.01i & \varepsilon & \varepsilon & \varepsilon & \varepsilon & \varepsilon & \varepsilon & \varepsilon \\ \varepsilon & \varepsilon & \varepsilon & \varepsilon & \varepsilon & 0.50 - 0.49i & 0.50 + 0.49i & \varepsilon & \varepsilon \\ 0.29 + 0.04i & 0.29 - 0.04i & \varepsilon & \varepsilon & 0.34 & \varepsilon & \varepsilon & \varepsilon & \varepsilon \\ \varepsilon & \varepsilon & \varepsilon & \varepsilon & \varepsilon & \varepsilon & \varepsilon & 0.50 + 0.46i & 0.50 - 0.46i \\ \varepsilon & \varepsilon & \varepsilon & \varepsilon & \varepsilon & 0.50 + 0.46i & 0.50 - 0.46i & \varepsilon & \varepsilon \end{bmatrix} \end{matrix} \quad (5.12)$$

In Sp_{nc} and P , the elements circled:

- in green: means that similar information may be drawn from both matrices.
- in red: means that different information may be drawn from both matrices.

The terms with a modulus inferior to the modulus of $0.1 \pm 0.1i$ are presented with ε .

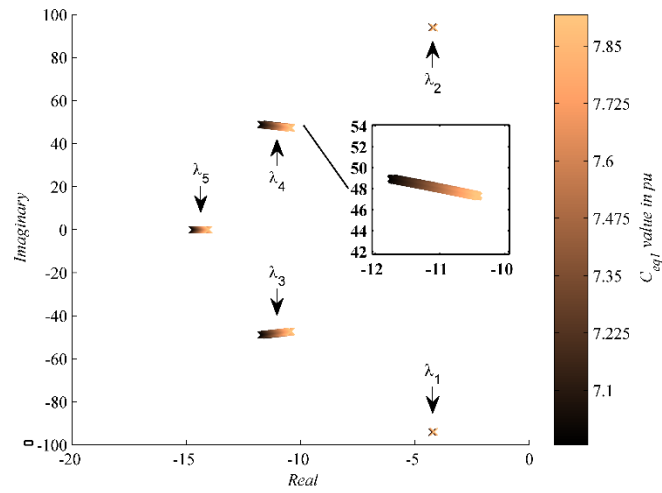
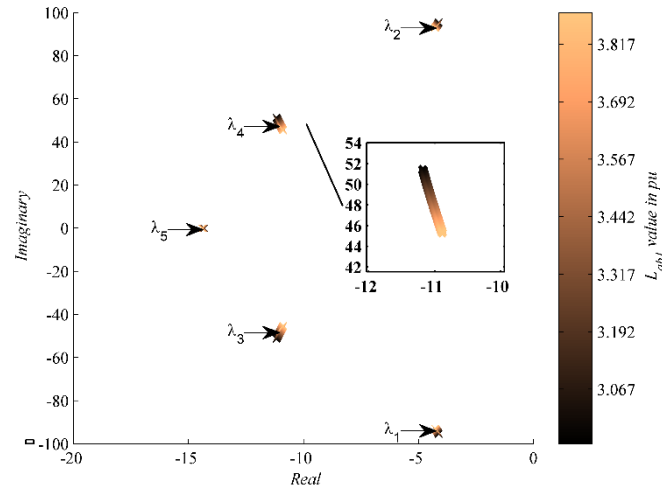
In this case, the results obtain with P and Sp_{nc} are nearly similar:

- λ_5 : P and Sp_{nc} confirm that this mode is mainly depending on the capacitors.
- $\lambda_{6,7}$ and $\lambda_{8,9}$: P and Sp_{nc} confirm that these modes are mainly associated with the AC current loop
- $\lambda_{1,2}$ are related to C_{eq3} (v_{dc3}), and L_{ab2} (i_{Lab2})
- $\lambda_{3,4}$ are related to C_{eq1} , (v_{dc1}), C_{eq2} (v_{dc2}) and L_{ab1} , (i_{Lab1})

There is only the natural coupling on the cable sections. In models where the coupling is not strong between parameters, the results of the parametric sensitivity and the participation factors can lead to similar results.

At this stage, an important remark has to be done about the elements of both matrices. In P , the numerical values have no physical meaning whereas in Sp_{nc} , it is possible to draw some information from these values. Indeed, each element represents the derivative of a pole with respect to a given parameter. Hence, a high modulus of an element compare with the other elements in the same column is relative to a high sensitivity of the pole to the parameter but the complex number gives also the direction of the evolution of the pole.

Figure 5.7 and Figure 5.8 presents the evolution of the nine poles with respect to C_{eq1} and L_{ab1} . The evolution of the λ_4 is relative to elements in Sp_{nc} matrix: $0.18 - 0.23i$ for C_{eq1} , $0.04 - 0.85i$ for L_{ab1} .


 Figure 5.7 Eigenvalue evolution for changing $C_{eq1} \pm 0.5$ pu .

 Figure 5.8 Eigenvalue evolution for changing $L_{abl} \pm 0.5$ pu .

B. Medium droop value

In this section, the droop value is set to 0.2 on both VSC stations; the eigenvalues are given in Table V.3.

 Table 5.6 Eigenvalues for $k_{droop} = 0.2$

Eigenvalues	Frequency (Hz)	Damping ratio
$\lambda_{1,2} = -10.53 \pm 89.7i$	14.37	0.044
$\lambda_{3,4} = -25.34 \pm 41.12i$	7.68	0.524
$\lambda_5 = -38.36$	-	1
$\lambda_{6,7} = 180.63 \pm 244.67i$	48.40	0.593
$\lambda_{8,9} = 184.10 \pm 243.78i$	47.61	0.602

Figure 5.9 presents the time domain simulation for the system subject to the same events as previously.

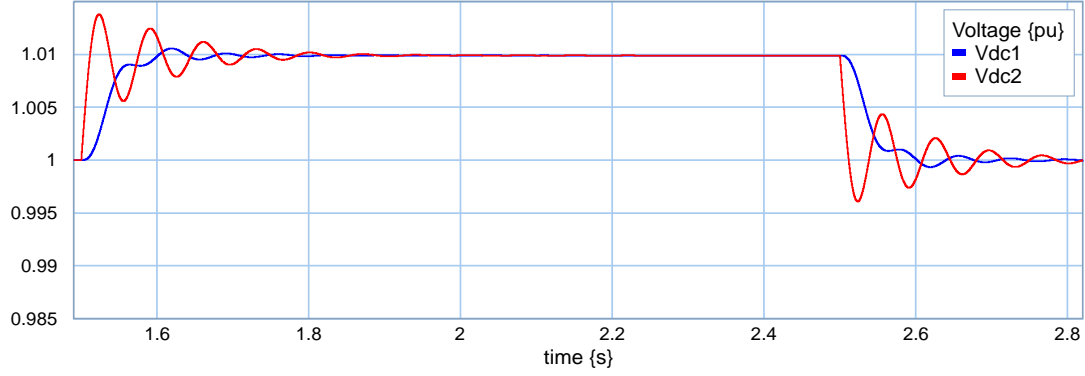


Figure 5.9 Voltage response of the VSC stations

$\lambda_{6,7}$ and $\lambda_{8,9}$ are nearly the same as previously which is normal since there are relative to the current loop.

λ_5 has increased which is consistent with the analysis proposed in (Rault et al. 2013), however a very important difference is noticed between Sp_{nc} and P . Sp_{nc} shows clearly that this pole not only depends on the capacitors but also on L_{ab1} , L_{ab2} , L_{f2} . This phenomena is not noticed in P . Moreover, the origin of $\lambda_{1,2}$ is different in Sp_{nc} and P .

For $\lambda_{3,4}$, the information given by P and Sp_{nc} can be considered as nearly similar.

$$Sp_{nc} = \begin{matrix} \begin{matrix} C_{eq1} \\ L_{ab1} \\ L_{f1} \\ C_{eq2} \\ L_{ab2} \\ L_{f2} \\ C_{eq3} \end{matrix} & \begin{matrix} \lambda_1 & \lambda_2 & \lambda_3 & \lambda_4 & \lambda_5 & \lambda_6 & \lambda_7 & \lambda_8 & \lambda_9 \end{matrix} \\ \begin{bmatrix} \epsilon & \epsilon & 0.24 + 0i & 0.24 - 0i & 0.69 & \epsilon & \epsilon & \epsilon & \epsilon \\ \epsilon & \epsilon & 0.17 + 0.76i & 0.17 - 0.76i & -0.26 & \epsilon & \epsilon & \epsilon & \epsilon \\ \epsilon & \epsilon & 0.07 + 0.18i & 0.07 - 0.18i & 0.45 & \epsilon & \epsilon & 0.99 + 0.12i & 0.95 - 0.12i \\ \epsilon & \epsilon & 0.12 + 0.16i & 0.12 - 0.16i & 0.35 & \epsilon & \epsilon & \epsilon & \epsilon \\ 0.13 + 0.95i & 0.13 - 0.95i & -0.22 + 0.43i & -0.22 - 0.43i & \epsilon & \epsilon & \epsilon & \epsilon & \epsilon \\ 0.11 + 0.1i & 0.11 - 0.1i & -0.08 + 0.14i & -0.08 - 0.14i & 0.23 & 0.95 + 0.13i & 0.95 - 0.13i & \epsilon & \epsilon \\ \epsilon & \epsilon & \epsilon & \epsilon & 0.28 & \epsilon & \epsilon & \epsilon & \epsilon \end{bmatrix} \end{matrix} \quad (5.13)$$

$$P = \begin{matrix} \begin{matrix} v_{dc1} \\ i_{L_{a1}} \\ i_{L_{f1}} \\ v_{dc2} \\ i_{L_{a2}} \\ i_{L_{f2}} \\ v_{dc3} \\ Int_1 \\ Int_2 \end{matrix} & \begin{matrix} \lambda_1 & \lambda_2 & \lambda_3 & \lambda_4 & \lambda_5 & \lambda_6 & \lambda_7 & \lambda_8 & \lambda_9 \end{matrix} \\ \begin{bmatrix} \epsilon & \epsilon & 0.17 - 0.26i & 0.17 + 0.26i & 0.56 & \epsilon & \epsilon & \epsilon & \epsilon \\ \epsilon & \epsilon & 0.44 + 0.15i & 0.44 - 0.15i & \epsilon & \epsilon & \epsilon & \epsilon & \epsilon \\ \epsilon & \epsilon & \epsilon & \epsilon & \epsilon & \epsilon & \epsilon & 0.48 - 0.50i & 0.48 + 0.50i \\ 0.10 - 0.15i & 0.10 + 0.15i & 0.24 - 0.03i & 0.24 + 0.03i & 0.26 & 0.03 + 0.14i & 0.03 - 0.14i & \epsilon & \epsilon \\ 0.43 - 0.01i & 0.43 + 0.01i & 0.08 + 0.12i & 0.08 - 0.12i & \epsilon & \epsilon & \epsilon & \epsilon & \epsilon \\ \epsilon & \epsilon & \epsilon & \epsilon & \epsilon & 0.49 - 0.50i & 0.49 + 0.50i & \epsilon & \epsilon \\ 0.33 + 0.11i & 0.33 - 0.11i & \epsilon & \epsilon & 0.24 & \epsilon & \epsilon & \epsilon & \epsilon \\ \epsilon & \epsilon & \epsilon & \epsilon & \epsilon & \epsilon & \epsilon & 0.48 + 0.36i & 0.48 - 0.36i \\ \epsilon & \epsilon & \epsilon & \epsilon & \epsilon & 0.49 + 0.36i & 0.49 - 0.36i & \epsilon & \epsilon \end{bmatrix} \end{matrix} \quad (5.14)$$

C. Small droop value

In this section, the droop value is set to 0.1 on both VSC, it leads to new values for the eigenvalues presented in Table 5.7.

Table 5.7 Eigenvalues for $k_{droop} = 0.1$

Eigenvalues	Frequency (Hz)	Damping ratio
$\lambda_{1,2} = -11.92 \pm 80.23i$	12.9	0.147
$\lambda_{3,4} = -44.60 \pm 8.07i$	7.36	0.984
$\lambda_5 = -81.58$	0	-
$\lambda_{6,7} = -157.60 \pm 282.89i$	51.53	0.486
$\lambda_{8,9} = -162.92 \pm 278.91i$	5148	0.506

The voltage response produced for this case is presented in Figure 5.10

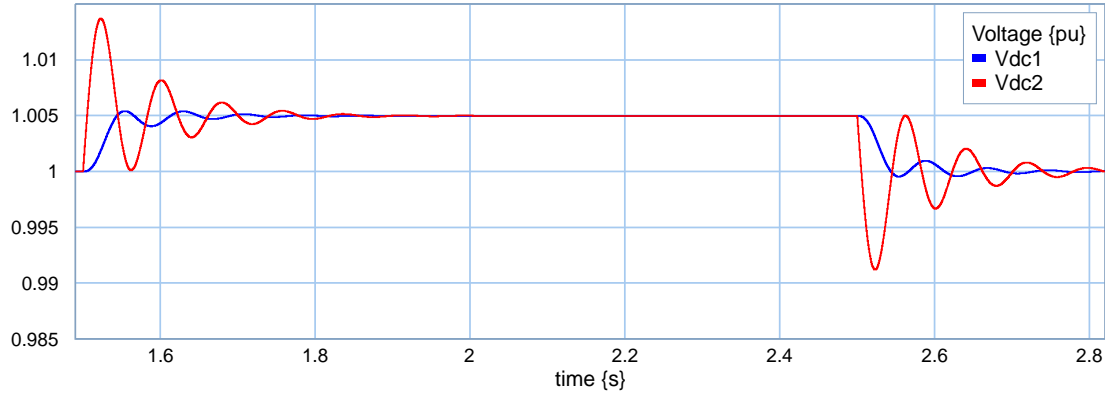


Figure 5.10 Voltage response.

The matrix Sp_{nc} is

$$\begin{matrix}
 \begin{matrix} C_{eq1} \\ L_{ab1} \\ L_{f1} \\ C_{eq2} \\ L_{ab2} \\ L_{f2} \\ C_{eq3} \end{matrix}
 \end{matrix}
 Sp_{nc} =
 \begin{matrix}
 \begin{matrix} \lambda_1 & \lambda_2 & \lambda_3 & \lambda_4 & \lambda_5 & \lambda_6 & \lambda_7 & \lambda_8 & \lambda_9 \end{matrix} \\
 \begin{bmatrix}
 \varepsilon & \varepsilon & \varepsilon & \varepsilon & 0.31 & \varepsilon & \varepsilon & \varepsilon & \varepsilon \\
 -0.02 + 0.18i & -0.02 - 0.18i & 0.05 + 0.41i & 0.05 - 0.41i & \varepsilon & \varepsilon & \varepsilon & \varepsilon & \varepsilon \\
 \varepsilon & \varepsilon & 0.05 - 0.14i & 0.05 + 0.14i & 0.94 & \varepsilon & \varepsilon & 0.98 + 0.22i & 0.98 - 0.22i \\
 \varepsilon & \varepsilon & 0.09 - 0.20i & 0.09 + 0.20i & \varepsilon & \varepsilon & \varepsilon & \varepsilon & \varepsilon \\
 0.28 + 0.90i & 0.28 - 0.90i & -0.08 + 0.78i & -0.08 - 0.78i & \varepsilon & \varepsilon & \varepsilon & \varepsilon & \varepsilon \\
 0.05 + 0.14i & 0.05 - 0.14i & 0.21 - 0.30i & 0.21 + 0.30i & \varepsilon & 0.97 + 0.22i & 0.97 - 0.22i & \varepsilon & \varepsilon \\
 -0.03 + 0.22i & -0.03 - 0.22i & \varepsilon & \varepsilon & \varepsilon & \varepsilon & \varepsilon & \varepsilon & \varepsilon
 \end{bmatrix}
 \end{matrix}
 \quad (5.15)$$

For this example the participation factors are,

5.3 Dynamic analysis of a three terminal MTDC

$$\begin{matrix}
 \begin{matrix}
 v_{dc1} \\
 i_{L_{a1}} \\
 i_{L_{j1}} \\
 v_{dc2} \\
 i_{L_{a2}} \\
 i_{L_{j2}} \\
 v_{dc3} \\
 Int_1 \\
 Int_2
 \end{matrix}
 \end{matrix}
 P =
 \begin{matrix}
 \begin{matrix}
 \lambda_1 & \lambda_2 & \lambda_3 & \lambda_4 & \lambda_5 & \lambda_6 & \lambda_7 & \lambda_8 & \lambda_9
 \end{matrix} \\
 \begin{bmatrix}
 \varepsilon & \varepsilon & 0 - 0.67i & 0 + 0.67i & 0.72 & \varepsilon & \varepsilon & 0.14 + 0.20i & 0.14 - 0.20i \\
 0.15 + 0.05i & 0.15 - 0.05i & 0.41 + 1.30i & 0.41 - 1.30i & \varepsilon & \varepsilon & \varepsilon & \varepsilon & \varepsilon \\
 \varepsilon & \varepsilon & \varepsilon & \varepsilon & \varepsilon & \varepsilon & \varepsilon & 0.45 - 0.49i & 0.45 + 0.49i \\
 \varepsilon & \varepsilon & 0.35 + 1.44i & 0.35 - 1.44i & \varepsilon & 0.15 + 0.23i & 0.15 - 0.23i & \varepsilon & \varepsilon \\
 0.43 - 0.06i & 0.43 + 0.06i & 0.09 + 1.30i & 0.09 - 1.30i & \varepsilon & \varepsilon & \varepsilon & \varepsilon & \varepsilon \\
 \varepsilon & \varepsilon & \varepsilon & \varepsilon & \varepsilon & 0.44 - 0.49i & 0.44 + 0.49i & \varepsilon & \varepsilon \\
 0.44 + 0.13i & 0.44 - 0.13i & 0.03 + 0.19i & 0.03 - 0.19i & \varepsilon & \varepsilon & \varepsilon & \varepsilon & \varepsilon \\
 \varepsilon & \varepsilon & \varepsilon & \varepsilon & 0.14 & \varepsilon & \varepsilon & 0.45 + 0.27i & 0.45 - 0.27i \\
 \varepsilon & \varepsilon & \varepsilon & \varepsilon & \varepsilon & 0.42 + 0.25i & 0.42 - 0.25i & \varepsilon & \varepsilon
 \end{bmatrix}
 \end{matrix}
 \quad (5.16)$$

From a general point of view, many differences are noticed between Sp_{nc} and P and it is nearly impossible to compare both matrices. $\lambda_{6,7}$ and $\lambda_{8,9}$ are still next to their theoretical value with a slight variation. Information given by P start to be wrong because an influence of v_{dc1} , v_{dc2} is noticed where as Sp_{nc} does not give this information.

The change of droop parameter involves clearly a coupling between the AC and the DC elements (mainly for λ_5 and for $\lambda_{1,2}$). Sp_{nc} shows this coupling while P points out no strong couplings.

One can conclude that when strong couplings are emerging between the different parts of the studied system, participation factors are not valid any more.

5.4 Dynamic analysis of HVDC system with MMC

As already mentioned, most of the HVDC links are now connected to AC system with MMC. For the high level control, one of the main differences between MMC and VSC is about the energy control. In the VSC, the capacitor is directly connected to the DC grid whereas, in the MMC, there is no direct connection. It is the reason why an energy loop has to be implemented in the MMC control as shown in Figure 4.25.

In this figure, the energy (W_{tot}) is controlled thanks to the DC power with the modulation of i_{dc} reference (i_{dc}^*). It is also possible to implement the control of energy with the AC current (i_{gd}^*). Both controls are compared in the sequel in term of dynamics. The section analyzes the dynamic behavior of a MMC in different study cases:

- One single MMC connected to a constant DC bus : energy controlled by DC power (section 5.4.1), AC power (section 5.4.2)
- One single MMC connected to a variable DC bus : constant energy reference (section 5.4.3), variable energy reference (section 5.4.4)
- An HVDC link with MMC

5.4.1 One MMC connected to a fixed voltage source: energy controlled by DC power

Let us suppose that the MMC station is connection to a constant DC voltage source. The MMC control has two aims:

- Controlling the MMC internal energy. In this section, the energy is controlled with the help of DC power.
- Controlling the power flowing through the converter thanks to the AC power.

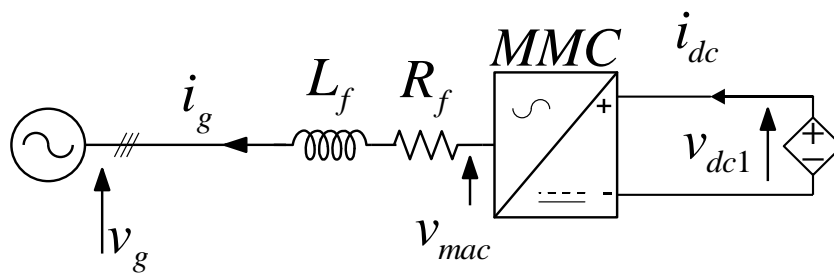


Figure 5.11 MMC connected to a fixed voltage source.

Table 5.8 Parameter values of one MMC station connected to a MTDC grid

Element	Value	Element	Value
P_b	1 GW	N	400
U_b	320 kV	R_f	0.512 Ω
f_b	50 Hz	L_f	58.7 mH

V_{dcb}	640 kV	C_{tot}	32.55 μF
L_{arm}	48.9 mH	R_{arm}	1.024 Ohm

The control settings are shown in Table 5.9.

Table 5.9 Control settings

Controller	Reference control parameters	Reference eigenvalues (rad/s)
AC current control for i_{gd} and i_{gq}	<i>Time response = 4 ms</i> <i>Damping coef. = 0.7</i>	$-525 \pm 535.6i$
DC current control	<i>Time response = 4ms</i> <i>Damping coef. = 0.7</i>	$-525 \pm 535.6i$
W_{tot} control	<i>Time response = 50ms</i> <i>Damping coef. = 0.7</i>	$-42.42 \pm 42.43i$

The system equations lead to the eigenvalues in Table 5.10.

Table 5.10 Eigenvalues with energy controlled by DC power.

Eigenvalues	Frequency (Hz)	Damping ratio
$\lambda_{1,2} = -42.1 \pm 42.78i$	9.55	0.701
$\lambda_{3,4} = -489.87 \pm 565.94i$	119.12	0.65
$\lambda_{5,6} = -531.16 \pm 534.84i$	119.36	0.704
$\lambda_{7,8} = -531.16 \pm 529.5i$	119.36	0.708

Looking at the control settings in Table 5.9, the eigenvalues can be easily understood.

- $\lambda_{1,2}$ is related to the control of the energy.
- $\lambda_{3,4}$ is related to the DC current loop.
- $\lambda_{5,6}$ and $\lambda_{7,8}$ are related to the AC current loop as they are very similar and in the control scheme are identical.

For the analysis of this model is important to clarify that the model uses the state variables that are expressed in per-unit using the representation introduced in section 2.3.2.

The PF matrix is

$$\begin{array}{c}
 \lambda_{1,2} \quad \lambda_{3,4} \quad \lambda_{5,6} \quad \lambda_{7,8} \\
 \begin{array}{c}
 v_{C_{tot}} \\
 i_{dc} \\
 i_{gd} \\
 i_{gq} \\
 Int_{i_{dc}} \\
 Int_{i_{gd}} \\
 Int_{i_{gq}} \\
 Int_{W_{tot}}
 \end{array}
 P = \begin{bmatrix}
 0.49 \pm 0.49i & \varepsilon & \varepsilon & \varepsilon \\
 \varepsilon & 0.5 \pm 0.51i & \varepsilon & \varepsilon \\
 \varepsilon & \varepsilon & \varepsilon & 0.5 \pm 0.5i \\
 \varepsilon & \varepsilon & 0.5 \pm 0.5i & \varepsilon \\
 \varepsilon & 0.5 \mp 0.43i & \varepsilon & \varepsilon \\
 \varepsilon & \varepsilon & \varepsilon & 0.5 \pm 0.5i \\
 \varepsilon & \varepsilon & 0.5 \pm 0.5i & \varepsilon \\
 0.5 \mp 0.49i & \varepsilon & \varepsilon & \varepsilon
 \end{bmatrix}
 \end{array} \quad (5.17)$$

To compare the PSM and the PF matrix the PSM is composed by the parameters most related to the state variables, energy storage parameters ($H_{C_{tot}}$, $H_{L_{eqdc}}$, $H_{L_{eqac}}$) and the parameters of the integrator in the controllers ($T_{i_{dc}}$, $T_{i_{gdq}}$, $T_{W_{tot}}$) which are in the same unit. The control for the dq AC grid is considered to be equal for the q and d axis so the control parameters are represented as with the same variable ($T_{i_{gdq}}$) to simplify the analysis and computation of the PSM.

$$\begin{array}{c}
 \lambda_{1,2} \quad \lambda_{3,4} \quad \lambda_{5,6} \quad \lambda_{7,8} \\
 \begin{array}{c}
 H_{C_{tot}} \\
 H_{L_{eqdc}} \\
 H_{L_{eqac}} \\
 T_{i_{dc}} \\
 T_{i_{gdq}} \\
 T_{W_{tot}}
 \end{array}
 Sp_{nc} = \begin{bmatrix}
 0.6 \mp 0.01i & \varepsilon & \varepsilon & \varepsilon \\
 -0.42 \mp 0.35i & 1 \mp 0.06i & \varepsilon & \varepsilon \\
 \varepsilon & \varepsilon & 0.98 \mp 0.01i & 0.98 \pm 0.01i \\
 \varepsilon & \varepsilon & \varepsilon & \varepsilon \\
 \varepsilon & \varepsilon & 0 \mp 1i & 0 \mp 1i \\
 0.01 \mp 0.58i & \varepsilon & \varepsilon & \varepsilon
 \end{bmatrix}
 \end{array} \quad (5.18)$$

The circled element is the only different element, compared to the PF matrix there are only two elements in the matrix with a different interpretation

Comparing P matrix and Sp_{nc} matrix leads to some interesting conclusions in this example.

- Both matrices lead to similar overall conclusions.
- Sp_{nc} gives more accurate conclusion on $\lambda_{1,2}$ mode. Indeed, since the energy is controlled by DC current, it is normal that this mode is depending on the $H_{L_{eqdc}}$.
- Sp_{nc} can lead to misleading conclusion since $\lambda_{3,4}$, the modes which are relative to the DC loop, do not seem to depend on the $T_{i_{dc}}$.

As presented in the example in section 5.2, the analysis of physical parameters and control parameters can hide valuable information, the analysis separating physical elements and control elements is performed, in this way.

The analysis for the energy storage elements is,

$$\begin{array}{c} \lambda_{1,2} \quad \lambda_{3,4} \quad \lambda_{5,6} \quad \lambda_{7,8} \\ \left[\begin{array}{c} H_{C_{tot}} \\ H_{L_{eqdc}} \\ H_{L_{eqac}} \end{array} \right] Sp_{nc} = \left[\begin{array}{c|c|c|c} 0.74 \mp 0.01i & \varepsilon & \varepsilon & \varepsilon \\ -0.51 \mp 0.43i & 1 \mp 0.06i & \varepsilon & \varepsilon \\ \varepsilon & \varepsilon & 1 \mp 0.01i & 1 \pm 0.01i \end{array} \right] \end{array} \quad (5.19)$$

The coupling in the first pair of eigenvalues is the result of controlling the energy using the dc energy, this coupling is not taken in to account in the PF matrix.

The control parameters the parametric analysis is

$$\begin{array}{c} \lambda_{1,2} \quad \lambda_{3,4} \quad \lambda_{5,6} \quad \lambda_{7,8} \\ \left[\begin{array}{c} T_{i_{dc}} \\ T_{i_{gdq}} \\ T_{W_{tot}} \end{array} \right] Sp_{nc} = \left[\begin{array}{c|c|c|c} \varepsilon & 0 \mp 1i & \varepsilon & \varepsilon \\ \varepsilon & \varepsilon & 0 \mp 1i & 0 \mp 1i \\ 0 \mp 1i & \varepsilon & \varepsilon & \varepsilon \end{array} \right] \end{array} \quad (5.20)$$

The analysis of the integral time confirms that each controller has an influenced on the particular eigenvalues relative to the loop where the integral parameter is involved in.

5.4.2 One MMC connected to a fixed voltage source: DC power mode and energy controlled by AC power

This case is very similar to the previous one except that the energy is controlled by the AC power. The power flowing through the converter is then controlled by DC power.

Since all the parameters for the MMC and the control are the same, the eigenvalues of the system are very similar to the previous ones as shown in Table 5.11.

Table 5.11 Eigenvalues for the DC link

Eigenvalues	Frequency (Hz)	Damping ratio
$\lambda_{1,2} = -41.53 \pm 41.25i$	9.31	0.709
$\lambda_{3,4} = -525.01 \pm 571.93i$	123.56	0.67
$\lambda_{5,6} = -531.16 \pm 534.84i$	119.96	0.704
$\lambda_{7,8} = -535.47 \pm 525.14i$	119.36	0.714

As previously, the origin of the eigenvalues is rather easy to find:

- $\lambda_{1,2}$ is related to the control of the energy.
- $\lambda_{3,4}$ is related to the DC current loop.
- $\lambda_{5,6}$ and $\lambda_{7,8}$ are related to the AC current loop as they are very similar and in the control scheme are identical.

Relatively similar to the previous example this initial guess is made in knowledge of the reference eigenvalues and “intuition”.

The PF matrix is

$$\begin{matrix}
 & \lambda_{1,2} & \lambda_{3,4} & \lambda_{5,6} & \lambda_{7,8} \\
 \begin{matrix} v_{C_{tot}} \\ i_{dc} \\ i_{gd} \\ i_{gq} \\ Int_{i_{dc}} \\ Int_{i_{gd}} \\ Int_{i_{gq}} \\ Int_{W_{tot}} \end{matrix} & P = & \begin{bmatrix} 0.46 \pm 0.47i & \varepsilon & \varepsilon & \varepsilon \\ \varepsilon & \varepsilon & \varepsilon & 0.5 \pm 0.51i \\ \varepsilon & 0.47 \pm 0.5i & \varepsilon & \varepsilon \\ \varepsilon & \varepsilon & 0.5 \pm 0.5i & \varepsilon \\ \varepsilon & \varepsilon & \varepsilon & 0.5 \mp 0.51i \\ \varepsilon & 0.5 \pm 0.46i & \varepsilon & \varepsilon \\ \varepsilon & \varepsilon & 0.5 \pm 0.5i & \varepsilon \\ 0.5 \mp 0.46i & \varepsilon & \varepsilon & \varepsilon \end{bmatrix}
 \end{matrix} \quad (5.21)$$

The PSM is

$$\begin{array}{c}
 \lambda_{1,2} \quad \lambda_{3,4} \quad \lambda_{5,6} \quad \lambda_{7,8} \\
 \begin{array}{c}
 H_{C_{tot}} \\
 H_{L_{eqdc}} \\
 H_{L_{eqac}} \\
 T_{i_{dc}} \\
 T_{i_{gdq}} \\
 T_{W_{tot}}
 \end{array}
 Sp_{nc} =
 \begin{bmatrix}
 0.6 \pm 0.01i & \varepsilon & \varepsilon & \varepsilon \\
 \varepsilon & \varepsilon & \varepsilon & 1 \mp 0.02i \\
 0.33 \mp 0.41i & 0.98 \mp 0.41i & 0.98 \mp 0.41i & \varepsilon \\
 \varepsilon & \varepsilon & \varepsilon & \varepsilon \\
 \varepsilon & 0 \mp 0.21i & 0 \mp 0.21i & \varepsilon \\
 0.03 \mp 0.60i & \varepsilon & \varepsilon & \varepsilon
 \end{bmatrix}
 \end{array} \quad (5.22)$$

As in the previous example Sp_{nc} is more accurate than participation factor since it highlights the dependence of $\lambda_{1,2}$ the mode which corresponds to the energy with the AC parameter which is normal due the choice on the control. It is also possible to separate the physical and control parameters but in this case, the information is similar.

$$\begin{array}{c}
 \lambda_{1,2} \quad \lambda_{3,4} \quad \lambda_{5,6} \quad \lambda_{7,8} \\
 \begin{array}{c}
 H_{C_{tot}} \\
 H_{L_{eqdc}} \\
 H_{L_{eqac}}
 \end{array}
 Sp_{nc} =
 \begin{bmatrix}
 0.76 \pm 0.01i & \varepsilon & \varepsilon & \varepsilon \\
 \varepsilon & \varepsilon & \varepsilon & 1 \pm 0.01i \\
 0.41 \mp 0.51i & -0.3 \mp 0i & 1 \mp 0.01i & \varepsilon
 \end{bmatrix}
 \end{array} \quad (5.23)$$

$$\begin{array}{c}
 \lambda_{1,2} \quad \lambda_{3,4} \quad \lambda_{5,6} \quad \lambda_{7,8} \\
 \begin{array}{c}
 T_{i_{dc}} \\
 T_{i_{gdq}} \\
 T_{W_{tot}}
 \end{array}
 Sp_{nc} =
 \begin{bmatrix}
 \varepsilon & \varepsilon & \varepsilon & 0 \mp 1i \\
 \varepsilon & 0 \mp 1i & 0 \mp 1i & \varepsilon \\
 0.05 \mp 1i & \varepsilon & \varepsilon & \varepsilon
 \end{bmatrix}
 \end{array} \quad (5.24)$$

This analysis can be used for the proportional constants parameters in the controllers.

$$\begin{array}{c}
 \lambda_{1,2} \quad \lambda_{3,4} \quad \lambda_{5,6} \quad \lambda_{7,8} \\
 \begin{array}{c}
 k_{i_{dc}} \\
 k_{i_{gdq}} \\
 k_{W_{tot}}
 \end{array}
 Sp_{nc} =
 \begin{bmatrix}
 \varepsilon & \varepsilon & \varepsilon & -0.70 \pm 0.71i \\
 \varepsilon & -1 \pm 0.02i & -1 \pm 0.2i & \varepsilon \\
 -0.67 \mp 0.74i & \varepsilon & \varepsilon & \varepsilon
 \end{bmatrix}
 \end{array} \quad (5.25)$$

This analysis can also be used for the proportional constants parameters in the controllers. The same information are drawn as for the integral parameter.

5.4.3 One MMC connected to a variable DC bus – energy reference constant

The variable DC bus is modelled by a capacitor associated to a current source (see Figure 5.12). This current source is modelling the current which could be delivered by another MMC connected on the same DC bus as in an HVDC link as it will be presented in section 5.4.4. C_{dc} is a simplified model of the cable which links both stations.

Since the voltage is not fixed, it has to be regulated. The MMC control has to aims:

- controlling the MMC internal energy. In this section, the energy is controlled with the help of AC power.
- controlling the DC voltage thanks to the DC power.

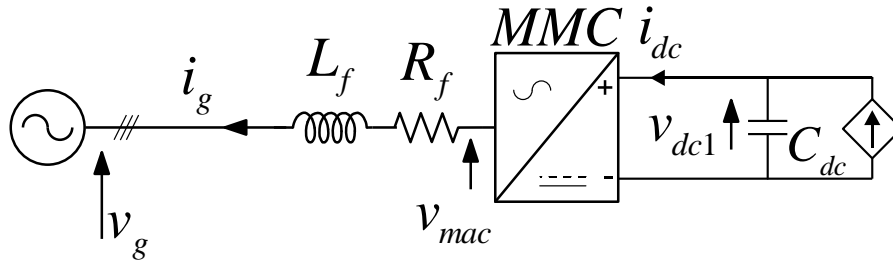


Figure 5.12 MMC connected to a variable voltage source.

With the same parameters values and the following control parameters.

Table 5.12 Control settings

Controller	Reference control parameters	Reference eigenvalues (rad/s)
AC current control for i_{gd} and i_{gq}	<i>Time response</i> = 4 ms <i>Damping coef.</i> = 0.7	$-525 \pm 535.6i$
DC current control	<i>Time response</i> = 4ms <i>Damping coef.</i> = 0.7	$-525 \pm 535.6i$
W_{tot} control	<i>Time response</i> = 50ms <i>Damping coef.</i> = 0.7	$-42.42 \pm 42.43i$
v_{dc1} control	<i>Time response</i> = 70ms <i>Damping coef.</i> = 0.7	$-30 \pm 30.6i$

Using the parameter values in Table 5.8 and the control settings in Table 5.12, the system equations leads to the eigenvalues in Table 5.13.

Table 5.13 Eigenvalues for the DC link

Eigenvalues	Frequency (Hz)	Damping ratio
$\lambda_{1,2} = -41.53 \pm 45.25i$	9.31	0.709
$\lambda_{3,4} = -60.25 \pm 60.52i$	13.59	0.705
$\lambda_{5,6} = -475.45 \pm 583.82i$	119.8	0.63
$\lambda_{7,8} = -525.01 \pm 571.93i$	123.56	0.67
$\lambda_{9,10} = -531.16 \pm 529.5i$	119.36	0.708

the eigenvalues can be related to:

- $\lambda_{1,2}$ is the control of the energy in the station.
- $\lambda_{5,6}$, $\lambda_{7,8}$ and $\lambda_{9,10}$ are related to the AC and DC current loops.
- $\lambda_{3,4}$: considering the numerical values, it is not so obvious to find the relationship between the eigenvalues and the parameters of the model.

The PF matrix is

$$P = \begin{matrix} & \begin{matrix} \lambda_{1,2} & \lambda_{3,4} & \lambda_{5,6} & \lambda_{7,8} & \lambda_{9,10} \end{matrix} \\ \begin{matrix} v_{dc1} \\ v_{C_{tot}} \\ i_{dc} \\ i_{gd} \\ i_{gq} \\ Int_{i_{dc}} \\ Int_{i_{gd}} \\ Int_{i_{gq}} \\ Int_{W_{tot}} \\ Int_{v_{dc1}} \end{matrix} & \begin{bmatrix} \varepsilon & 0.48 \pm 0.5i & \varepsilon & \varepsilon & \varepsilon \\ 0.46 \pm 0.47i & \varepsilon & \varepsilon & \varepsilon & \varepsilon \\ \varepsilon & \varepsilon & 0.49 \pm 0.52i & \varepsilon & \varepsilon \\ \varepsilon & \varepsilon & \varepsilon & 0.47 \pm 0.5i & \varepsilon \\ \varepsilon & \varepsilon & \varepsilon & \varepsilon & 0.5 \pm 0.5i \\ \varepsilon & \varepsilon & 0.50 \mp 0.4i & \varepsilon & \varepsilon \\ \varepsilon & \varepsilon & \varepsilon & 0.5 \pm 0.46i & \varepsilon \\ \varepsilon & \varepsilon & \varepsilon & \varepsilon & 0.5 \mp 0.5i \\ 0.5 \mp 0.46i & \varepsilon & \varepsilon & \varepsilon & \varepsilon \\ \varepsilon & 0.51 \mp 0.48i & \varepsilon & \varepsilon & \varepsilon \end{bmatrix} \end{matrix} \quad (5.26)$$

The PSM is

$$\begin{array}{c}
 \lambda_{1,2} \quad \lambda_{3,4} \quad \lambda_{5,6} \quad \lambda_{7,8} \quad \lambda_{9,10} \\
 \begin{array}{c}
 H_{C_{dc}} \\
 H_{C_{tot}} \\
 H_{L_{eqdc}} \\
 H_{L_{eqac}} \\
 T_{i_{dc}} \\
 T_{i_{gdq}} \\
 T_{W_{tot}} \\
 T_{v_{dc1}}
 \end{array}
 \end{array}
 Sp_{nc} = \begin{bmatrix}
 \varepsilon & 0.38 \mp 0i & \varepsilon & \varepsilon & \varepsilon \\
 0.6 \pm 0.01i & \varepsilon & \varepsilon & \varepsilon & \varepsilon \\
 \varepsilon & -0.1 \mp 0.91i & 1 \mp 0.08i & \varepsilon & \varepsilon \\
 0.33 \mp 0.41i & \varepsilon & \varepsilon & 0.98 \mp 0.01i & 0.98 \pm 0.01i \\
 \varepsilon & \varepsilon & \varepsilon & \varepsilon & \varepsilon \\
 \varepsilon & \varepsilon & \varepsilon & 0 \mp 0.21i & 0 \mp 21i \\
 0.03 \mp 0.6i & \varepsilon & \varepsilon & \varepsilon & \varepsilon \\
 \varepsilon & \varepsilon & \varepsilon & \varepsilon & \varepsilon
 \end{bmatrix} \quad (5.27)$$

The conclusions which can be drawn from this comparison are similar to the previous examples. Sp_{nc} analysis give more accurate information on the system since it highlights clearly the relation between the modes linked with the internal energy and the energy stored in the DC bus with their respective storage element, which is normal, but also with the internal loops.

- $\lambda_{1,2}$: the mode associated with the internal energy depends on $H_{C_{tot}}$ and $H_{L_{eqdc}}$ since the energy is controlled by AC power.
- $\lambda_{3,4}$: the mode associated with the DC bus energy depends on $H_{C_{dc}}$ and $H_{L_{eqdc}}$ since the voltage is controlled by DC power.

Separating physical elements and Control elements

$$\begin{array}{c}
 \lambda_{1,2} \quad \lambda_{3,4} \quad \lambda_{5,6} \quad \lambda_{7,8} \quad \lambda_{9,10} \\
 \begin{array}{c}
 H_{C_{dc}} \\
 H_{C_{tot}} \\
 H_{L_{eqdc}} \\
 H_{L_{eqac}}
 \end{array}
 \end{array}
 Sp_{nc} = \begin{bmatrix}
 \varepsilon & 0.38 \pm 0i & \varepsilon & \varepsilon & \varepsilon \\
 0.76 \mp 0.01i & \varepsilon & \varepsilon & \varepsilon & \varepsilon \\
 \varepsilon & -0.1 \mp 0.92i & 1 \mp 0.08i & \varepsilon & \varepsilon \\
 0.41 \mp 0.51i & \varepsilon & \varepsilon & 1 \mp 0i & 1 \pm 0i
 \end{bmatrix} \quad (5.28)$$

The analysis shows that the internal energy storage in the MMC in the total capacitance $H_{C_{tot}}$ is important for the control of the energy and the control of the voltage is performed through the equivalent DC inductance $H_{L_{eqdc}}$.

The control parameters for the integral time,

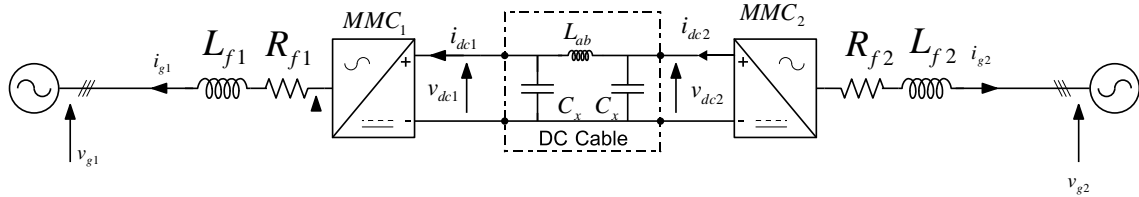
$$\begin{matrix} \lambda_{1,2} & \lambda_{3,4} & \lambda_{5,6} & \lambda_{7,8} & \lambda_{9,10} \\ \begin{matrix} T_{i_{dc}} \\ T_{i_{gdq}} \\ T_{W_{tot}} \\ T_{v_{dc1}} \end{matrix} \end{matrix} S p_{nc} = \begin{bmatrix} \varepsilon & \varepsilon & 0 \mp 1i & \varepsilon & \varepsilon \\ \varepsilon & \varepsilon & \varepsilon & 0 \mp 1i & 0 \mp 1i \\ 0.05 \mp 1i & \varepsilon & \varepsilon & \varepsilon & \varepsilon \\ \varepsilon & 0.03 \mp 1i & \varepsilon & \varepsilon & \varepsilon \end{bmatrix} \quad (5.29)$$

5.4.4 Two terminal MMC DC link (MMC1 Power mode W controlled by dc Power, MMC2 voltage mode W controlled by Ac Power)

Considering the model given in section 4.4.5, two MMC stations compose the system. One of the stations controls its energy and power (MMC₁) and the link and the other (MMC₂) controls the voltage of the link. Both stations have a control loop of the internal energy as already explained in Chapter 4. The system has 20 state variables for this complex problem the use of the parametric sensitivity is proposed.

The free-motion equations have no particular form, in other words, is not possible to know much from them if it does have a diagonal dominance or if there are couplings between the state equations.

Considering the structure in Figure 4.30



HVDC link with MMC stations

Using the parameters in Table 5.14.

Table 5.14 Parameters of the MMC stations

Element	Value	Element	Value
P_b	1 GW	N	400
U_b	320 kV	R_f	0.521 Ohms
f_b	50 Hz	L_f	58.7 mH
V_{dcb}	640 kV	Cable length l	300 km
L_{arm}	48 mH	C_{tot}	32.55 μF
R_{arm}	1.024 Ohm	L_{ab}	3.739 mH / km
$C_{x1,2}$	0.2469 μF	R_{ab}	5.346 m Ω / km

The control scheme has the following settings

Table 5.15 Control settings MMC1

Controller	Setting	Prospect eigenvalue (rad/s)
AC current control	<i>Time response = 4 ms</i> <i>Dammping coef. = 0.7</i>	$-525 \pm 535.6i$
DC current control	<i>Time response = 4 ms</i> <i>Dammping coef. = 0.7</i>	$-525 \pm 535.6i$
W_{tot} control	<i>Time response = 40 ms</i> <i>Dammping coef. = 0.7</i>	$-53.02 \pm 53.04i$

Table 5.16 Control settings MMC1

Controller	Setting	Prospect eigenvalue (rad/s)
AC current control	<i>Time response = 4 ms</i> <i>Dammping coef. = 0.7</i>	$-525 \pm 535.6i$
DC current control	<i>Time response = 4 ms</i> <i>Dammping coef. = 0.7</i>	$-525 \pm 535.6i$
W_{tot} control	<i>Time response = 40 ms</i> <i>Dammping coef. = 0.7</i>	$-53.02 \pm 53.04i$
v_{dc2} control	<i>Time response = 70 ms</i> <i>Dammping coef. = 0.7</i>	$-30 \pm 30.6i$

Because of its complexity, the complete set of equations is not presented.

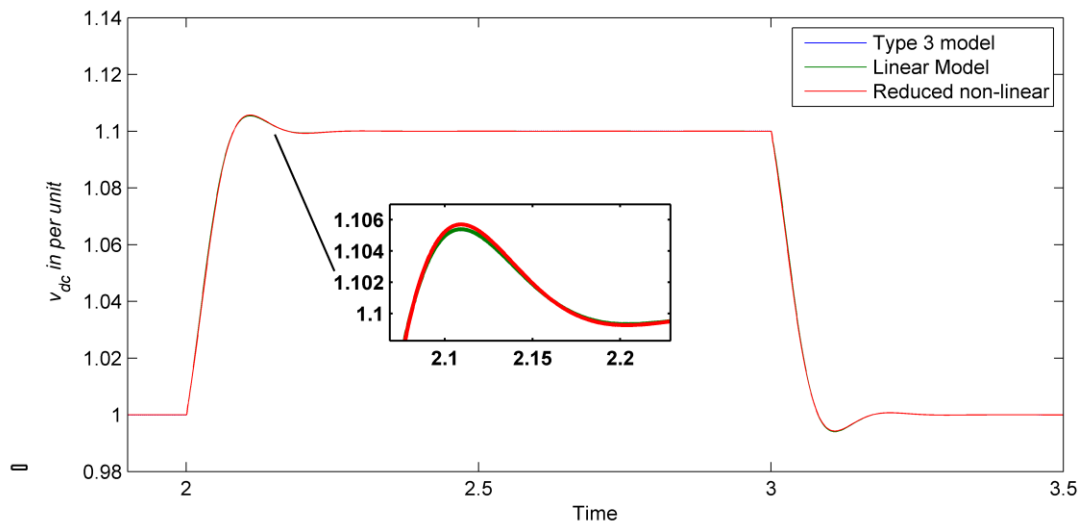


Figure 5.13 Voltage response for a change of voltage reference

Figure 5.13 presents the voltage response for a change of the voltage reference from the MTDC equivalent, increasing 0.1pu of the power in $t = 2s$ and decreasing 0.1pu in $t = 3s$.

The system equations lead to the eigenvalues in Table 5.17.

Table 5.17 Eigenvalues for the DC link

Eigenvalues (rad/s)	Frequency (Hz)	Damping ratio
$\lambda_{1,2} = -22.11 \pm 32.49i$	6.25	0.56
$\lambda_3 = -43.49$	–	1
$\lambda_{4,5} = -52.95 \pm 52.74i$	11.89	0.708
$\lambda_{6,7} = -88.18 \pm 152.69i$	28.55	0.5
$\lambda_{8,9} = -251.45 \pm 1610.17i$	259.3	0.15
$\lambda_{10,11} = -404.75 \pm 671.98i$	124.85	0.51
$\lambda_{12,13} = -426.16 \pm 426.64i$	95.97	0.706
$\lambda_{14,15} = -426.16 \pm 422.36i$	95.49	0.71
$\lambda_{16} = -468.53$	–	1
$\lambda_{17,18} = -527.32 \pm 550.86i$	121.36	0.69
$\lambda_{19,20} = -531.16 \pm 529.50i$	119.3	0.7

From Table 5.17 it is possible to anticipate the link between some eigenvalues with a damping ratio near to 0.7 and the controllers of the MMC stations. However, it is not straightforward to have an intuition on all the present 20 eigenvalues.

From the system matrix in **per-unit** and the eigenvalues the PF matrix is presented in equation (5.30). The sub index 1 and 2 indicate the station MMC1 or MMC2 respectively.

According to the PF the eigenvalues have the following contributions

	$\lambda_{1,2}$	λ_3	$\lambda_{4,5}$	$\lambda_{6,7}$	$\lambda_{8,9}$	$\lambda_{10,11}$	$\lambda_{12,13}$	$\lambda_{14,15}$	λ_{16}	$\lambda_{17,18}$	$\lambda_{19,20}$
$H_{C_x 1}$	ε	ε	ε	$0.13 \pm 0.07i$	ε	ε	ε	ε	ε	ε	ε
$H_{C_{tot} 1}$	ε	ε	$0.25 \pm 0.01i$	ε	ε	ε	ε	ε	ε	ε	ε
$H_{L_{eqac} 1}$	ε	ε	ε	ε	ε	ε	$0.99 \mp 0.01i$	$0.99 \pm 0.01i$	ε	ε	ε
$H_{L_{eqdc} 1}$	ε	ε	$-0.09 \pm 0.89i$	$0.43 \pm 0.81i$	ε	$0.99 \pm 0.17i$	ε	ε	ε	ε	ε
$H_{C_x 2}$	ε	ε	ε	ε	ε	ε	ε	ε	ε	ε	ε
$H_{C_{tot} 2}$	$0.67 \pm 0.29i$	ε	ε	ε	ε	ε	ε	ε	ε	ε	ε
$H_{L_{eqac} 2}$	$-0.03 \pm 0.42i$	ε	ε	ε	ε	ε	ε	ε	ε	$0.97 \mp 0.01i$	$0.99 \pm 0.01i$
$H_{L_{eqdc} 2}$	ε	ε	ε	ε	$0.62 \pm 0.79i$	ε	ε	ε	1	$-0.11 \pm 0.09i$	ε
H_{Lab}	ε	ε	ε	$0.05 \pm 0.35i$	ε	ε	ε	ε	ε	ε	ε
$Ti_{i_g 1}$	ε	ε	ε	ε	ε	ε	$0 \pm 0.17i$	$0 \pm 0.17i$	ε	ε	ε
$Ti_{i_{dc} 1}$	ε	ε	ε	ε	ε	ε	ε	ε	ε	ε	ε
$Ti_{W_{tot} 1}$	ε	ε	$0.02 \pm 0.38i$	ε	ε	ε	ε	ε	ε	ε	ε
$Ti_{i_g 2}$	ε	ε	ε	ε	ε	ε	ε	ε	ε	$0.01 \pm 0.21i$	$0.01 \pm 0.21i$
$Ti_{i_{dc} 2}$	ε	ε	ε	ε	ε	ε	ε	ε	ε	ε	ε
$Ti_{v_{dc} 2}$	$-0.09 \pm 0.26i$	0.31	ε	ε	ε	ε	ε	ε	ε	ε	ε
$Ti_{W_{tot} 2}$	$0.28 \pm 0.31i$	0.93	ε	ε	ε	ε	ε	ε	ε	ε	ε

(5.30)

$$Sp_{nc} = \begin{matrix} & \begin{matrix} \lambda_{1,2} & \lambda_3 & \lambda_{4,5} & \lambda_{6,7} & \lambda_{8,9} & \lambda_{10,11} & \lambda_{12,13} & \lambda_{14,15} & \lambda_{16} & \lambda_{17,18} & \lambda_{19,20} \end{matrix} \\ \begin{matrix} v_{dc1} \\ v_{C_{tot}1} \\ i_{gd1} \\ i_{gq1} \\ i_{dc1} \\ v_{dc2} \\ v_{C_{tot}2} \\ i_{gd2} \\ i_{gq2} \\ i_{dc2} \\ i_{Lab} \\ Int_{i_{gd}1} \\ Int_{i_{gq}1} \\ Int_{i_{dc}1} \\ Int_{W_{tot}1} \\ Int_{i_{gd}2} \\ Int_{i_{gq}2} \\ Int_{i_{dc}2} \\ Int_{v_{dc}2} \\ Int_{W_{tot}2} \end{matrix} & \begin{bmatrix} \varepsilon & \varepsilon & \varepsilon & 0.43 \pm 0.26i & \varepsilon & 0.07 \pm 0.16i & \varepsilon & \varepsilon & \varepsilon & \varepsilon & \varepsilon \\ \varepsilon & \varepsilon & 0.48 \pm 0.5i & \varepsilon & \varepsilon & \varepsilon & \varepsilon & \varepsilon & \varepsilon & \varepsilon & \varepsilon \\ \varepsilon & \varepsilon & \varepsilon & \varepsilon & \varepsilon & \varepsilon & 0.5 \pm 0.5i & \varepsilon & \varepsilon & \varepsilon & \varepsilon \\ \varepsilon & \varepsilon & \varepsilon & \varepsilon & \varepsilon & \varepsilon & \varepsilon & 0.5 \pm 0.5i & \varepsilon & \varepsilon & \varepsilon \\ \varepsilon & \varepsilon & \varepsilon & \varepsilon & \varepsilon & 0.45 \pm 0.52i & \varepsilon & \varepsilon & \varepsilon & \varepsilon & \varepsilon \\ \varepsilon & \varepsilon & \varepsilon & \varepsilon & 0.44 \pm 0.09i & \varepsilon & \varepsilon & \varepsilon & \varepsilon & \varepsilon & \varepsilon \\ 0.49 \pm 0.31i & \varepsilon & \varepsilon & \varepsilon & \varepsilon & \varepsilon & \varepsilon & \varepsilon & \varepsilon & \varepsilon & \varepsilon \\ \varepsilon & \varepsilon & \varepsilon & \varepsilon & \varepsilon & \varepsilon & \varepsilon & \varepsilon & \varepsilon & 0.48 \pm 0.51i & \varepsilon \\ \varepsilon & \varepsilon & \varepsilon & \varepsilon & \varepsilon & \varepsilon & \varepsilon & \varepsilon & \varepsilon & \varepsilon & 0.50 \pm 0.50i \\ \varepsilon & \varepsilon & \varepsilon & \varepsilon & 0.45 \pm 0.25i & \varepsilon & \varepsilon & \varepsilon & \varepsilon & \varepsilon & \varepsilon \\ \varepsilon & \varepsilon & \varepsilon & 0.52 \pm 0.21i & \varepsilon & \varepsilon & \varepsilon & \varepsilon & \varepsilon & \varepsilon & \varepsilon \\ \varepsilon & \varepsilon & \varepsilon & \varepsilon & \varepsilon & \varepsilon & 0.5 \pm 0.5i & \varepsilon & \varepsilon & \varepsilon & \varepsilon \\ \varepsilon & \varepsilon & \varepsilon & \varepsilon & \varepsilon & \varepsilon & \varepsilon & 0.5 \pm 0.5i & \varepsilon & \varepsilon & \varepsilon \\ \varepsilon & \varepsilon & \varepsilon & \varepsilon & \varepsilon & 0.46 \pm 0.28i & \varepsilon & \varepsilon & \varepsilon & \varepsilon & \varepsilon \\ \varepsilon & \varepsilon & 0.52 \pm 0.48i & \varepsilon & \varepsilon & \varepsilon & \varepsilon & \varepsilon & \varepsilon & \varepsilon & \varepsilon \\ \varepsilon & \varepsilon & \varepsilon & \varepsilon & \varepsilon & \varepsilon & \varepsilon & \varepsilon & \varepsilon & 0.51 \pm 0.48i & \varepsilon \\ \varepsilon & \varepsilon & \varepsilon & \varepsilon & \varepsilon & \varepsilon & \varepsilon & \varepsilon & \varepsilon & \varepsilon & 0.50 \pm 0.50i \\ \varepsilon & \varepsilon & \varepsilon & \varepsilon & 0.10 \pm 0.13i & \varepsilon & \varepsilon & \varepsilon & 0.81 & \varepsilon & \varepsilon \\ 0.24 \pm 0.32i & 0.53 & \varepsilon & \varepsilon & \varepsilon & \varepsilon & \varepsilon & \varepsilon & \varepsilon & \varepsilon & \varepsilon \\ 0.22 \pm 0.03i & 0.59 & \varepsilon & \varepsilon & \varepsilon & \varepsilon & \varepsilon & \varepsilon & \varepsilon & \varepsilon & \varepsilon \end{bmatrix} \end{matrix} \quad (5.31)$$

According to the PF the eigenvalues have the following contributions

From the matrix Sp_{nc} the following can be stated.

Table 5.18 Most important **parameters** for the eigenvalues

	Eigenvalues	Parameters
Voltage and Energy in MMC2	$\lambda_{1,2} = -22.11 \pm 32.49i$	$H_{C_{tot}2}, H_{L_{eqac}2}, Ti_{v_{dc}2}, Ti_{W_{tot}2}$
	$\lambda_3 = -43.49$	$Ti_{v_{dc}2}, Ti_{W_{tot}2}$
Energy in MMC1	$\lambda_{4,5} = -52.95 \pm 52.74i$	$H_{C_{tot}1}, H_{L_{eqdc}1}, Ti_{W_{tot}1}$
DC physical couplings MMC1	$\lambda_{6,7} = -88.18 \pm 152.69i$	$H_{C_x1}, H_{L_{eqdc}1}, H_{Lab},$
Equivalent inductance MMC2	$\lambda_{8,9} = -251.45 \pm 1610.17i$	$H_{L_{eqdc}2}$
DC current control MMC1	$\lambda_{10,11} = -404.75 \pm 671.98i$	$H_{L_{eqdc}1}$
AC current control MMC1 (dq frame)	$\lambda_{12,13} = -426.16 \pm 426.64i$	$H_{L_{eqac}1}, Ti_{i_g1}$
	$\lambda_{14,15} = -426.16 \pm 422.36i$	$H_{L_{eqac}1}, Ti_{i_g1}$
DC current control MMC2	$\lambda_{16} = -468.53$	$H_{L_{eqdc}2}$
AC current control MMC2 (dq frame)	$\lambda_{17,18} = -527.32 \pm 550.86i$	$H_{L_{eqac}2}, Int_{i_{gd}2}$
	$\lambda_{19,20} = -531.16 \pm 529.50i$	$H_{L_{eqac}2}, Int_{i_{gq}2}$

 Table 5.19 **State variables** with most contribution to the eigenvalues

Eigenvalues	states
$\lambda_{1,2} = -22.11 \pm 32.49i$	$v_{C_{tot}2}, Int_{v_{dc}2}, Int_{W_{tot}2}$
$\lambda_3 = -43.49$	$Int_{v_{dc}2}, Int_{W_{tot}2}$
$\lambda_{4,5} = -52.95 \pm 52.74i$	$v_{C_{tot}1}, Int_{W_{tot}1}$
$\lambda_{6,7} = -88.18 \pm 152.69i$	v_{dc1}, i_{Lab}
$\lambda_{8,9} = -251.45 \pm 1610.17i$	$v_{dc2}, i_{dc2}, Int_{i_{dc}2}$
$\lambda_{10,11} = -404.75 \pm 671.98i$	$v_{dc1}, i_{dc1}, Int_{i_{dc}1}$
$\lambda_{12,13} = -426.16 \pm 426.64i$	$i_{gd1}, Int_{i_{gd}1}$
$\lambda_{14,15} = -426.16 \pm 422.36i$	$i_{gq1}, Int_{i_{gq}1}$
$\lambda_{16} = -468.53$	$Int_{i_{dc}2}$
$\lambda_{17,18} = -527.32 \pm 550.86i$	$i_{gd2}, Int_{i_{gd}2}$
$\lambda_{19,20} = -531.16 \pm 529.50i$	$i_{gq2}, Int_{i_{gq}2}$

Comparing both tables leads to the following conclusions:

- Same results for the 8 eigenvalues related to AC current loops ($\lambda_{12,13}$, $\lambda_{14,15}$, $\lambda_{17,18}$, $\lambda_{19,20}$).
- Similar results on energy control ($\lambda_{1,2}$, $\lambda_{4,5}$) where the Sp_{nc} is a little bit more accurate.
- Similar results for the 4 poles relative to DC current loops. Participation factors give wrong information because it suggests an influence of v_{dc1} , v_{dc2} on these poles. This information is not found in Sp_{nc} matrix.
- $\lambda_{6,7}$ is the only eigenvalue where a coupling is noticed between a converter and the inductance H_{Lab} . Some rather similar information are drawn from participation factor except for H_{Leqdc1} .
- Similar results are noticed also on the eigenvalue λ_3 but it is difficult to understand the physical meanings of this eigenvalue.
- Different results are noticed on λ_{16} but it is also difficult to understand the physical meanings on this pole.

The parametric sensitivity helps in this case to understand how the eigenvalues are related to the explicit parameters in the matrix of the linear system. Nevertheless, the physical relationships of the parameters may help also to understand how non-explicit parameters relate to the eigenvalues.

Let's take the example of the length of the cable. The parameter has an influence on L_{ab} . As seen previously only the eigenvalue $\lambda_{6,7}$ is relative but H_{Lab1} so, it is possible to anticipate that only this pole will be sensitive to the length. Figure 5.16 (circled eigenvalues) confirms this affirmation.

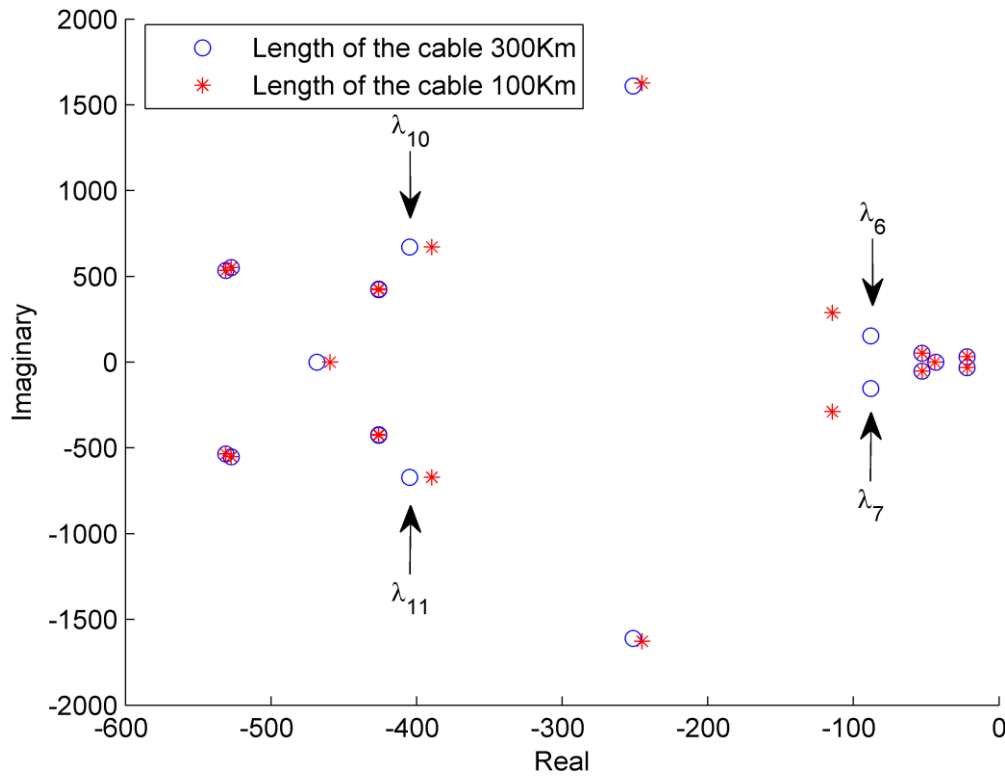


Figure 5.14 Eigenvalues changing the cable length from 300Km to 100Km.

The analysis of a system with many eigenvalues is a complex task but as the automatic tool in MATLAB® performs all the partial derivatives, the result of the analysis is obtained in few seconds.

5.5 Conclusions

The analysis of the different models of the VSC and MMC station shows the efficacy of the parametric sensitivity analysis. However for reasonable dynamics a large part of the information given by the participation factor are correct. The comparison with the participation factors shows clearly the limitation of the participation factors when the systems are strongly coupled in case of high dynamics for the system

From the technical point of view, the parametric sensitivity analysis shows the nature of the different eigenvalues taking into account for any kind of parameters in the model. New insight on the couplings and interactions between elements (or subsystems) can be envisaged with this technique.

Chapter 6 General Conclusions and Perspectives

In this thesis, it has been presented a review of the participation factor matrix as an analysis tool showing some limitations. Nonetheless, its application is valid depending on the properties of the model.

From the easy interpretation of the PF and the accurate information of the parametric sensitivity analysis, a methodology has been proposed using the parametric sensitivity for modal analysis in LTI models. A new form of modal analysis is presented in Chapter 3, including the formulation of the Parametric Sensitivity Matrix (PSM).

The PSM has the advantage of having normalized elements, where the information is organized, clear and useful. It has been shown that the per unit approach is mandatory to obtain consistent results. The interpretation of the elements in the PSM is not limited to real numbers but also to complex number for the sensitivities. Each element of the matrix describes the first order sensitivity of the eigenvalue.

The PSM can give a measurement of the change of the eigenvalues for changes of the parameters, and it can be used for different purposes as,

- Stability analysis
- Tuning of control parameters
- Analysis and selection of new parameters
- Analysis of coupling in different subsystems and parameters

The purpose of this thesis is to show that the PSM is a better alternative for the analysis of DC networks.

The analysis of the different models of the VSC and reduced model of a MMC station shows the efficacy of the parametric sensitivity analysis. The comparison with the participation factors shows how the participation factors have a limitation when the systems are strongly coupled.

An automatic analysis tool was implemented for the MMC models in the MATLAB ® environment. Appendix A describes the routine of parametric analysis for the models described in this chapter. This computational tool is suitable for any LTI system, having the appropriated inputs. The efficacy of the implementation allows having an analytical model and the analysis for a point of operation in less than one minute for a complex model of 20 state variables.

This thesis is part of the collaborative effort with Julian Freytes and Samy Akkari, where the perspectives is to applied the defined methodology to more complex MMC models and use it on MTDC networks.

In the short term:

- Use of the PSM in a larger MTDC network
- Analysis of a MMC in AC unbalanced operating point
- Study of the evolution of the energy in the system subject to a variation on a given parameter to determine the most active eigenvalues
- Possible reduction and validation of its dynamics using the activity analysis (Louca, Stein, and Hulbert 2010) and the PSM.
- Use of the PSM for evaluate the couplings between subsystems developing a metric to measure the index of coupling.

In the long term

- Develop a general formulation for linear systems of the PSM.
- Include a second order derivative on the sensitivity for the PSM.

Scientific contribution

From the work of this thesis two papers were published in international conference and one journal paper has been submitted in an international journal.

Barrera Gallegos, Noe, Genevieve Dauphin-Tanguy, and Xavier Guillaud. 2016. “Modal Sensitivity of a Reduced Equivalent HVDC-VSC System.” In International Conference on Control, Decision and Information Technologies.

Barrera-gallegos, Noé, Geneviève Dauphin-Tanguy, and Xavier Guillaud. 2014. “Bond Graph Model Analysis of an Offshore Wind Farm.” In 11th International Conference on Bond Graph Modeling and Simulation, 832–38.

Barrera Gallegos, Noe, Julian Freytes, Genevieve Dauphin-Tanguy, and Xavier Guillaud. 2016. “Comparison between Participation Factors and Parametric Sensitivity Methodology for dynamic analysis on a MTDC system” in review for the Special Issue on Advances in High-Voltage Transmission Systems

Bibliography

- Abed, Eyad H., Munther a. Hassouneh, and Wael a. Hashlamoun. 2009. "Modal Participation Factors Revisited: One Definition Replaced by Two." *Proceedings of the American Control Conference*, 1140–45. doi:10.1109/ACC.2009.5160012.
- Abildgaard, Elisabeth N., and Marta Molinas. 2012. "Modelling and Control of the Modular Multilevel Converter (MMC)." *Energy Procedia* 20 (Mmc): 227–36. doi:10.1016/j.egypro.2012.03.023.
- Akkari, Samy. 2016. "Control of a Multi-Terminal HVDC (MTDC) System and Study of the Interactions between the MTDC and the AC Grids." Université Paris-Saclay.
- Alden, R. T H, and F. A. Qureshy. 1985. "Eigenvalue Tracking Due to Parameter Variation." *IEEE Transactions on Automatic Control* 30 (9): 923–25. doi:10.1109/TAC.1985.1104080.
- Arabi, S., G.J. Rogers, D.Y. Wong, P. Kundur, and M.G. Lauby. 1991. "Small Signal Stability Program Analysis of SVC and HVDC in AC Power Systems." *IEEE Transactions on Power Systems* 6 (3): 1147–53. doi:10.1109/59.119259.
- Barrera-Gallegos, Noe, Genevieve Dauphin-Tanguy, and Xavier Guillaud. 2016. "Modal Sensitivity of a Reduced Equivalent HVDC-VSC System." In *2016 International Conference on Control, Decision and Information Technologies (CoDIT)*, 588–93. IEEE. doi:10.1109/CoDIT.2016.7593628.
- Beddard, A., and M. Barnes. 2015. *Modelling of MMC-HVDC Systems – An Overview*. *Energy Procedia*. Vol. 80. Elsevier B.V. doi:10.1016/j.egypro.2015.11.423.
- Beerten, Jef, Salvatore D Arco, and Jon Suul. 2015. "Identification and Small-Signal Analysis of Interaction Modes in VSC MTDC Systems." *IEEE Transactions on Power Delivery* 8977 (c): 888–97. doi:10.1109/TPWRD.2015.2467965.
- Bergna Diaz, Gilbert, Jon Are Suul, and Salvatore D'Arco. 2015. "Small-Signal State-Space Modeling of Modular Multilevel Converters for System Stability Analysis." In *2015 IEEE Energy Conversion Congress and Exposition (ECCE)*, 5822–29. IEEE. doi:10.1109/ECCE.2015.7310477.
- Bernal-Perez, S., S. Ano-Villalba, R. Blasco-Gimenez, and N. Aparicio. 2012. "Wind Power Plant Control for the Connection to Multiterminal HVdc Links." *2012 IEEE Energy Conversion Congress and Exposition, ECCE 2012*, 2873–79. doi:10.1109/ECCE.2012.6342372.
- Chapman, Stephen J. 2010. *Electric Machinery Fundamentals. Antimicrobial Agents and Chemotherapy*. Vol. 58. doi:10.1088/1751-8113/44/8/085201.
- Chaudhuri, Nilanjan Ray, Balarko Chaudhuri, Rajat Mujumder, and Amirnaser Yazdani. 2014. *Multi-Terminal Direct-Current Grids: Modeling, Analysis and Control*.
- Choi, Kang Min, Sang Won Cho, Man Gi Ko, and In Won Lee. 2004. "Higher Order Eigensensitivity Analysis of Damped Systems with Repeated Eigenvalues." *Computers and Structures* 82 (1): 63–69. doi:10.1016/j.compstruc.2003.08.001.
- Cole, Stijn, Student Member, Jef Beerten, and Ronnie Belmans. 2010. "Generalized Dynamic VSC MTDC Model for Power System Stability Studies" 25 (3): 1655–62.
- D'Arco, Salvatore, Jon Are Suul, and Olav Fosso. 2014a. "Automatic Tuning of Cascaded Controllers for Power Converters Using Eigenvalue Parametric Sensitivities." *IEEE Transactions on Industry Applications* 51 (2): 1–1. doi:10.1109/TIA.2014.2354732.
- D'Arco, Salvatore, Jon Are Suul, and Olav B. Fosso. 2014b. "Small-Signal Modelling and Parametric Sensitivity of a Virtual Synchronous Machine." In *2014 Power Systems Computation Conference*, 1–9. doi:10.1109/PSCC.2014.7038410.

- D'Arco, Salvatore, Jon Are Suul, and Olav B. Fosso. 2015. "Small-Signal Modeling and Parametric Sensitivity of a Virtual Synchronous Machine in Islanded Operation." *International Journal of Electrical Power & Energy Systems* 72. Elsevier Ltd: 3–15. doi:10.1016/j.ijepes.2015.02.005.
- D'Arco, Salvatore, Jon Are Suul, and Marta Molinas. 2014. "Implementation and Analysis of a Control Scheme for Damping of Oscillations in VSC-Based HVDC Grids." *16th International Power Electronics and Motion Control Conference and Exposition*, 586–93. doi:10.1109/EPEPEMC.2014.6980558.
- Delarue, P, F Gruson, and X Guillaud. 2013. "Energetic Macroscopic Representation and Inversion Based Control of a Modular Multilevel Converter." In *2013 15th European Conference on Power Electronics and Applications, EPE 2013*, 1–10. doi:10.1109/EPE.2013.6631859.
- Determination, Numerical. n.d. "Of Eigenvalues and Eigenvectors," 1–4.
- Eslami, Mansour. 1994. *Theory of Sensitivity in Dynamic Systems*. Berlin, Heidelberg: Springer Berlin Heidelberg. doi:10.1007/978-3-662-01632-9.
- Freytes, J, S Akkari, J Dai, F Gruson, P Rault, and X Guillaud. 2016. "Small-Signal State-Space Modeling of an HVDC Link with Modular Multilevel Converters." Inproceedings. In *2016 IEEE 17th Workshop on Control and Modeling for Power Electronics (COMPEL)*, 1–8. doi:10.1109/COMPEL.2016.7556693.
- Gao, Wenzhong, Ziping Wu, Jianhui Wang, and Shusheng Gu. 2013. "A Review of Inertia and Frequency Control Technologies for Variable Speed Wind Turbines." *2013 25th Chinese Control and Decision Conference (CCDC)*, 2527–33. doi:10.1109/CCDC.2013.6561366.
- Gershgorin, S. 1931. "Über Die Abgrenzung Der Eigenwerte Einer Matrix." *Bulletin de l'Académie Des Sciences de l'URSS*, no. 6: 749–54.
- Holttinen, Hannele. 2012. "Wind Integration: Experience, Issues, and Challenges." *Wiley Interdisciplinary Reviews: Energy and Environment* 1 (3): 243–55. doi:10.1002/wene.18.
- Hsu, Yuan-Yih, and Chern-Lin Chen. 1987. "Identification of Optimum Location for Stabiliser Applications Using Participation Factors." *IEE Proceedings C Generation, Transmission and Distribution* 134 (3): 238. doi:10.1049/ip-c.1987.0037.
- Ismunandar, Christian. 2010. "Control of Multi-Terminal VSC-HVDC for Offshore Wind Power Integration." *TUDeft, Master's Thesis*. http://repository.tudelft.nl/assets/uuid:bc13cdc7-6c4f-4ab6-894d-90bcd2d47337/MSc_thesis_Chris_Aug2010.pdf?origin=publication_detail.
- Jacobi, Carl Gustav Jacob. 1856. "Über Ein Leichtes Verfahren Die in Der Theorie Der Säculärstörungen Vorkommenden Glenichungen Numerich Aufzulösen." *Crelle's J.*, 51–94.
- Kalcon, Giddani O., Grain P. Adam, Olimpo Anaya-Lara, Stephen Lo, and Kjetil Uhlen. 2012. "Small-Signal Stability Analysis of Multi-Terminal VSC-Based DC Transmission Systems." *IEEE Transactions on Power Systems* 27 (4): 1818–30. doi:10.1109/TPWRS.2012.2190531.
- Krause, Paul C, Oleg Wasynczuk, and Scott D Sudhoff. 2002. "Analysis of Electric Machinery and Drive Systems." *Power Engineering*. doi:10.1109/9780470544167.
- Kundur, Prabha. 2007. *Power System Stability and Control*. McGraw-Hill, Inc.
- Kundur, Prabha, Jonh Paserba, Venkat Ajarapu, Göran Andersson, Anjan Bose, Claudio Canizares, Nikos Hatziaargyriou, et al. 2004. "Definition and Classification of Power System Stability IEEE/CIGRE Joint Task Force on Stability Terms and Definitions." *IEEE Transactions on Power Systems* 19 (3): 1387–1401. doi:10.1109/TPWRS.2004.825981.
- Li, Li, Yujin Hu, Xuelin Wang, and Ling Ling. 2013. "Eigensensitivity Analysis of Damped Systems with Distinct and Repeated Eigenvalues." *Finite Elements in Analysis and Design* 72: 21–34. doi:10.1016/j.finel.2013.04.006.

- Liang, Jun, Oriol Gomis-Bellmunt, and Dirk Van Hertem. 2016. "HVDC Grids: For Offshore and Supergrid of the Future," 528.
- Meyer, Carl D. 2000. *Matrix Analysis and Applied Linear Algebra*. SIAM.
- Meyer, D., and K. Veselić. 1980. "On Some New Inclusion Theorems for the Eigenvalues of Partitioned Matrices." *Numerische Mathematik* 34 (4): 431–37. doi:10.1007/BF01403679.
- Mohan, Ned, Tore M Undeland, and William P Robbins. 2003. *Power Electronics: Converters, Applications and Design*. 3rd Editio. Wiley and Sons.
- Moler, Cleve, and Charles Van Loan. 2003. "Nineteen Dubious Ways to Compute the Exponential of a Matrix, Twenty-Five Years Later." *SIAM Review* 45 (1): 3–49. doi:10.1137/S00361445024180.
- Mondal, Debasish, Abhijit Chakrabarti, and Aparajita Sengupta. 2014. *Power System Small Signal Stability Analysis and Control*. First Ed. Elsevier Inc.
- Morgan, B.S. 1966. "Computational Procedure for the Sensitivity of an Eigenvalue." *Electronics Letters* 2 (6): 197. doi:10.1049/el:19660166.
- Okba, Mohamed H., Mohamed H. Saied, M. Z. Mostafa, and T. M. Abdel- Moneim. 2012. "High Voltage Direct Current Transmission - A Review, Part I." In *2012 IEEE Energytech*, 1–7. IEEE. doi:10.1109/EnergyTech.2012.6304650.
- Pagola, F. Luis, Ignacio J. Perez-Arriaga, and George C. Verghese. 1989. "On Sensitivities, Residues and Participations: Applications to Oscillatory Stability Analysis and Control." *IEEE Transactions on Power Systems* 4 (1): 278–85. doi:10.1109/59.32489.
- Pal, Bikash, and Balarko Chaudhuri. 2005. *Robust Control in Power Systems*. doi:10.1007/b136490.
- Paraskevopoulos, P., C. Tsonis, and S. Tzafestas. 1974. "Eigenvalue Sensitivity of Linear Time-Invariant Control Systems with Repeated Eigenvalues." *IEEE Transactions on Automatic Control* 19 (5): 610–12. doi:10.1109/TAC.1974.1100638.
- Peralta, Jaime, Hani Saad, Sebastien Denner, and Jean Mahseredjian. 2012. "Dynamic Performance of Average-Value Models for Multi-Terminal VSC-HVDC Systems." *IEEE Power and Energy Society General Meeting*, 1–8. doi:10.1109/PESGM.2012.6345610.
- Peralta, Jaime, Hani Saad, Sébastien Denner, Jean Mahseredjian, and Samuel Nguéfeu. 2012. "Detailed and Averaged Models for a 401-Level MMC-HVDC System." *IEEE Transactions on Power Delivery* 27 (3): 1501–8. doi:10.1109/TPWRD.2012.2188911.
- Perez-Arriaga, I.J. 1981. "Selective Modal Analysis With Applications to Electric Power Systems." Massachusetts Institute of Technology.
- Perez-Arriaga, I.J., L Rouco, F.L. Pagola, and J.L. Sancha. 1988. "The Role of Participation Factors in Reduced Order Eigenanalysis of Large Power Systems." 1988., *IEEE International Symposium on Circuits and Systems*. IEEE, 923–27. doi:10.1109/ISCAS.1988.15074.
- Perez-Arriaga, I.J., G.C. Verghese, and F.C. Schweppe. 1982. "Selective Modal Analysis with Applications to Electric Power Systems, PART I: Heuristic Introduction." *IEEE Transactions on Power Apparatus and Systems* PAS-101 (9): 3117–25. doi:10.1109/TPAS.1982.317524.
- Perez-Arriaga, Ignacio J., George C. Verghese, F. Luis Pagola, Jos??Luis Sancha, and Fred C. Schweppe. 1990. "Developments in Selective Modal Analysis of Small-Signal Stability in Electric Power Systems." *Automatica* 26 (2): 215–31. doi:10.1016/0005-1098(90)90117-Z.
- Perveen, Rehana, Nand Kishor, and Soumya R. Mohanty. 2014. "Off-Shore Wind Farm Development: Present Status and Challenges." *Renewable and Sustainable Energy Reviews* 29. Elsevier: 780–92. doi:10.1016/j.rser.2013.08.108.
- Porter, Brian, and Roger Crossley. 1972. *Modal Control: Theory and Applications*. Taylor and Francis Ltd.

- Quarteroni, Alfio, Riccardo Sacco, and Fausto Saleri. 2007. *Numerical Mathematics. Texts in Applied Mathematics*. Vol. 37. Texts in Applied Mathematics. Springer New York. doi:10.1007/b98885.
- Rault, P., F. Colas, X. Guillaud, and S. Nguefeu. 2012. "Method for Small Signal Stability Analysis of VSC-MTDC Grids." *2012 IEEE Power and Energy Society General Meeting* 3: 1–7. doi:10.1109/PESGM.2012.6345318.
- Rault, P., X. Guillaud, F. Colas, and S. Nguefeu. 2013. "Investigation on Interactions between AC and DC Grids." *2013 IEEE Grenoble Conference PowerTech, POWERTECH 2013* 3. doi:10.1109/PTC.2013.6652229.
- Saad, H, S Denetiere, J Mahseredjian, P Delarue, X Guillaud, J Peralta, and S Nguefeu. 2014. "Modular Multilevel Converter Models for Electromagnetic Transients." *IEEE Transactions on Power Delivery* 29 (3): 1481–89. doi:10.1109/TPWRD.2013.2285633.
- Saad, Hani, Xavier Guillaud, Jean Mahseredjian, Sebastien Denetiere, and Samuel Nguefeu. 2015. "MMC Capacitor Voltage Decoupling and Balancing Controls." *IEEE Transactions on Power Delivery* 30 (2): 704–12. doi:10.1109/TPWRD.2014.2338861.
- Samimi, Shabab. 2015. "Modélisation et Commande Des Convertisseurs MMC En Vue de Leur Intégration Dans Le Réseau Électrique." Ecole centrale de Lille.
- Shen, L., M. Barnes, J.V. Milanovic, and R. Preece. 2012. "Control of VSC HVDC System Integrated with AC Network." *10th IET International Conference on AC and DC Power Transmission (ACDC 2012)*, 51–51. doi:10.1049/cp.2012.1954.
- Sheng, Li Sheng Li, E.H. Abed, M.a. Hassounh, Huizhong Yang Huizhong Yang, and M.S. Saad. 2010. "Mode in Output Participation Factors for Linear Systems." *American Control Conference (ACC), 2010*, 956–61.
- Smed, Thomas. 1993. "Feasible Eigenvalue Sensitivity for Large Power Systems." *IEEE Transactions on Power Systems* 8 (2): 555–63. doi:10.1109/59.260827.
- Thams, Florian, Jon Are Suul, Salvatore D'Arco, Marta Molinas, and Friedrich Wilhelm Fuchs. 2015. "Stability of DC Voltage Droop Controllers in VSC HVDC Systems." In *2015 IEEE Eindhoven PowerTech*, 1–7. IEEE. doi:10.1109/PTC.2015.7232614.
- Tschirhart, Paul, Alan Sussman, and Eyad H. Abed. 2014. "Using Participation Factors to Improve the Consistency and Accuracy of Prony Analysis for Voltage Stability Monitoring Applications." *2014 IEEE PES Innovative Smart Grid Technologies Conference, ISGT 2014*. doi:10.1109/ISGT.2014.6816391.
- Varga, Richard S. 2000. *Matrix Iterative Analysis*. New York. Vol. 27. Springer Series in Computational Mathematics. Berlin, Heidelberg: Springer Berlin Heidelberg. doi:10.1007/978-3-642-05156-2.
- Vasca, F., and G.C. Verghese. 1999. "Adimensional Models and Participation Factors for the Analysis of Induction Motor Dynamics." *ISIE '99. Proceedings of the IEEE International Symposium on Industrial Electronics (Cat. No.99TH8465)* 2. doi:10.1109/ISIE.1999.798659.
- Verghese, G., I. Perez-arriaga, and F. Schweppe. 1982. "Selective Modal Analysis With Applications to Electric Power Systems, Part II: The Dynamic Stability Problem." *IEEE Transactions on Power Apparatus and Systems* PAS-101 (9): 3126–34. doi:10.1109/TPAS.1982.317525.
- Wang, Kai, Xiaobo Hu, Wei Sun, Haishun Sun, and Ke Zhang. 2014. "DC Voltage Control and Power Dispatch Study of a Five-Terminal DC Grid Based on Average-Value VSC Model." *POWERCON 2014 - 2014 International Conference on Power System Technology: Towards Green, Efficient and Smart Power System, Proceedings*, no. Powercon: 2285–92. doi:10.1109/POWERCON.2014.6993784.
- Wang, Xi-Fan, Yonghua Song, and Malcolm Irving. 2008. *Modern Power Systems Analysis*. Springer.

- Wenyuan, Wang, A Beddard, M Barnes, and O Marjanovic. 2014. "Analysis of Active Power Control for VSC-HVDC." *Power Delivery, IEEE Transactions on* 29 (4): 1978–88. doi:10.1109/TPWRD.2014.2322498.
- Wu, Jie, Zhi Xin Wang, Lie Xu, and Guo Qiang Wang. 2014. "Key Technologies of VSC-HVDC and Its Application on Offshore Wind Farm in China." *Renewable and Sustainable Energy Reviews* 36. Elsevier: 247–55. doi:10.1016/j.rser.2014.04.061.
- Yazdani, Amirnaser, and Reza Iravani. 2010. *Voltage-Sourced Converters in Power Systems*. Hoboken, NJ, USA: John Wiley & Sons, Inc. doi:10.1002/9780470551578.

Appendix A. *Automatic routine for parametric sensitivity analysis*

For the analysis of the parametric sensitivity in different models an automatic routine was developed. The parametric sensitivity analysis described in Chapter 3 has the following inputs

- the analytic equations of the linear (or linearized) model.
- the list of parameters to analyze
- the list of all the parameters
- the list of the parameter values

With these inputs, the automatic routine follows the next flow chart.

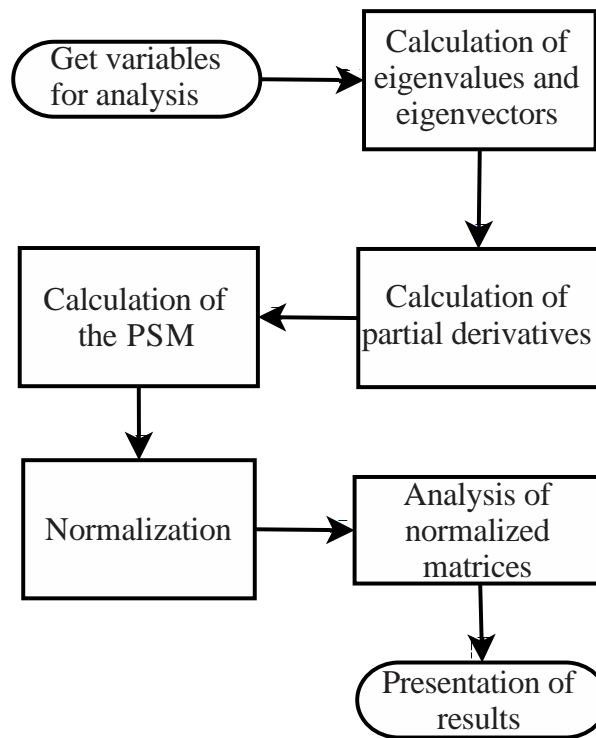


Figure A.1 General flow chart for the parametric sensitivity analysis.

For the stages in the flow chart different functions were developed, for the examples in section 5.4 the function to get the variables has,

```
%  
*****  
% [Par,vals,A_sys]=getvariab()  
% This function gives the necessary matrices for the parametric  
sensitivity  
% analysis.  
% Par is the matrix of parameters contained on the matrix of the system  
% Asys is the matrix of the system in symbolic form  
% vals is the matrix of the parameter values in the same order as Par
```

```
% v1 (11/01/2016) Noe Barrera G.
% v2 (11/03/2016) Julian Freytes
% v2.1 (14/03/2016) Noe Barrera G. added state names for PF analysis
% v3 (23/08/16) Noe B New version adpted to have the elemetrts for
% HVDC.link of Julian
% v4 (21/08/2016) Julian F New version adopted for MMC DQ control
% % % % % % % % % % % % % % % %
function [Par,vals,A_sys_sym,A_sys_num, state_names]=PS_getvariab()
tic
addpath([cd '/a01_GeneralFunctions/']);
run('a00_RUNME_MMC_Pmode_Symb.m')
run('a00_RUNME_MMC_Pmode_Num.m')
Struct = MMC1;
A_sys_sym= Struct.A_sys_sym;
A_sys_num= Struct.A_sys;
Par = symvar(A_sys_sym);
vals = zeros(1,length(Par));

for i = 1:length(Par)
    Index = SeekAndReturnIndex_Sym(char(Par(i)), Struct.Parameters);
    vals(i) = Struct.Parameters.num(Index);
end

vals= vals';

state_names=Struct.States.sym;
rmpath([cd '/a01_GeneralFunctions/']);
disp('Computing time for PS_getvariab:')
```

The computation of the eigenvalues, eigenvectors and the sensitivity matrices have the following code,

```
Asysnum = A_sys_num;

% PFF = PS_PartFact(Asysnum);
[Vi,lamd]=eig(Asysnum);           %%Rigth eigenvector and eigenvalues
Uti=inv(Vi);                     %%transponse of the left
eigenvector
Ui=transpose(Uti);               %%Left eigenvector
```

The calculation of the partial derivatives is performed using the tool of differentiation in MATLAB®.

Each row of the PSM is computed in a loop

```
%
*****
% [Spnl]=parSens(Asys,PP,all,values,S)
% This function calculate the parametric sensitivity for a given
parameter
%
% 'PP' is the parameter of the analysis [1x1]
%
```



```

% 'Asys' is the system matrix in symbolic representation
%
% 'all' is the vector of all paramters in symbolic representation
%
% 'values' is the vector of paramter values in the same order as 'all'
%
% 'S' are the sensitivity matrices of the system
%
% 'Spnl' is the output vector with the parametric sensitivity respect to
PP
% for all eigenvalues
%   v1 11/02/2016      Noe-----noebg20@gmail.com
%   v1.5 10/10/2016    Julian   added
%*****

function [Spnl]=PS_parSens(Asys,PP,all,values,S)
Spnl=zeros(1,length(Asys));          %%variable inicialization

    PDi=expand(diff(Asys,PP));          %%partial
differentiation
    a01_NoValues
tic
    PDi_num=(eval(PDi));                %%sustitution,

tic
    for k=1:length(Asys)
        for j=1:length(Asys)
            for i=1:length(Asys)
                Spnl(k)=Spnl(k)+(S(j,i,k)*PDi_num(j,i));    %%definition of
sensitivity according to the chain rule
            end
        end
    end
end
toc

```

For the normalization the function used is

```

%
%*****
% function [Spnl]=normaliz(SP,RC)
% This function calculate the normalization using L2-norm
%
% 'SP' is the parametric sensitivity matrix
%
% 'RC' is the mode of normalization
% % % % % 'rows' or 'columns'
%
% 'Spnl' is the matrix SP normalized
%
% v1.1 (11/01/2016) Noe Barrera G.
% % % % % % % % % % % % % % % %
function [Spnl]=PS_normaliz(SP,RC)

[a,b]=size(SP);
Spnl=zeros(a,b);

```

```

if strcmp(RC,'rows')
    for i=1:a
        for k=1:b
            Spnl(i,k)=SP(i,k)/norm(SP(i,:),2);
        end
    end
else if strcmp(RC,'columns')

    for i=1:b
        for k=1:a
            Spnl(k,i)=SP(k,i)/norm(SP(:,i),2);
        end
    end
else
    error('-----NORMALIZATION NOT SPECIFIED-----use help
normaliz-----')
end
end
end

```

The analysis and the presentation of the results in the workspace performed by the following function.

```

%
%*****
% [tot]=show_results(SP, lamd, param2)
% This function show the results of the parametric sensitivity analysis
%
% SP is the matrix of parameters sensitivities normalized
% lamd is the vector of eigenvalues
% param2 is the vector of parameter analysis in symbolic
% KoA is a character to select the kind of analysis by 'rows' or
% 'columns'
%
% v2.2 (11/03/2016) Noe Barrera G. noebg20@gmail.com
% v2.3 (22/03/2016) Noe Barrera G. labels e--->n
% % % % % % % % % % % % % % % % %
function [tot]=PS_show_results(SP, lamd, param2,KoA)
esp=' ';
epsil='_____n'; %%text for the values
which are smaller than abs(0.1+0.1i)
disp('')
disp(' The order of the eigenvalues is ')
disp('')
[a,b]=size(SP);
tot=cell(a+1,b+1);
for i=1:length(lamd)
    disp([num2str(char(181)),'_',num2str(i),' =
',num2str(lamd(i,i),'%6.2f' )])
    if i>=10
        tx1='====';
        tx2='===';
    elseif i>=100
        tx1='====';
        tx2='==';
    elseif i>=1000
        tx1='====';
        tx2='=';
    else
        tx1='====';
    end
end

```

```

        tx2='===';
    end

    tot(1,i+1)={strcat(tx1,num2str(char(181)),'_',num2str(i),tx2)};
end
sl=zeros(length(param2),1);
for i=1:length(param2)
    v=char(param2(i));
    sl(i)=length(v);
end
maxi=max(sl);
tem='/' ;
for i=1:(maxi+4)

    tem=strcat(tem,'/');
end

tot(1,1)={tem};
for i=1:length(param2)
    v=char(param2(i));

    for k=1:(maxi+5)-sl(i)
        v=strcat(v,'_');
    end

    tot(i+1,1)={v};
end
tot(i+1,1)={v};

for i=2:a+1
    for j=2:b+1
        if imag(SP(i-1,j-1))==0
            SP(i-1,j-1)=complex(SP(i-1,j-1),1e-25);
        end
        if real(SP(i-1,j-1))>=0
            if (abs(SP(i-1,j-1))<abs(0.1+0.1i))
                tot(i,j)={epsil};
            else
                tot(i,j)={strcat('+',num2str(SP(i-1,j-1),'%6.2f' ))};
            end
        else
            if (abs(SP(i-1,j-1))<abs(0.1+0.1i))
                tot(i,j)={epsil};
            else
                tot(i,j)={num2str(SP(i-1,j-1),'%6.2f' )};
            end
        end
    end
end

end

if strcmp(KoA,'rows')
    disp('-----')
    disp('|           The parametric sensitivity matrix normalized by rows
is,      |')
```

```

disp('-----')
elseif strcmp(KoA,'columns')
disp('-----')
disp('|      The parametric sensitivity matrix normalized by
columns is,   |')
disp('-----')
end
for i=1:b
if i==1
temp=strcat(tot(:,1), {' '},tot(:,2));
else
temp=strcat(temp, {' '},tot(:,i+1));
end
end

textttot=char(temp);

disp(textttot);

text0=strcat({' ',''}, {' '}, {esp},{char(144)});
%-----tables construction-----
temp1=cell(a+1,b+1);
if strcmp(KoA,'rows')
disp('-----')
disp('by rows: The most influenced eigenvalues of the system by each
parameter are:')
disp('-----')
temp1(:,1)=tot(:,1);
for i=2:a+1

for j=2:b+1
if strcmp(char(tot(i,j)), '____n____')
temp1(i,j)={' '};
else
temp1(i,j)={strcat(char(181), '_ ', num2str(j-
1),char(text0))};
end

end

end

for i=1:b
if i==1
tet=strcat(temp1(:,1), {' '},temp1(:,2));
else
tet=strcat(tet, {' '},temp1(:,i+1));
end

end

disp(char(tet))
else

```

```
if strcmp(KoA,'columns')
    disp('-----')
    disp('by columns: The most the most important parameter for each
eigenvalue are,')
    disp('-----')

    transt=transpose(tot);

temp2(:,1)=transt(:,1); %([2:a+1],1);
for i=2:b+1

    for j=2:a+1
        if strcmp(char(transt(i,j)), '____n____')
            temp2(i,j)={' '};
        else
            temp2(i,j)={strcat(char(param2(j-1)),char(text0))};
        end
    end

end

for i=1:a
    if i==1
        tet=strcat(temp2(:,1), {' '},temp2(:,2));
    else
        tet=strcat(tet, {' '},temp2(:,i+1));
    end

end

disp(char(tet))

else
    warning('See help for selection of anlysis')
    error('The selected analysis does not exist please seletc only
rows or columns as string')

end

end
disp('The elements with ____n____ teir value is less than the modulus of
(0.1+-0.1i)')
```

Sensibilité Paramétrique pour l'Analyse Dynamique des Réseaux à Courant Continu

Ce travail de thèse a pour finalité de présenter différentes méthodologies pour l'analyse de réseaux à courant continu haute tension (HVDC).

La théorie fondamentale de l'analyse de sensibilité s'applique sur analyse des systèmes électriques de puissance dans les différents étapes de la production et la transmission de l'énergie. Des outils de bases concernant cette théorie sont devenus populaires et très utilisés.

En pratique, les facteurs de participation représentent un exemple de ces outils, utilisés depuis longtemps. Ils ont été proposés par (Perez-Arriaga et al., 1982). Nous présentons la théorie fondamentale de la sensibilité analytique dans laquelle les facteurs de participation sont basés. Pour une bonne compréhension de ces éléments de base de cette théorie, quelques exemples sont présentés. Nous présentons une formulation différente pour l'analyse par sensibilité paramétrique (Barrera Gallegos et al., 2016). Enfin, les deux méthodologies sur des exemples des réseaux HVDC. Notre comparaison permet d'exposer les limites de l'utilisation des facteurs de participation sur des réseaux HVDC. En conclusion, la nouvelle méthodologie est plus générale comparée aux facteurs de participation. Également, la nouvelle méthodologie, par sensibilité paramétrique, nous donne plus d'informations sur les caractéristiques dynamiques des réseaux HVDC.

Mot clefs : Analyse modale, Sensibilité paramétrique, facteurs de participation, Réseaux à courant continu.

Parametric sensitivity for analysis of dc networks

The work presented in this thesis presents different methodology for parametric sensitivity of high voltage dc networks(HVDC).

The fundamental theory of modal analysis has been applied for analysis of the power electrical systems in its different stages of production and transmission of energy. Tools derived from these fundamentals have become popular with its use. Among the tools used in dynamic analysis, participation factors have been used for a long time. Proposed by (Perez-Arriaga et al., 1982), they give a metric for relating states and eigenvalues of a system. The participation factors is a tool that helps in the reduction of systems.

Firstly, we present the fundamentals of the sensitivity analysis upon which the participation factors are based on. The principle is illustrated with several examples.

We propose a new formulation for sensitivity analysis using parametric sensitivity (Barrera Gallegos et al., 2016).

In the latter, the application of participation factors and parametric sensitivity analysis is performed using HVDC networks. This comparison exposes the limitation of the participation factors for the general analysis of HVDC grids.

In conclusion, the new methodology is a better and general alternative compared to traditional participation factors employed for analysis of HVDC grids. In addition, the new technique of parametric sensitivity produces several novel information related to the dynamic characteristics of the HVDC grid.

Key words: Modal analysis, parametric sensitivity, participation factors, high voltage direct current grids.